High Energy Cosmic Ray Anisotropy with IceCube Observatory

Paolo Desiati, for the IceCube Collaboration

WIPAC & Department of Astronomy
University of Wisconsin - Madison

<desiati@wipac.wisc.edu>

Vulcano Workshop 2014 - Frontier Objects in Astrophysics and Particle Physics
Vulcano (ME) - Italy - May 23, 2014

cosmic ray observations

- **galactic** cosmic rays produced below 10^8-10^9 GeV
- **spectral features** from acceleration mechanisms & propagation effects
- **source distribution** in Galaxy and our neighborhood
- **magnetic field** configurations in local interstellar medium
- **anisotropy**

Gaisser, Stanev, Tilav, 2013 - arXiv:1303.3565

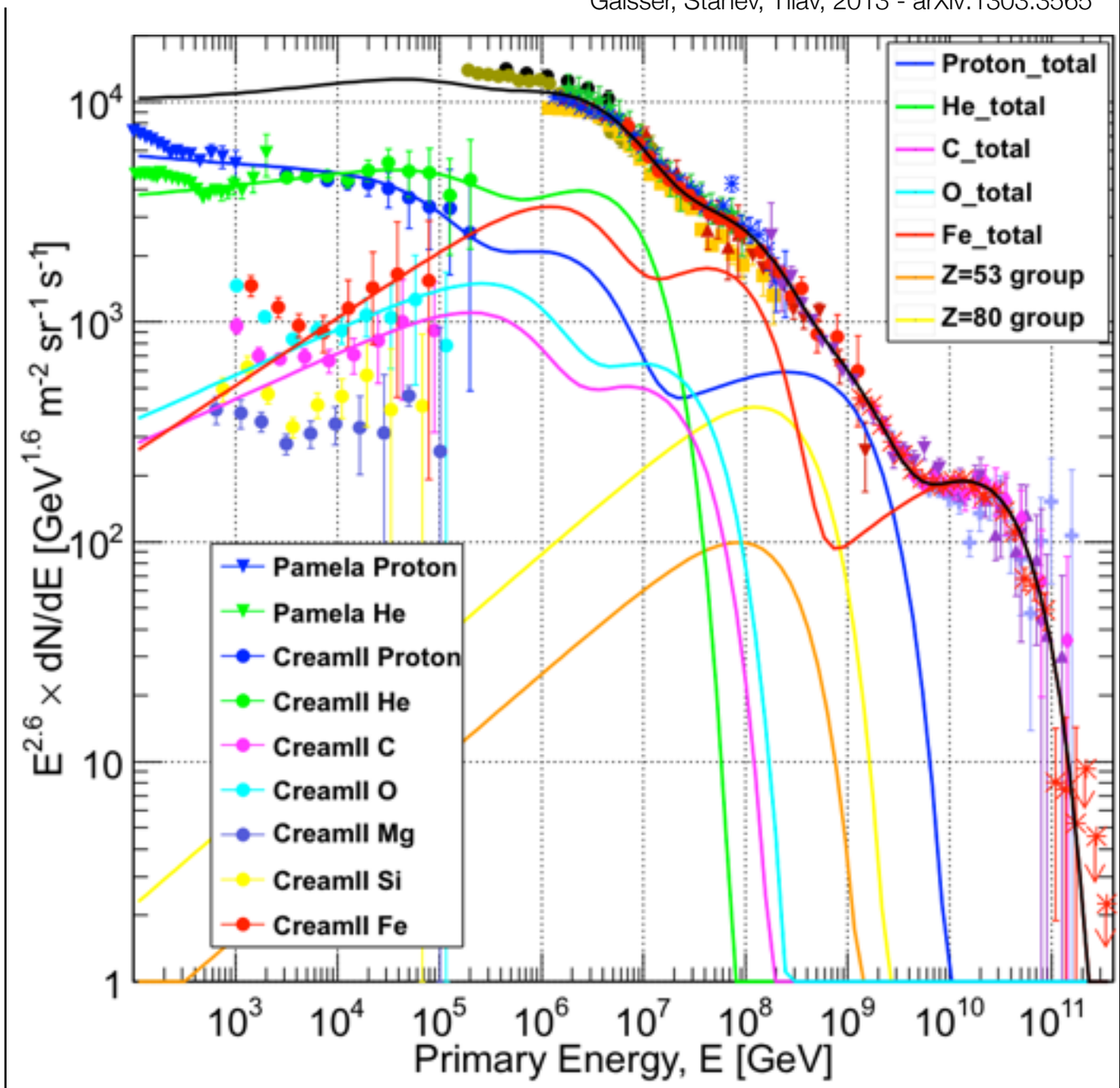

cosmic ray anisotropy observations

the legacy

~10^{-3}

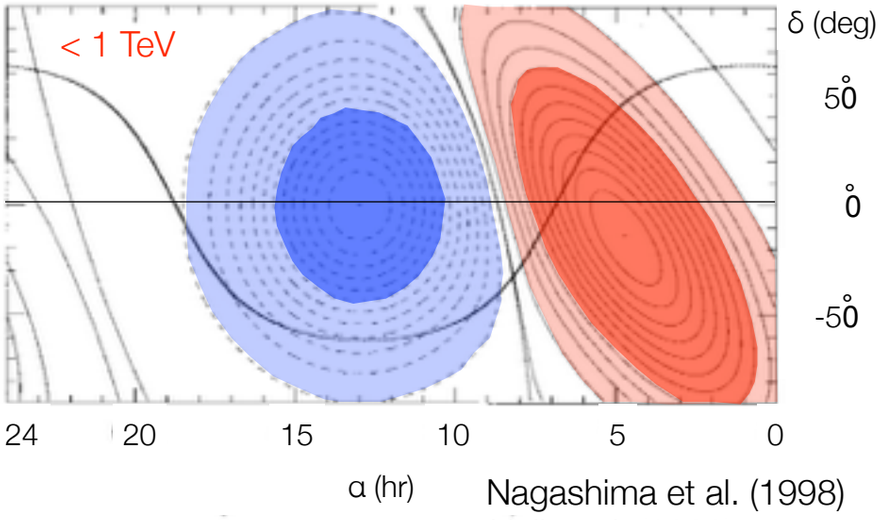

Nagashima et al. (1998)
Hall et al. (1999)

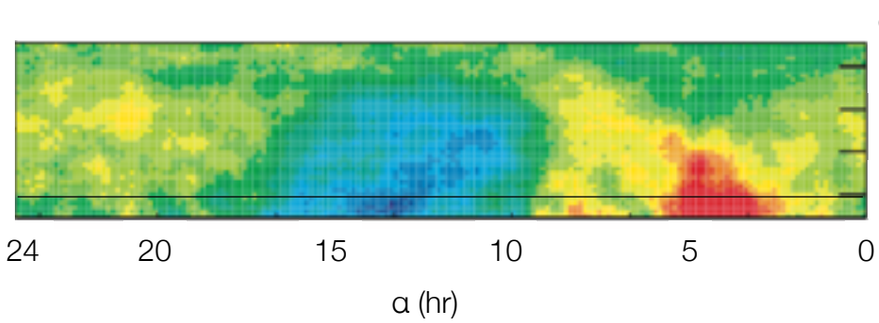

4 TeV

Tibet ASγ
Amenomori et al. (2006)

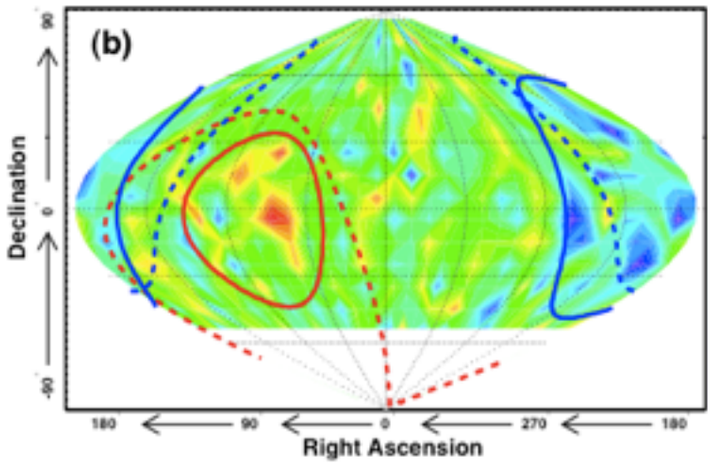

10 TeV

Super Kamiokande
Guillian et al. (2007)

equatorial coordinates

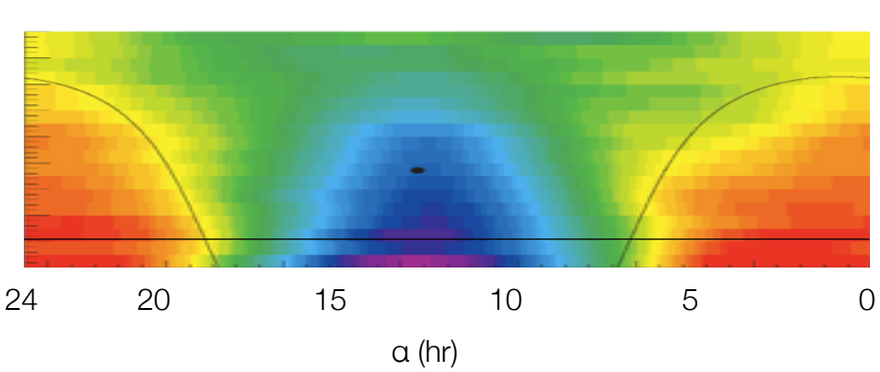

5 TeV

Milagro
Abdo et al. (2009)

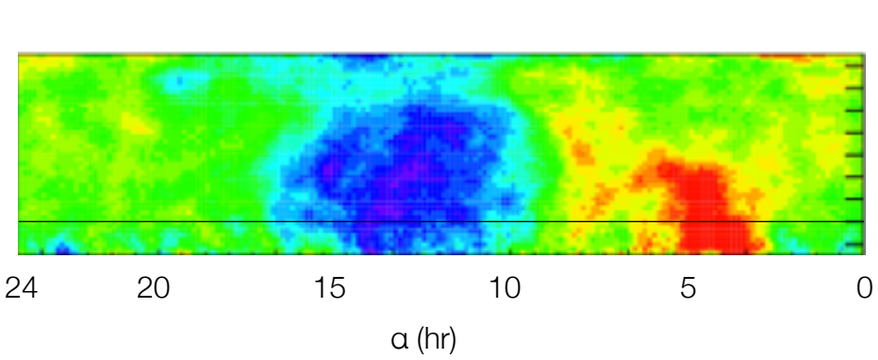

4 TeV

ARGO-YBJ
Zhang et al. (2009)

cosmic ray anisotropy observations

the legacy

1-5 TeV

$\sim 10^{-4}$

Tibet-III

Amenomori et al. ICRC 2007

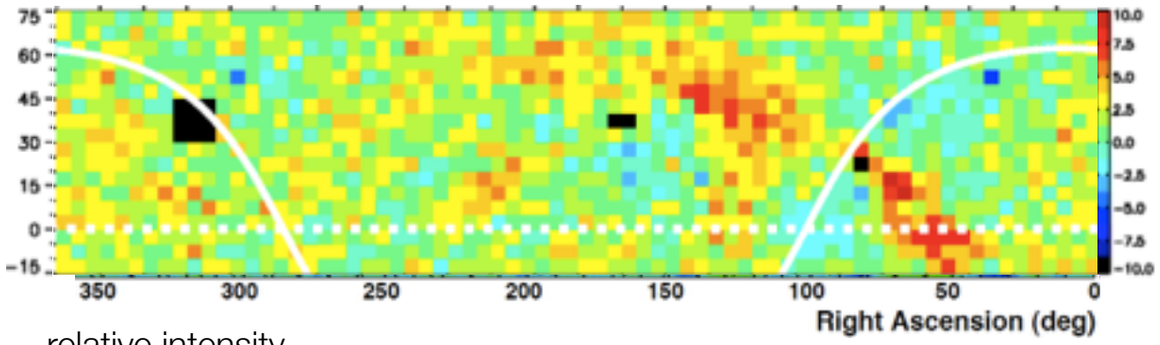

relative intensity

ARGO-YBJ

Vernetto et al. (2009)
Iuppa et al. (2011)
Bartoli et al. (2013)

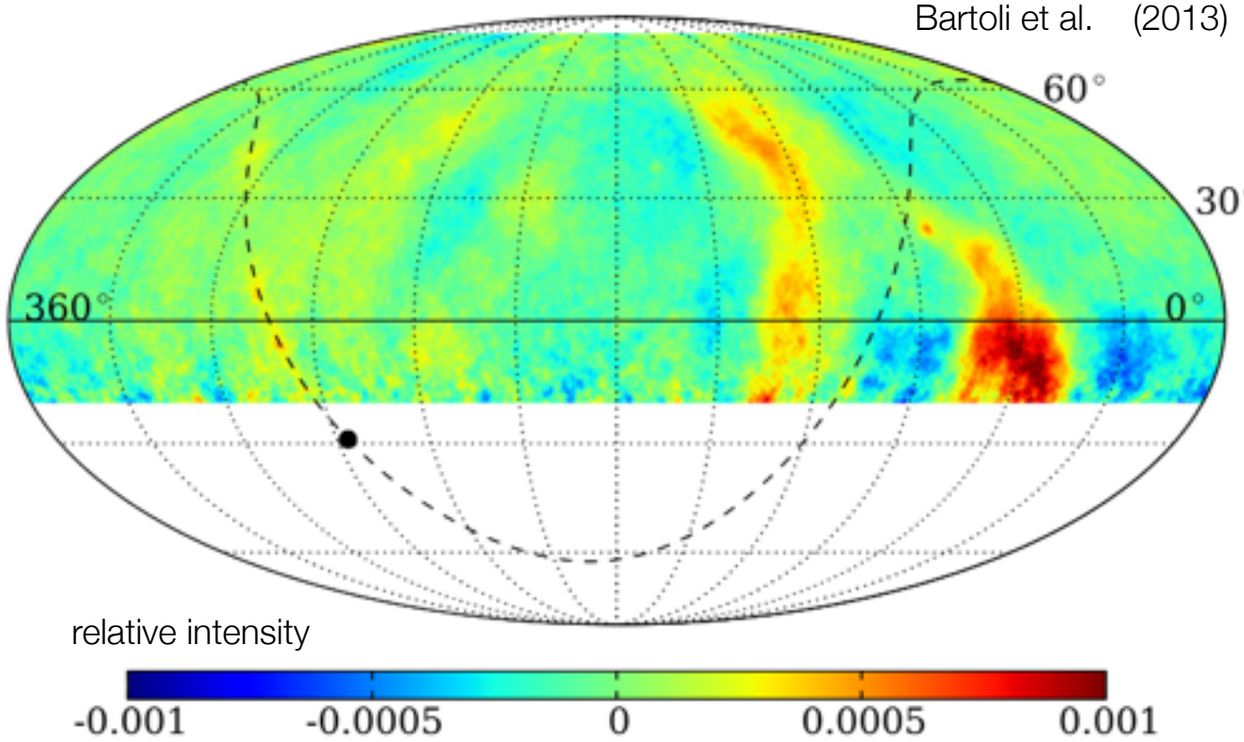

Milagro

Abdo et al. (2008)

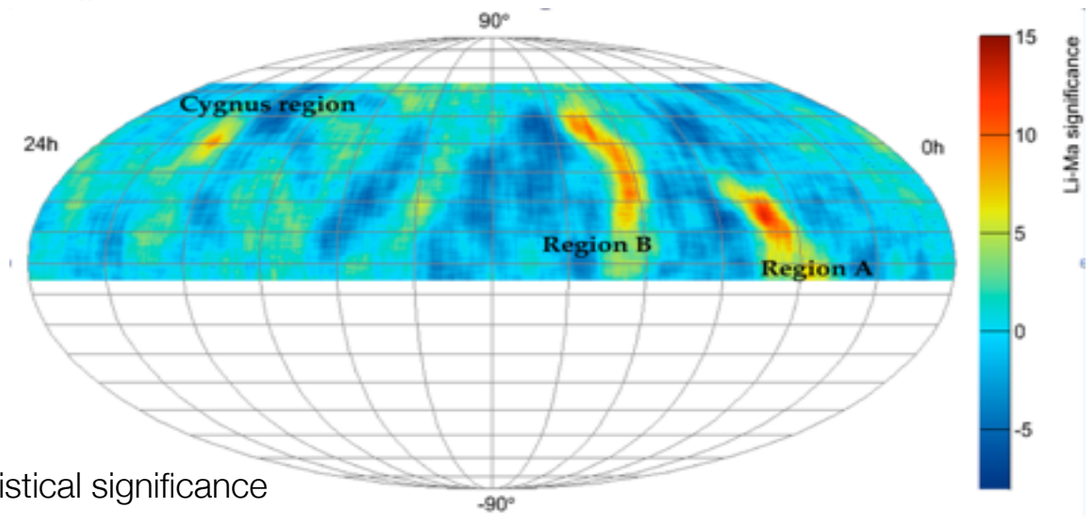

statistical significance

HAWC

BenZvi et al. ICRC 2013

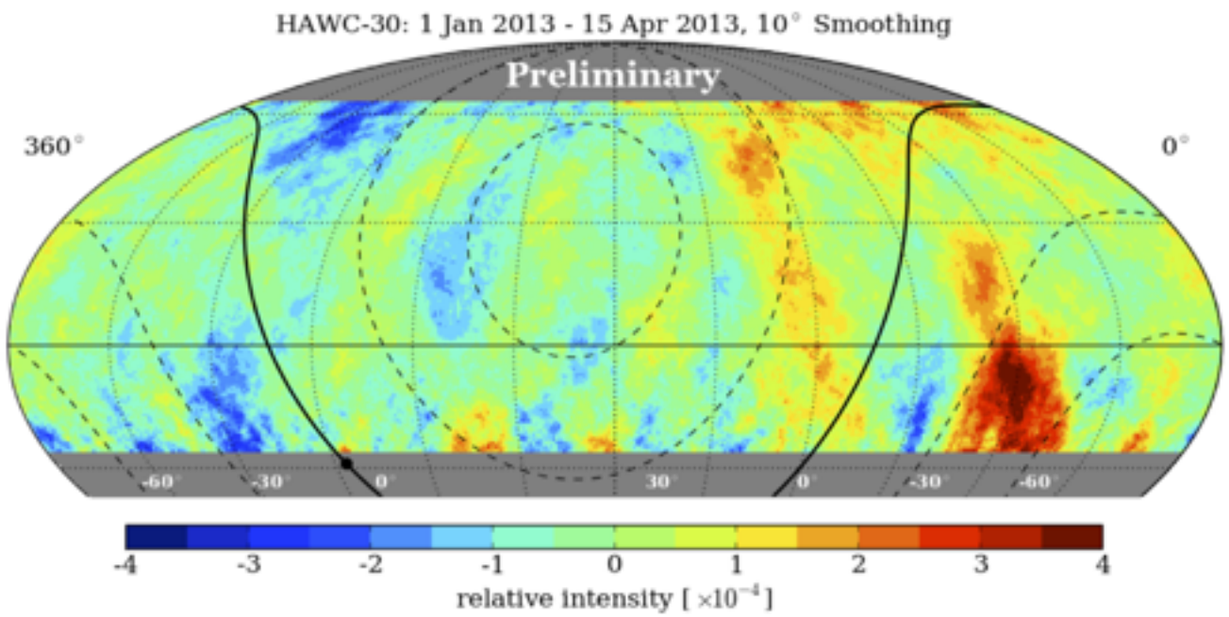

spectral feature associated to anisotropy

Milagro

Abdo et al. (2008)

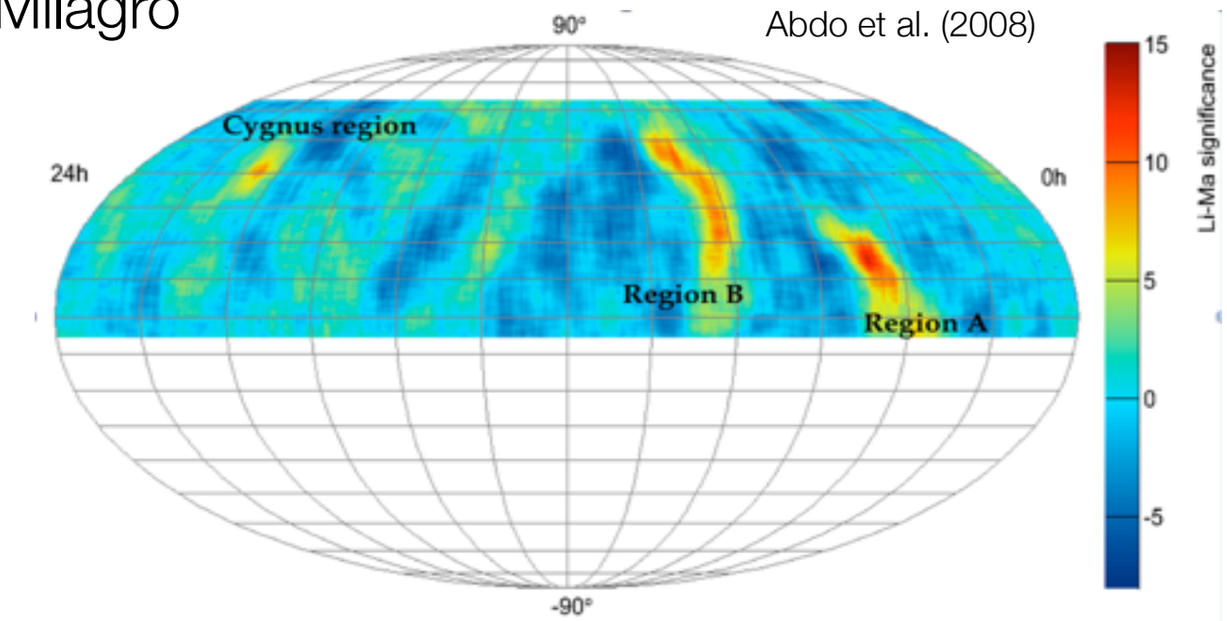

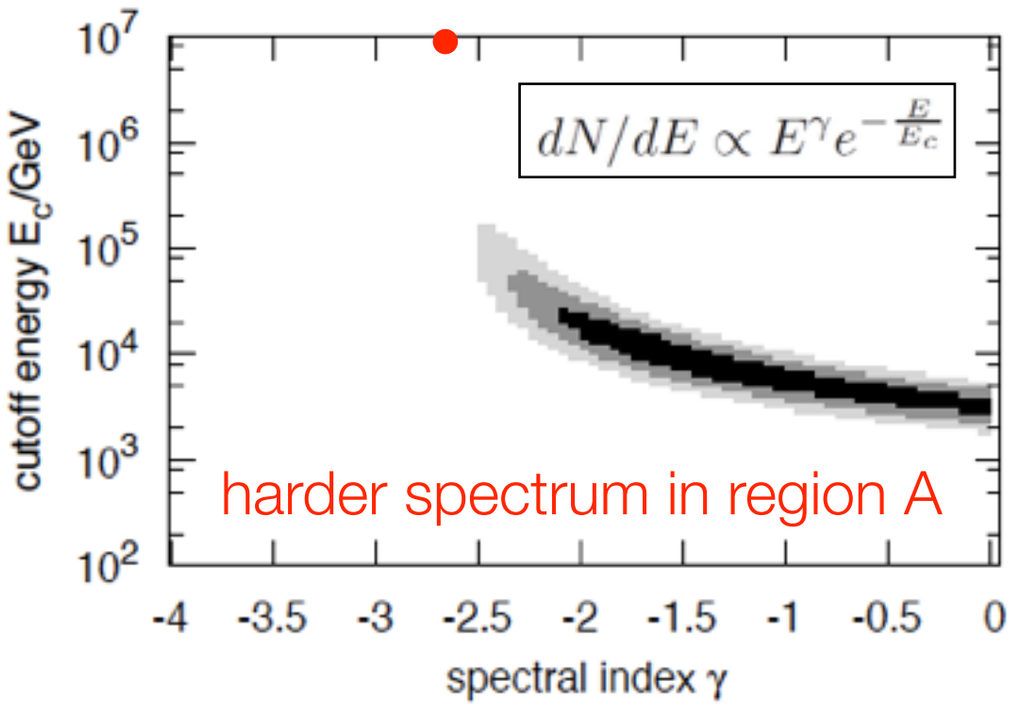

ARGO-YBJ

Bartoli et al. (2013)

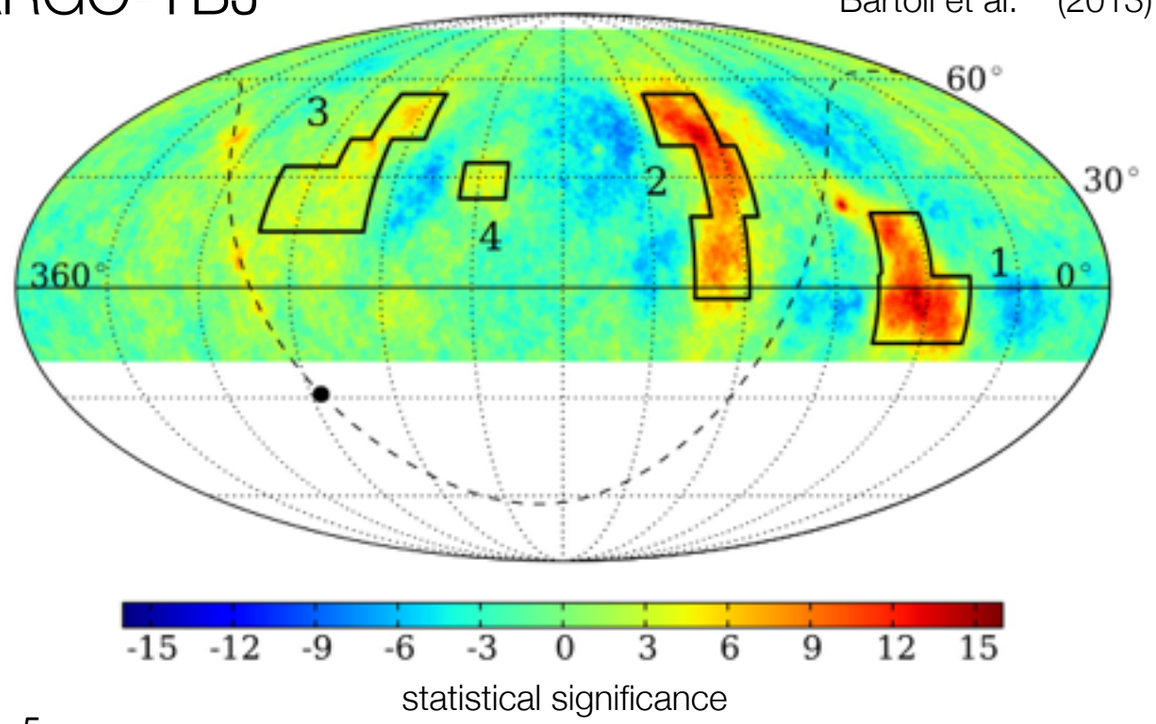

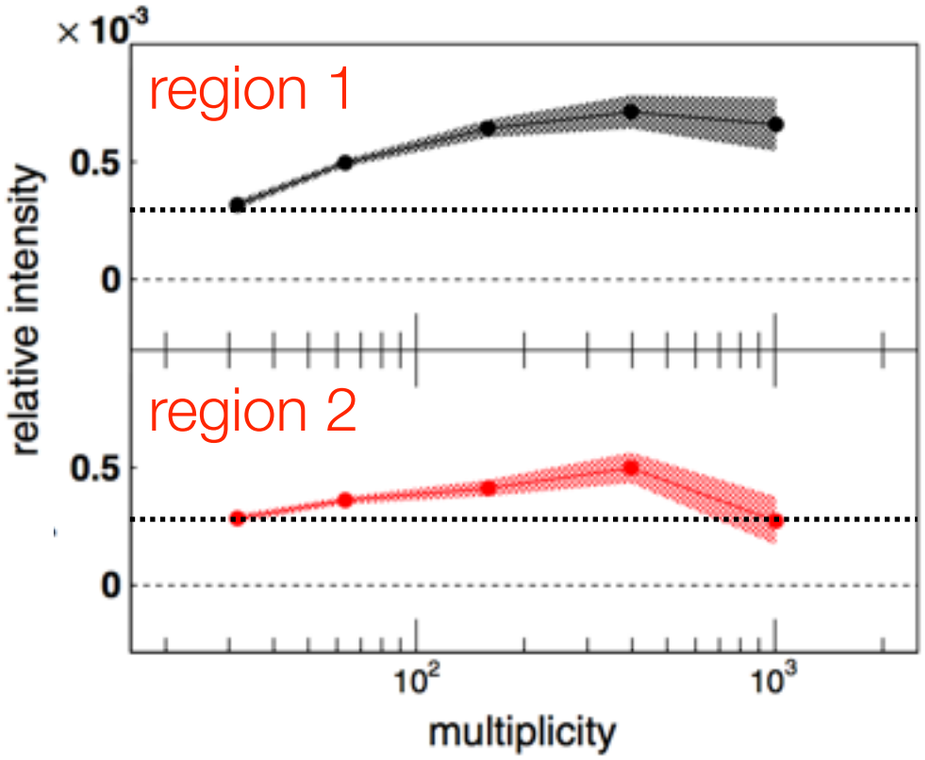

The IceCube Collaboration

Collaborating Organizations

Chiba University
Clark Atlanta University
Deutsches Elektronen-Synchrotron
Ecole Polytechnique Fédérale de Lausanne
Georgia Institute of Technology
Humboldt Universität
Lawrence Berkeley National Laboratory
Ohio State University
Pennsylvania State University
Ruhr-Universität Bochum
RWTH Aachen University
Southern University and A&M College
Stockholm University
Stony Brook University
Sungkyunkwan University
Technische Universität München
Universität Bonn
Universität Dortmund
Universität Mainz
Universität Wuppertal
Université libre de Bruxelles
Université de Mons
University of Adelaide
University of Alabama
University of Alberta
University of Alaska Anchorage
University of California-Berkeley
University of California-Irvine
University of Canterbury
University of Delaware
University of Geneva
University of Gent
University of Kansas
University of Maryland
University of Oxford
University of Wisconsin-Madison
University of Wisconsin-River Falls
Uppsala Universitet
Vrije Universiteit Brussel

growing IceCube
& historical data

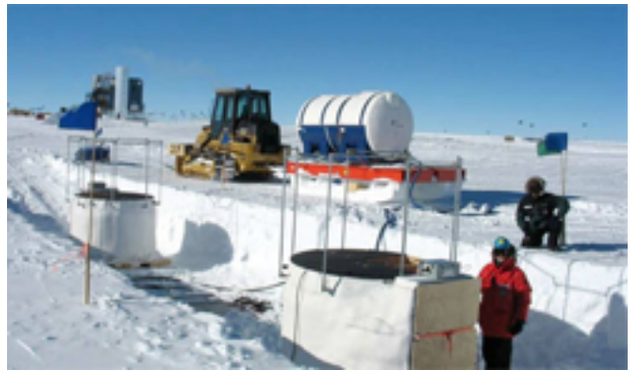

@ 2835 m altitude (680 g/cm²)

Digital Optical Module - DOM
with 10” PMT &
local DAQ electronics

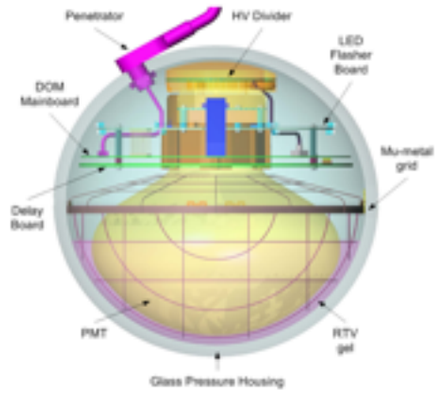

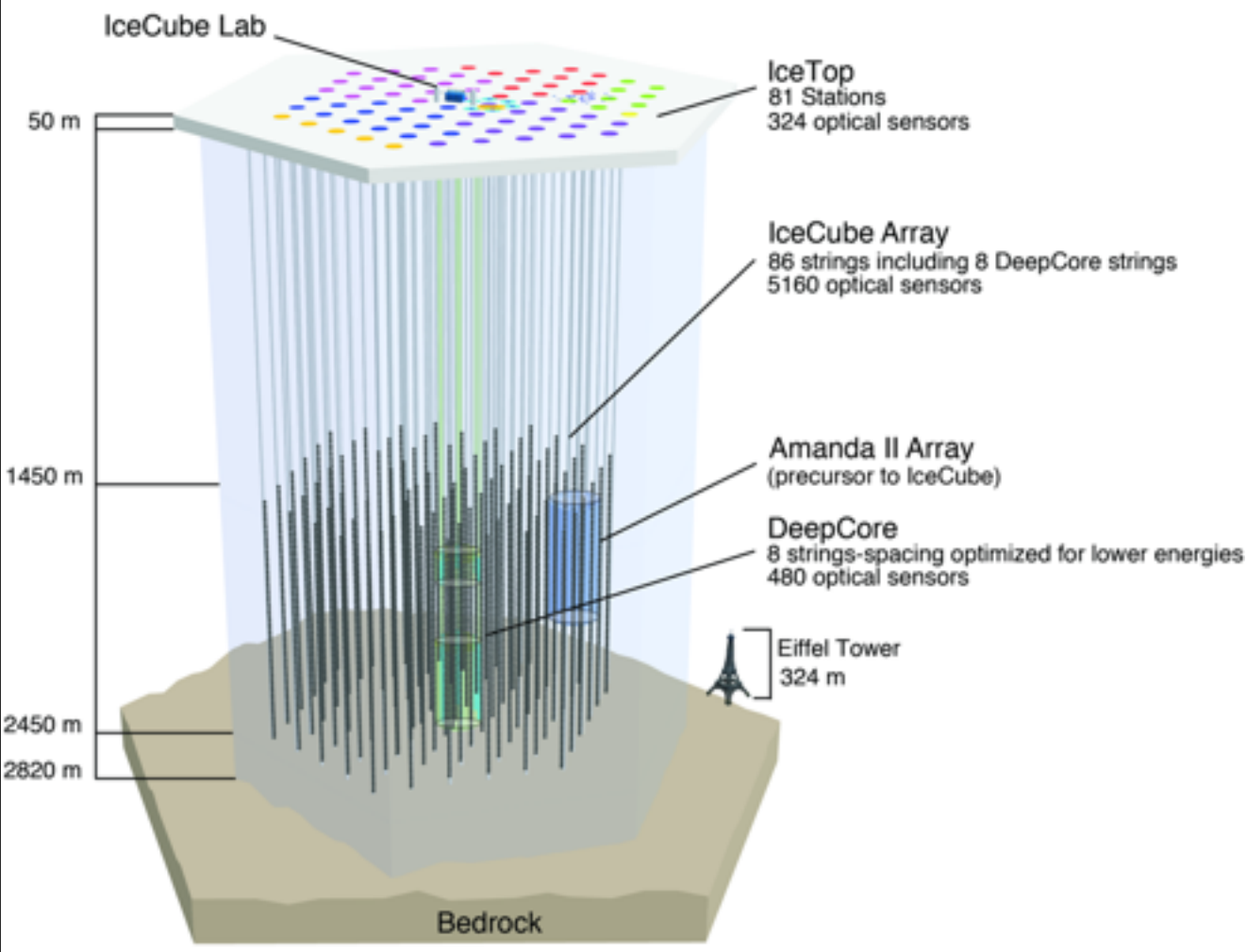

AMANDA - μ bundle rate (>1 TeV) ~**100 Hz**
2×10^9 events/yr
data from 2000-2006
decommissioned in 2009

IceCube - μ bundle rate (>1 TeV) ~ **2.2 kHz**
7×10^{10} events/yr
sensitive to asymmetries $O(10^{-5})$

IceTop - CR shower rate (>200 TeV) ~ **35 Hz**
1×10^9 events/yr
sensitive to asymmetries $O(10^{-4})$

cosmic ray anisotropy large scale
IceCube

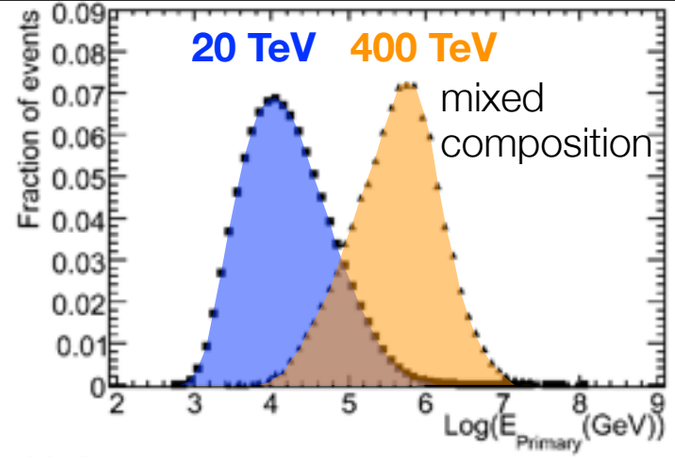

relative intensity equatorial coordinates

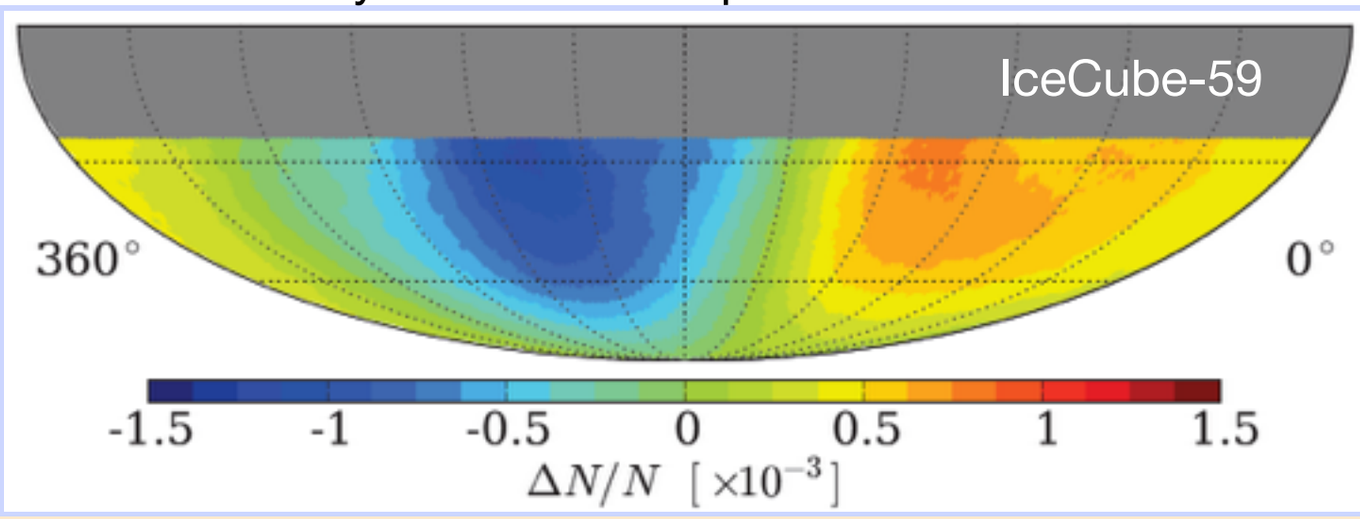

20 TeV

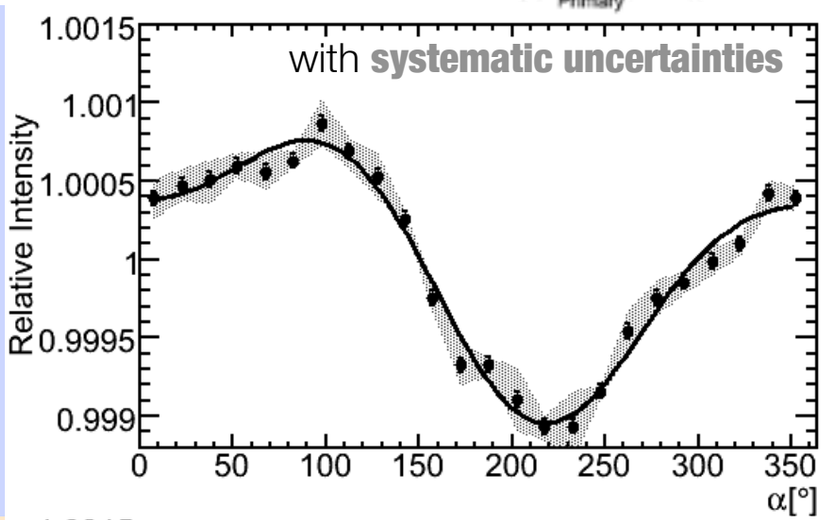

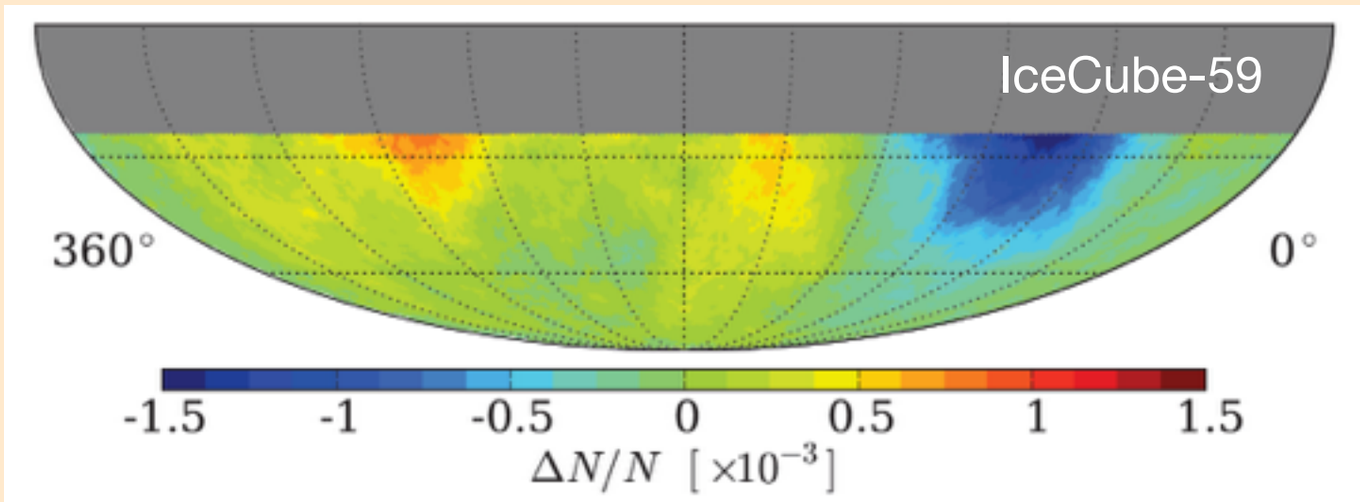

400 TeV

deficit
6.3 σ_{post}

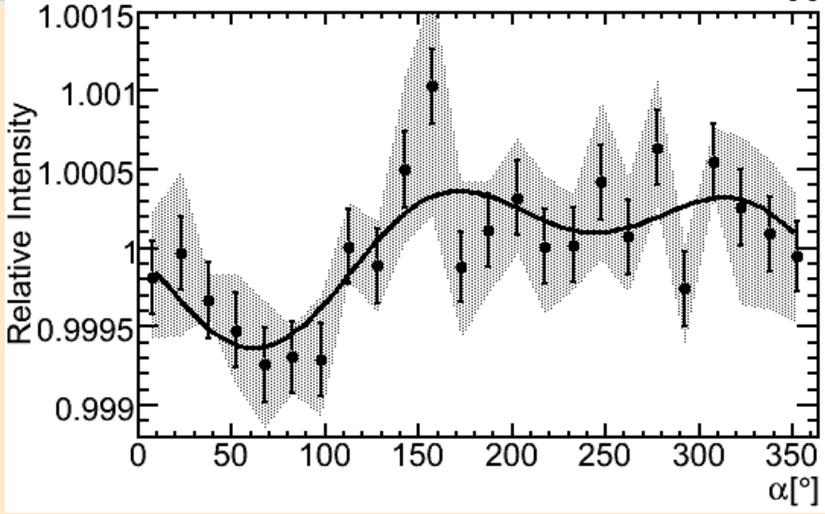

NOTE: anisotropy is **not a dipole**
topology changes above ~ 100 TeV

IC59 Abbasi et al., ApJ, **746**, 33, 2012

IC22 Abbasi et al., ApJ, **718**, L194, 2010

EAS-TOP Aglietta et al., ApJ 692, L130, 2009

a known anisotropy

Earth's motion around the Sun

Compton & Getting, Phys. Rev. 47, 817 (1935)
Gleeson, & Axford, Ap&SS, 2, 43 (1968)

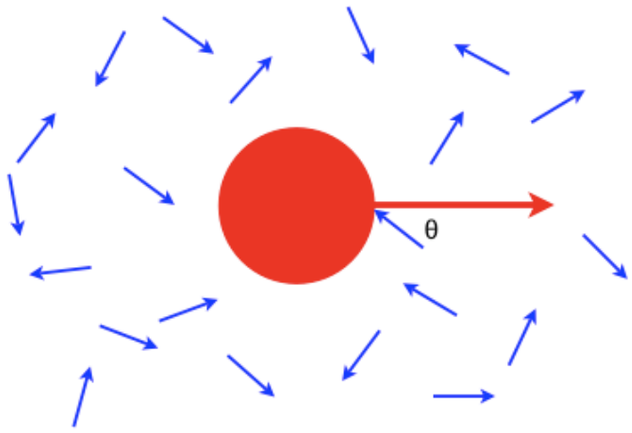

$$\frac{\Delta I}{I} = (\gamma + 2)\frac{v}{c}\cos\theta$$

v = 29.8 ± 0.5 km/s

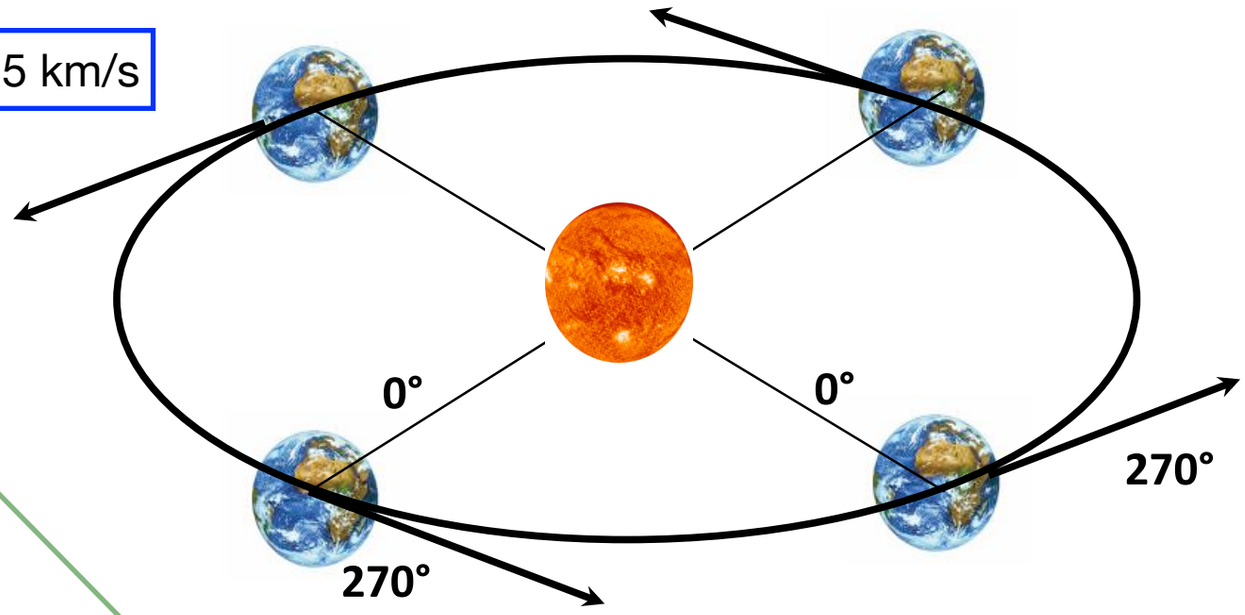

Hörandel, Astrop. Phys. 19, 193, 2003

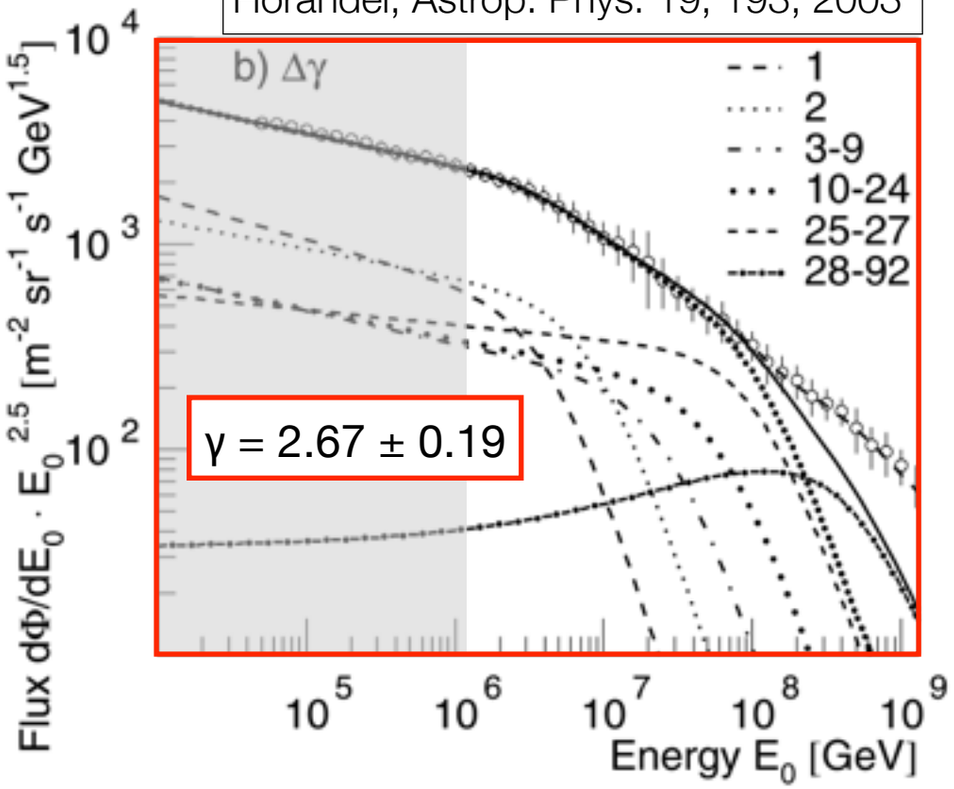

point spread function

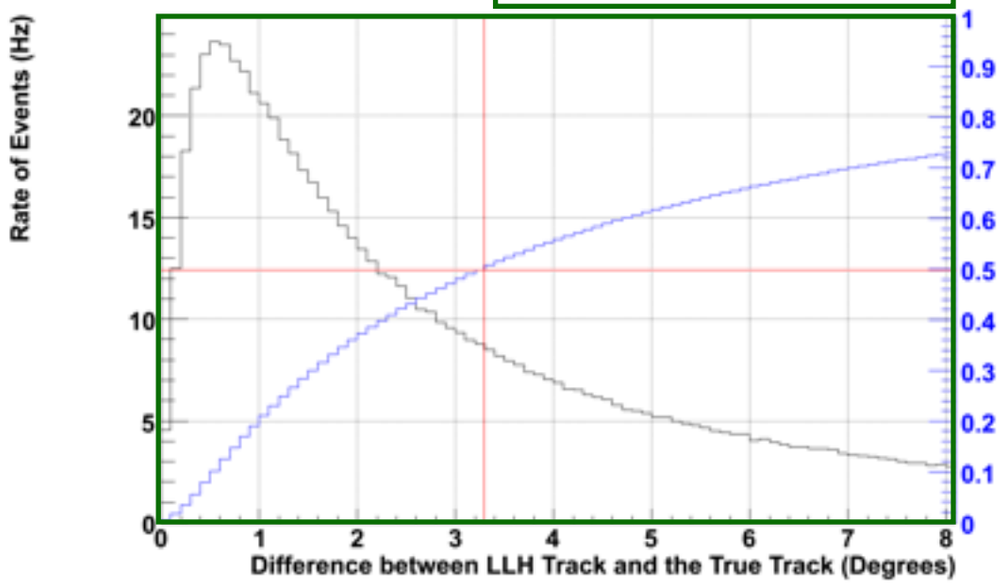

a known anisotropy

Earth's motion around the Sun

- the observation of the **solar dipole** supports the observation of the sidereal anisotropy in cosmic ray arrival direction

- **NO Compton-Getting Effect** signature from galactic rotation observed

relative intensity

α [°] - α_{SUN} [°]

IC59 Abbasi et al., ApJ, **746**, 33, 2012

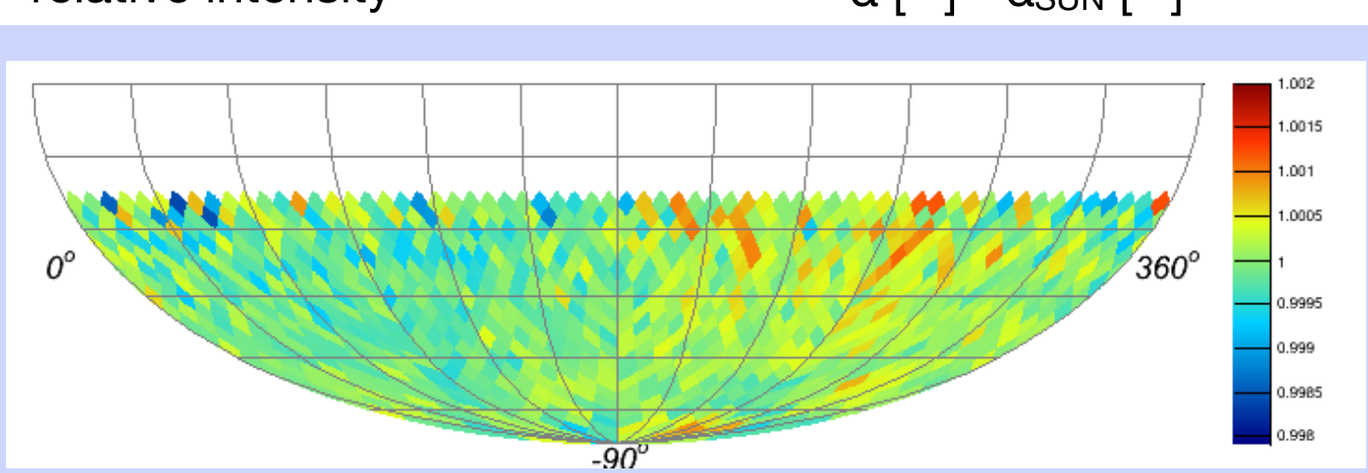

20 TeV

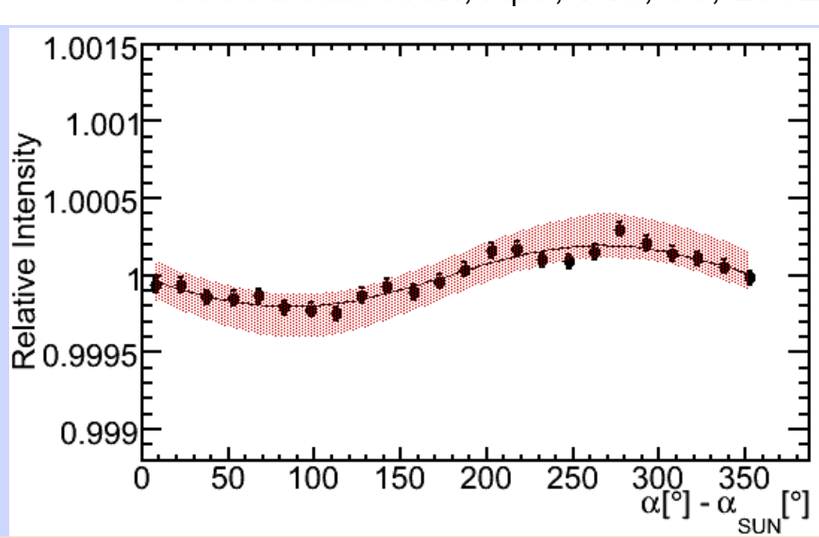

Abbasi et al., ApJ, **746**, 33, 2012

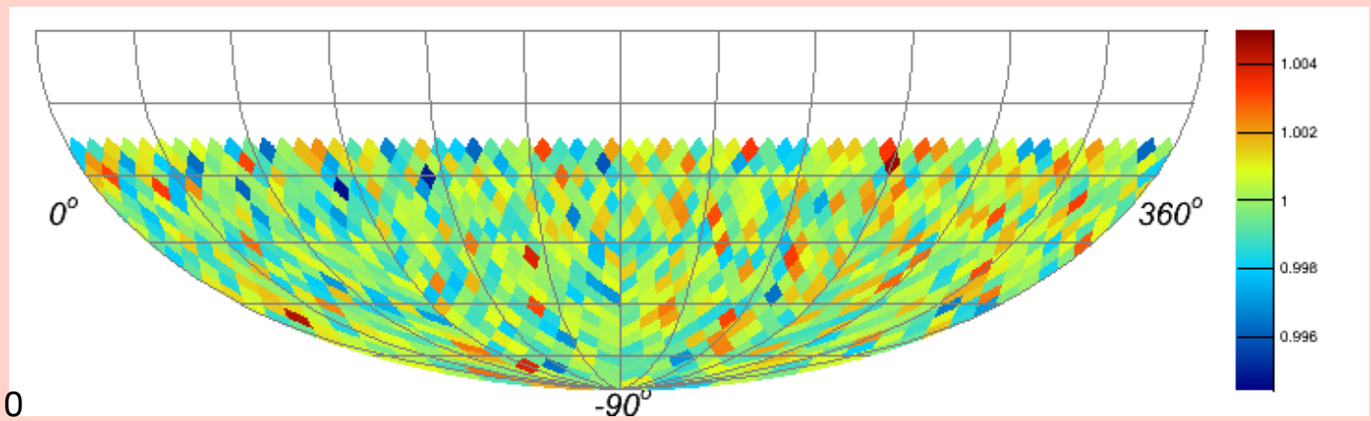

400 TeV

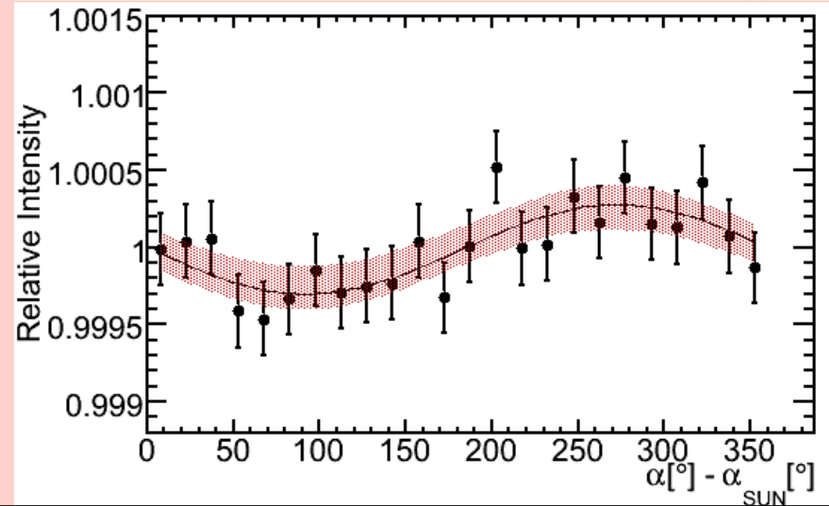

cosmic ray anisotropy large scale IceTop

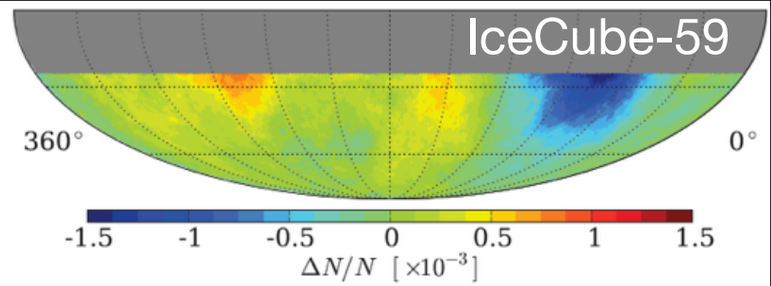

relative intensity equatorial coordinates

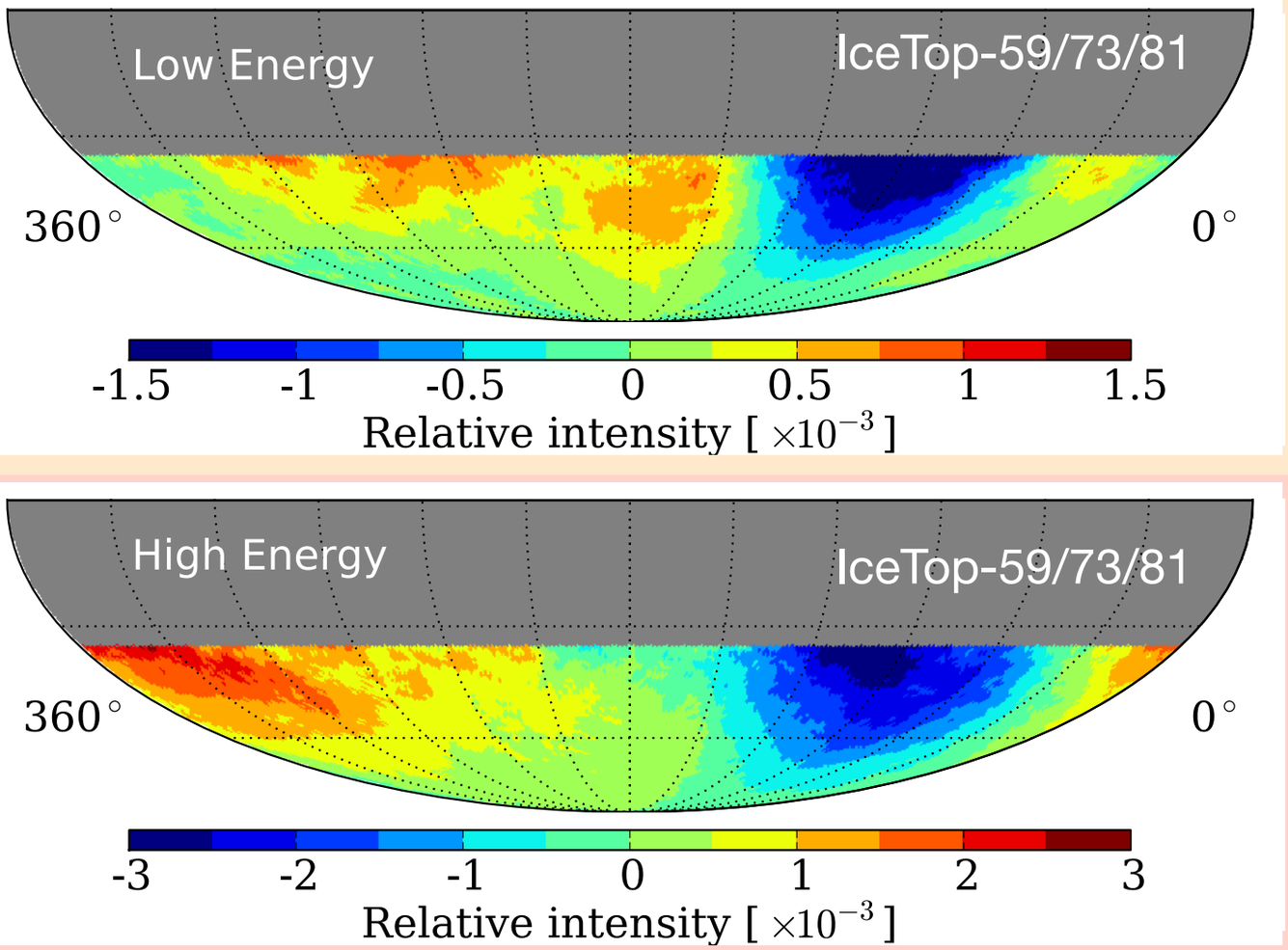

deficit
7 σ_{post}

400 TeV

2 PeV

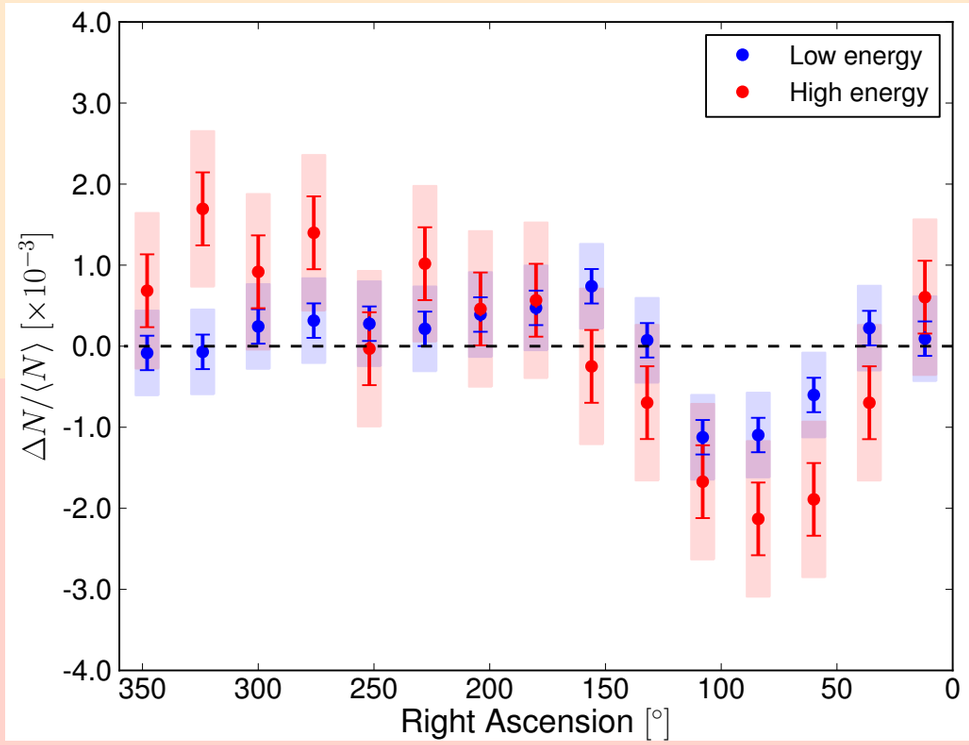

Aartsen et al., ApJ, **765**, 55, 2013

NOTE: global topology does not change above ~400 TeV

deficit amplitude increases with energy

cosmic ray anisotropy

large scale

IceCube IceTop

20 TeV

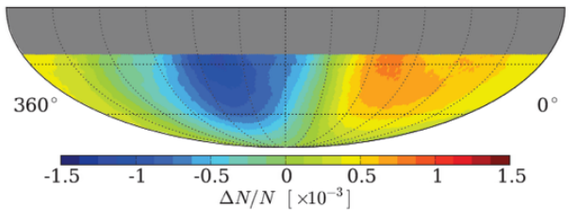

400 TeV

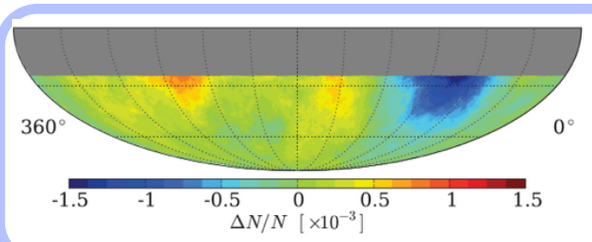

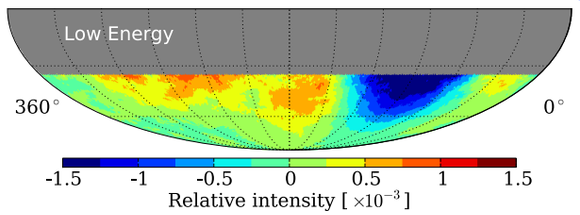

2 PeV

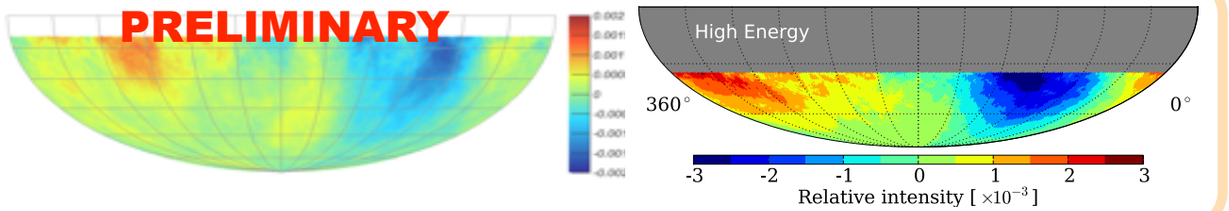

10 PeV

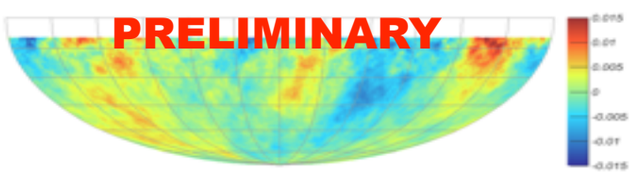

Gaisser, Stanev, Tilav, 2013 - arXiv:1303.3565

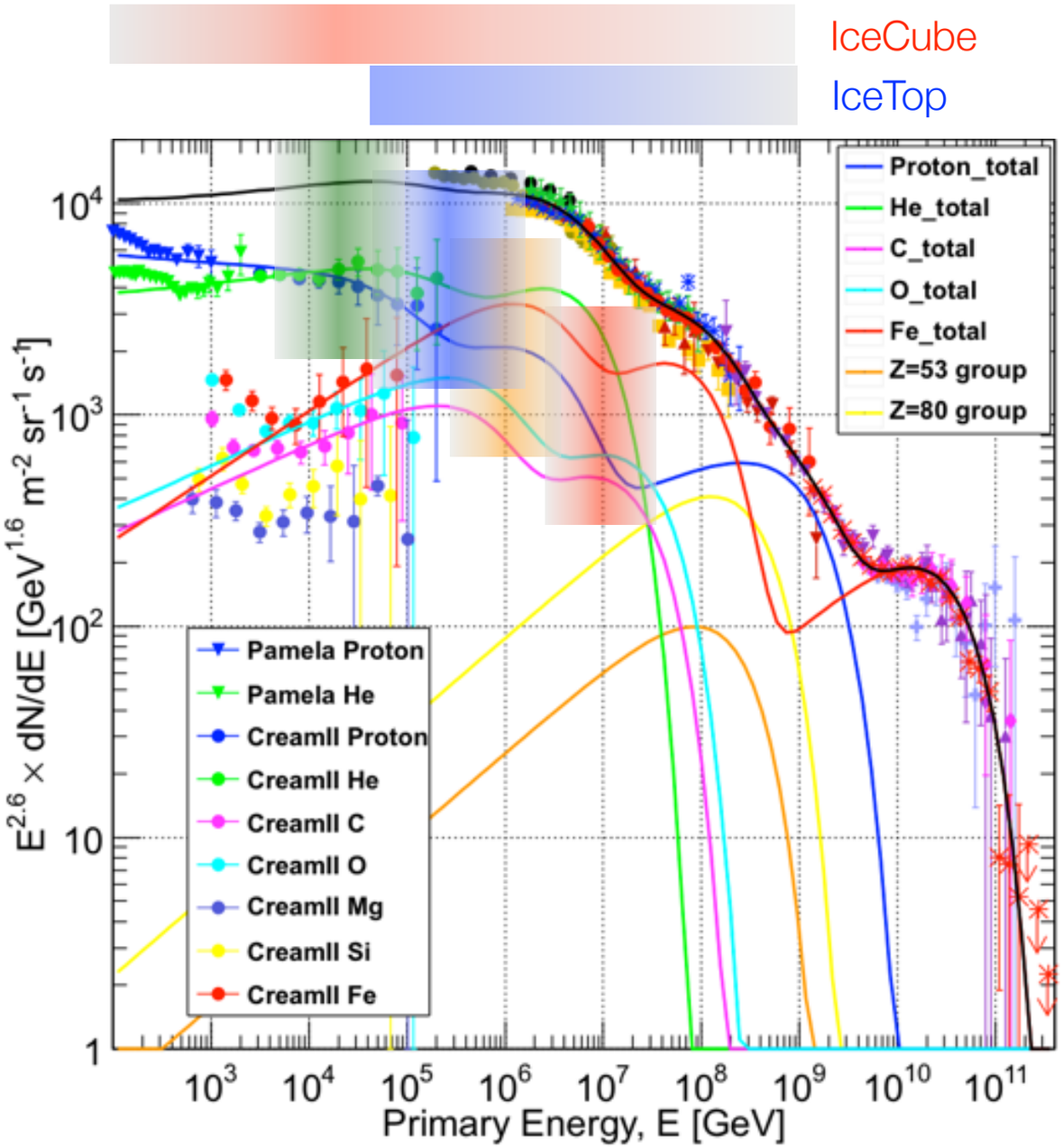

- extend observation above PeV range
- primary mass dependency
- primary spectrum at excess/deficit

cosmic ray anisotropy small scale
IceCube

relative intensity

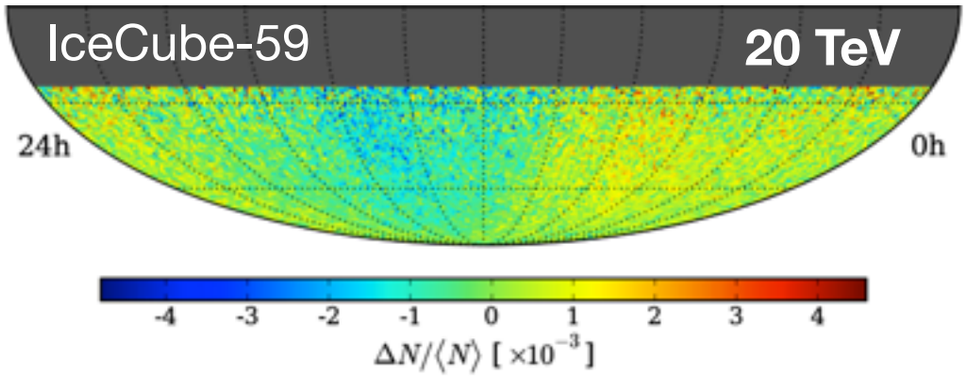

raw map

χ^2/ndf = 14743.4 / 14187 (prob = 0.05%)

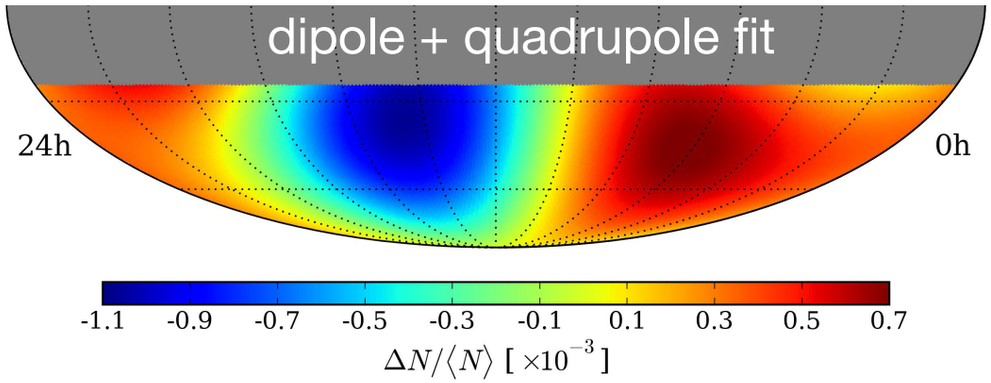

Abbasi et al., ApJ, **740**, 16, 2011

filter high CR density gradient structures

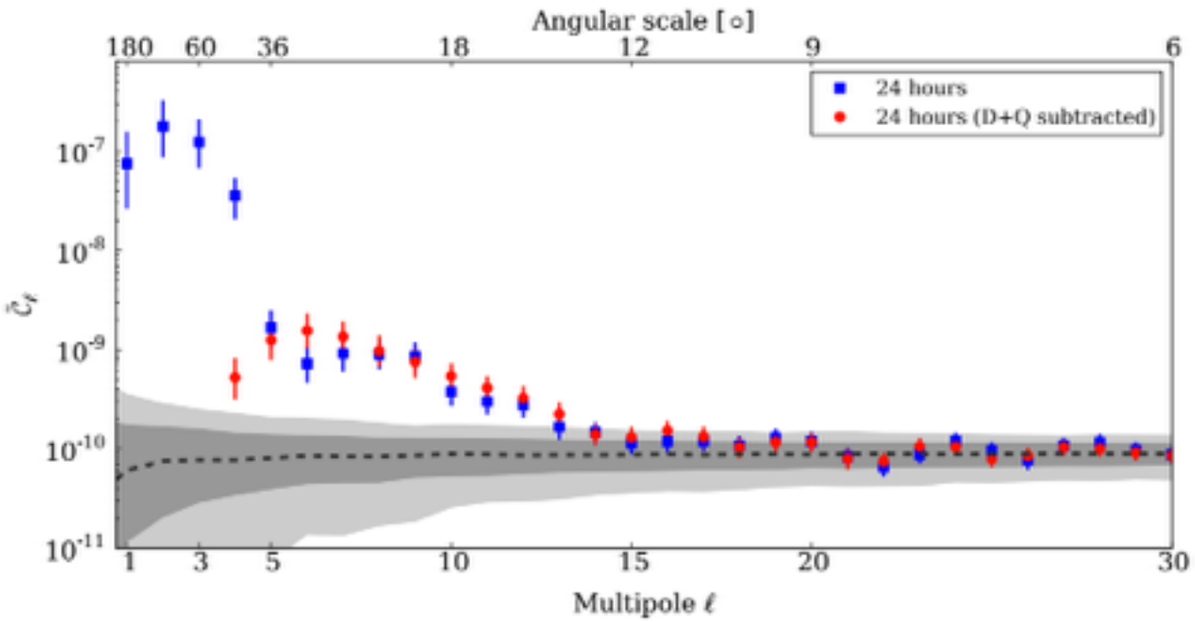

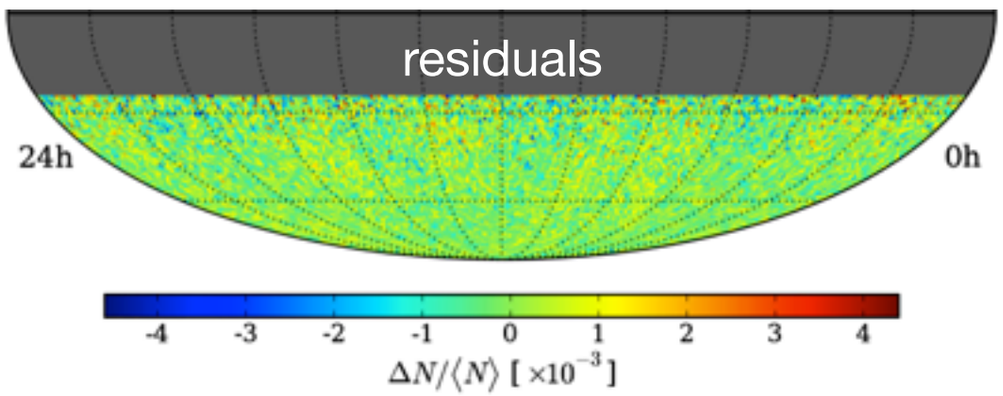

cosmic ray anisotropy

Tibet-III

Amenomori et al., ICRC 2011

5 TeV

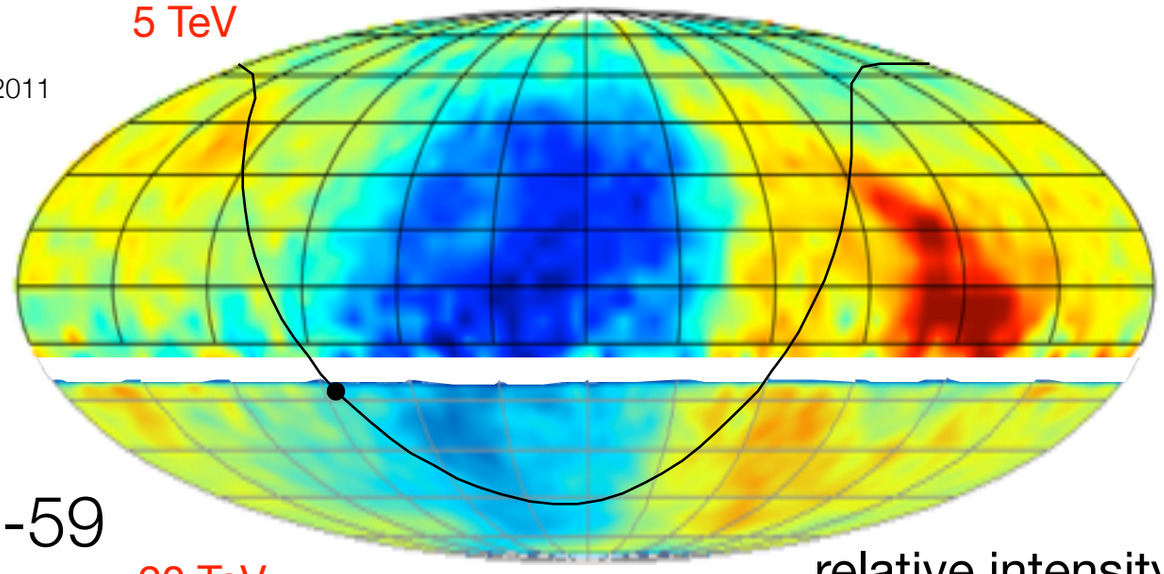

IceCube-59

Abbasi et al., ApJ, **746**, 33, 2012

20 TeV

relative intensity

- full sky map at comparable energy (**IceCube-ARGO/HAWC**)
  - to better determine low ℓ spherical harmonic components
  - to analyze fine angular structures across the sky

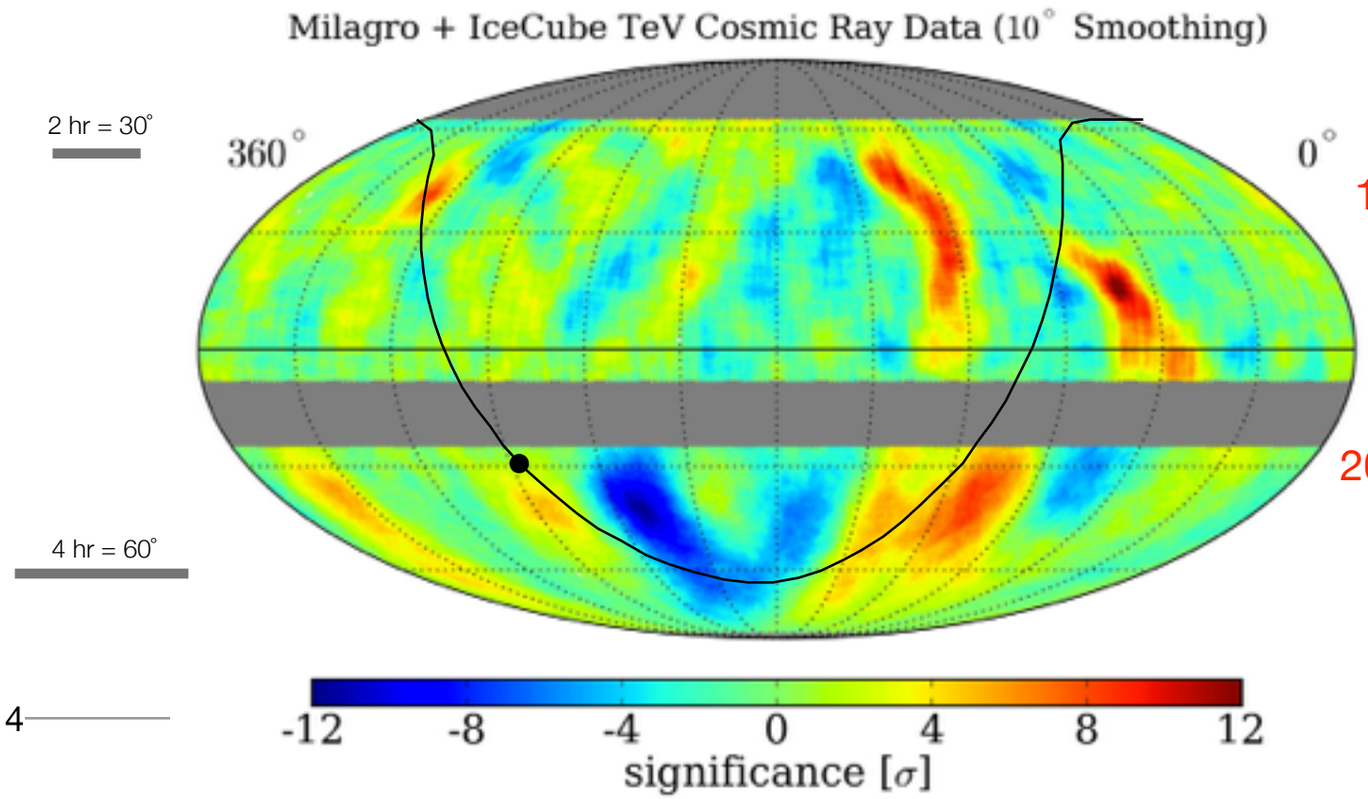

1 TeV

Milagro

Abdo et al., PRL, **101**, 221101, 2008

20 TeV

IceCube-59

Abbasi et al., ApJ, **740**, 16, 2011

equatorial coordinates

cosmic ray anisotropy observations

Bartoli et al. (2013)

ARGO-YBJ

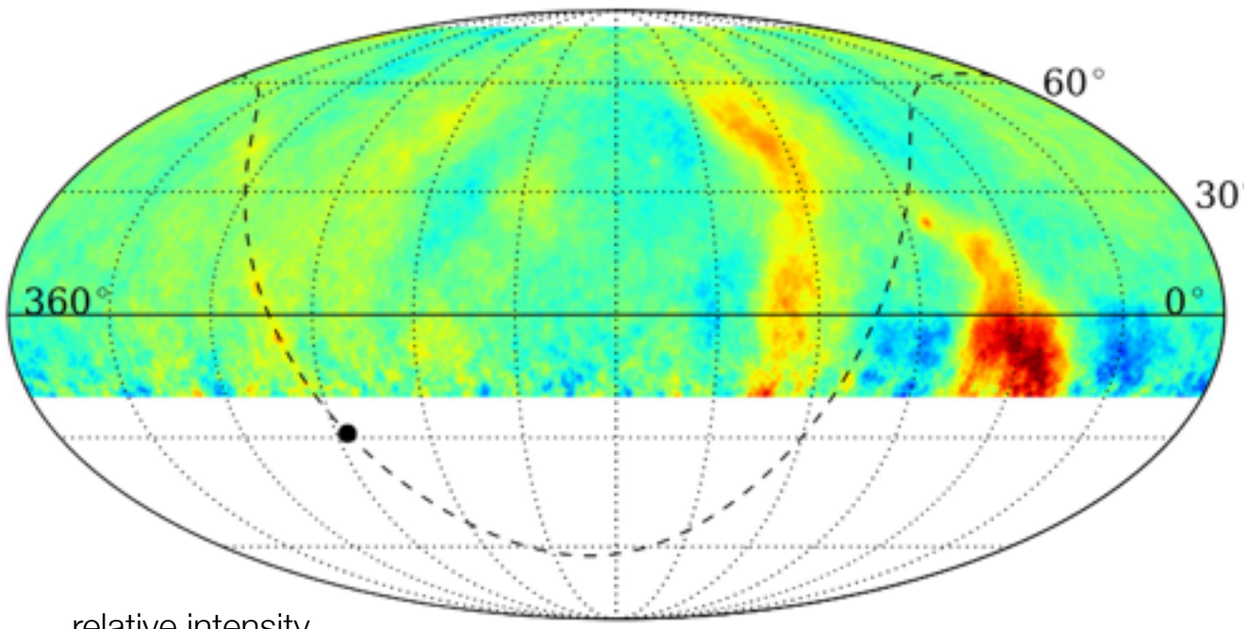

relative intensity

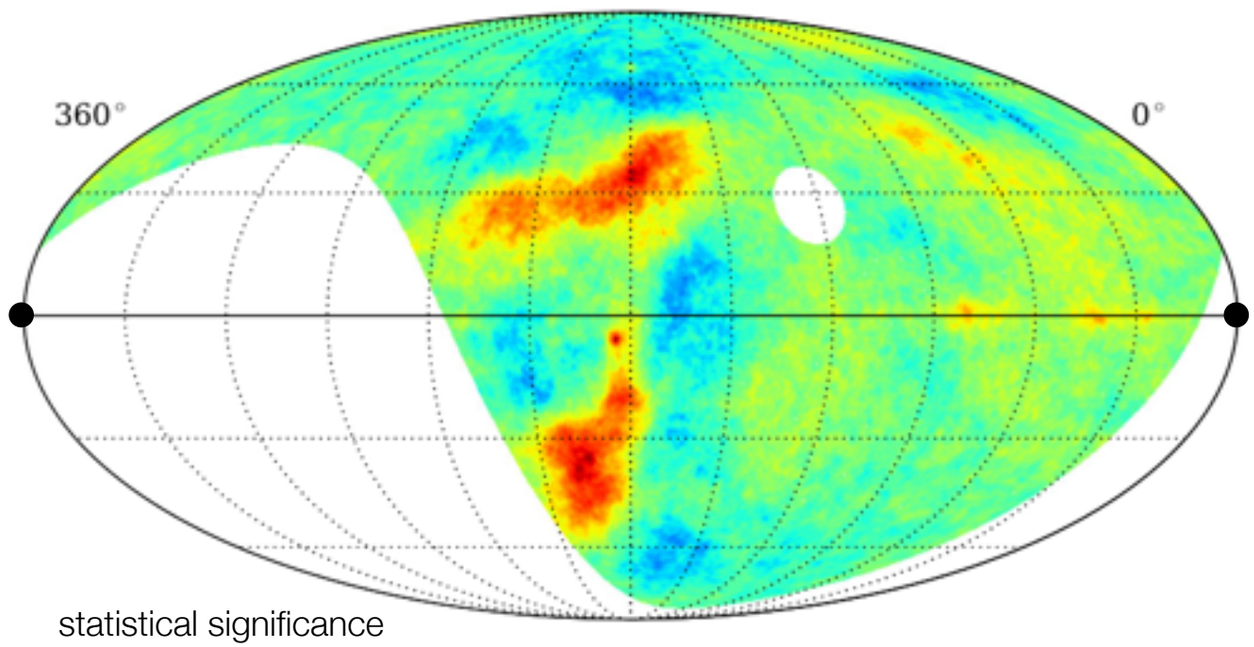

statistical significance

cosmic ray anisotropy

IceCube 2007-2012

PRELIMINARY

relative intensity equatorial coordinates

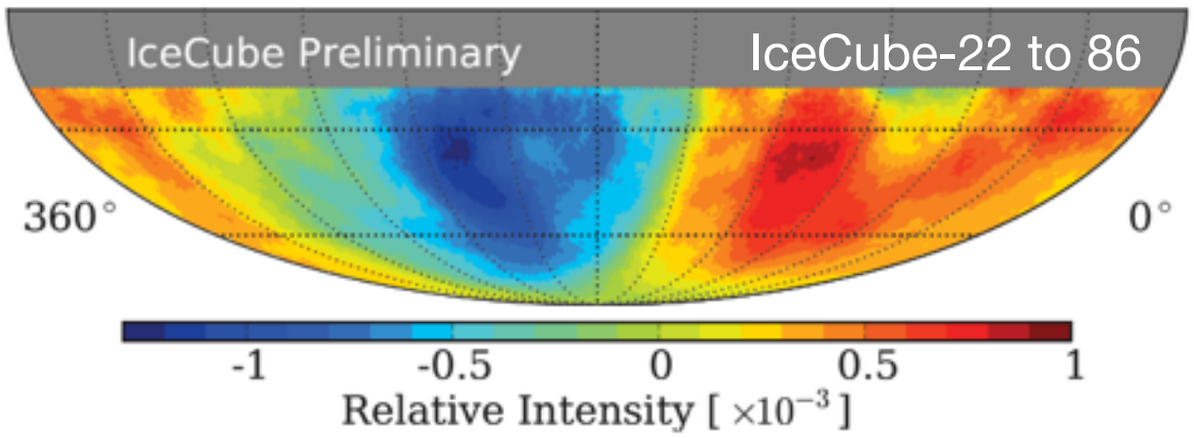

- 1.4×10^{11} events from 2007 to 2012
- sensitivity to **5° structures** with relative intensity of **O(10^{-4})**

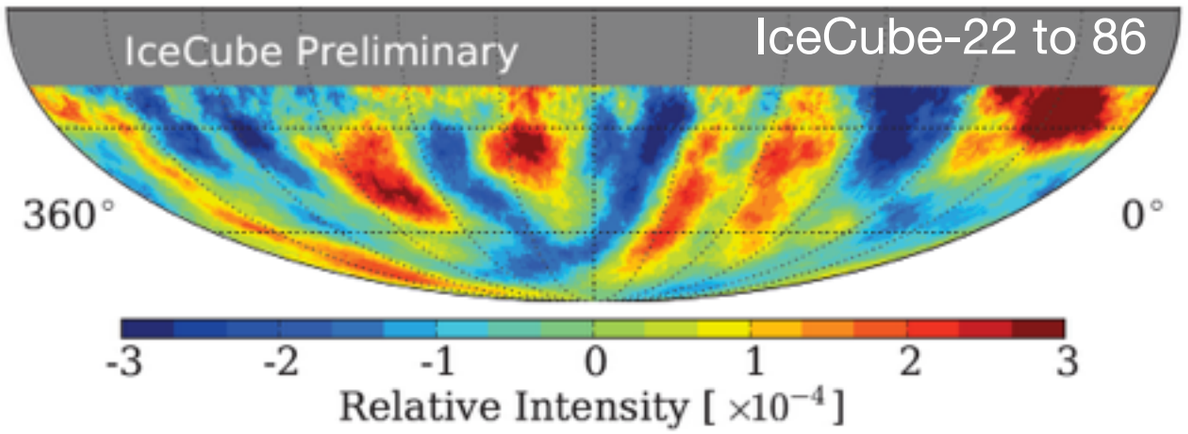

5° smoothing

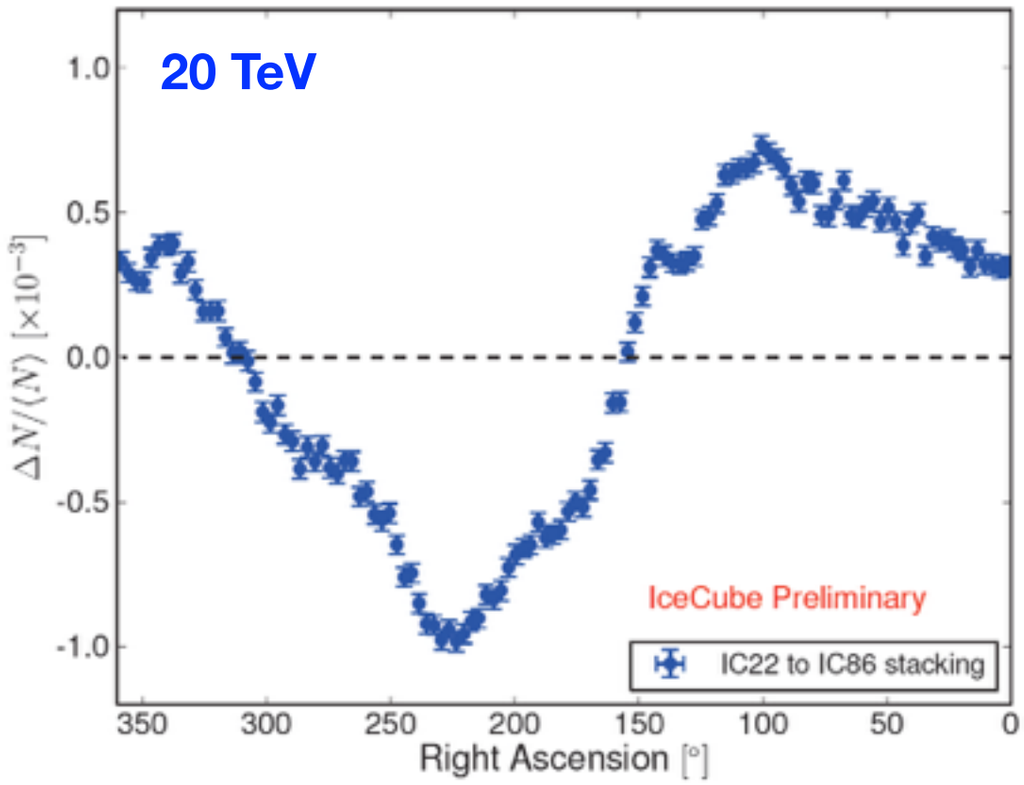

cosmic ray anisotropy

AMANDA-IceCube 2000-2011

PRELIMINARY

20 TeV

relative intensity equatorial coordinates

AMANDA

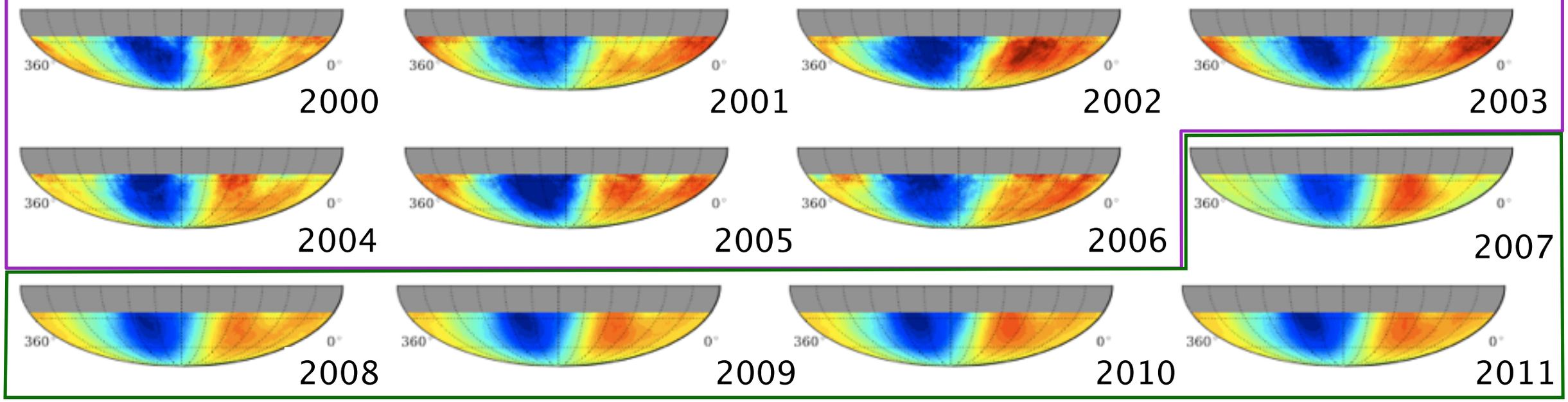

IceCube

- AMANDA and IceCube yearly data show long **time-scale stability** of global anisotropy within statistical uncertainties

  - no apparent effect correlated to solar cycles

cosmic ray anisotropy

AMANDA-IceCube 2000-2011

PRELIMINARY

20 TeV

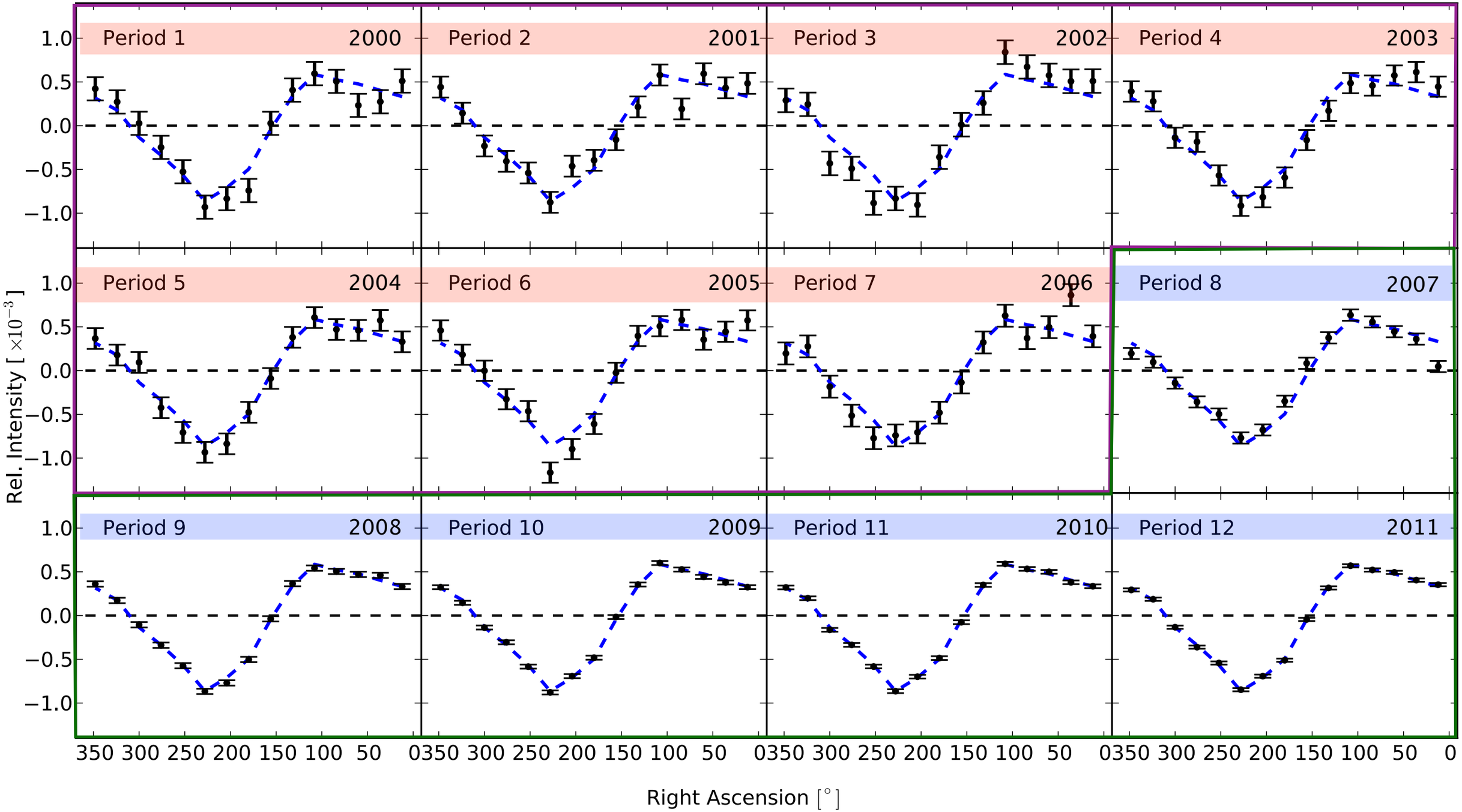

cosmic ray anisotropy

probing sources & propagation of cosmic rays ?

- stochastic effect of **nearby & recent sources** & temporal correlations

Erlykin & Wolfendale, Astropart. 2006

Blasi & Amato, 2011

Ptuskin+, 2012

Pohl & Eichler, 2012

Sveshnikova+, 2013

dipole amplitude

Sveshnikova+, 2013

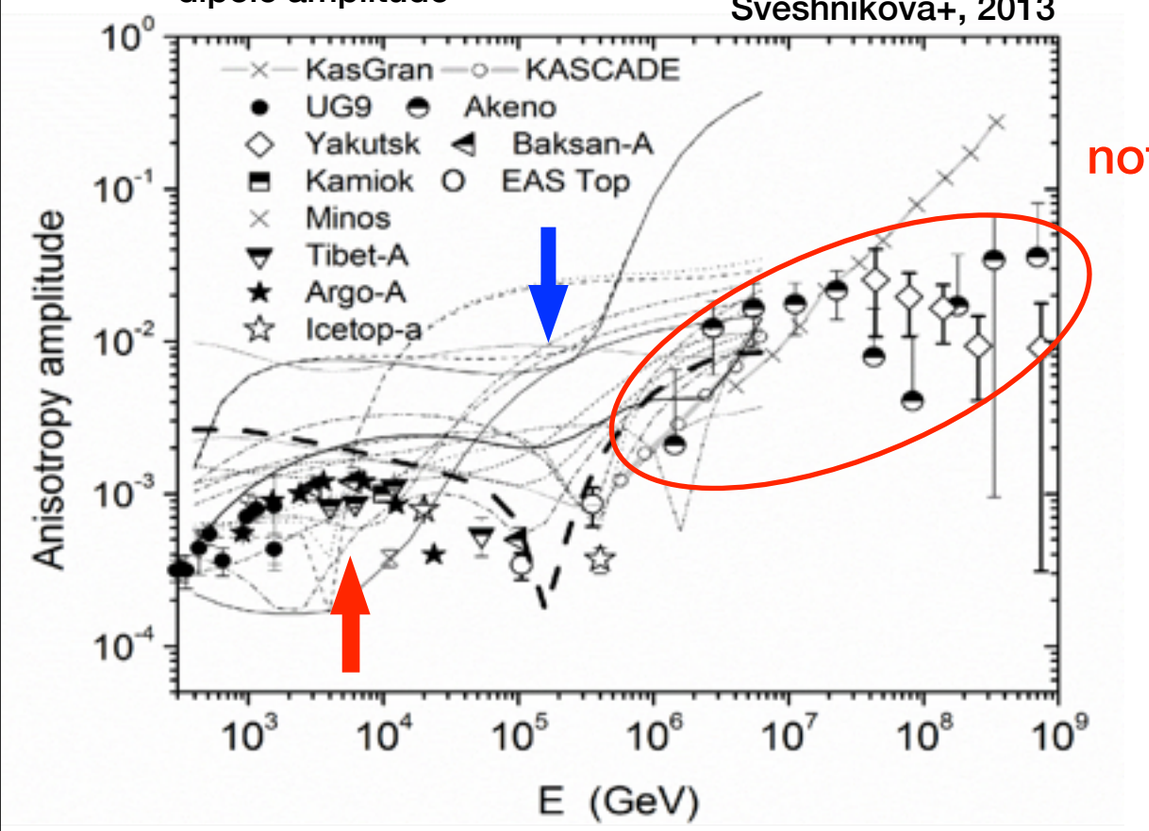

not dipole observations

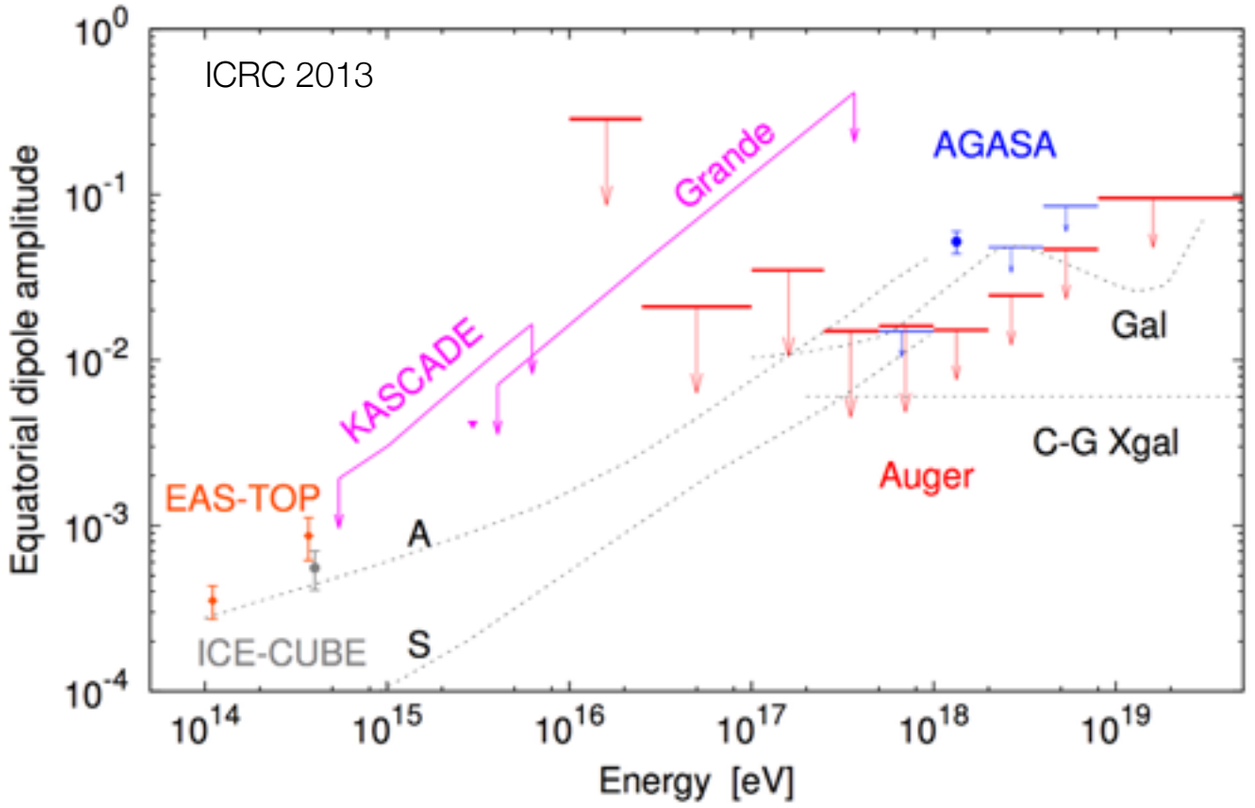

dipole components of the anisotropy

cosmic ray anisotropy

probing magnetic field turbulence ?

- propagation effect from turbulent realization of interstellar magnetic field within scattering mean free path

Giacinti & Sigl, 2012

Biermann+, 2012

Yan & Lazarian, 2008

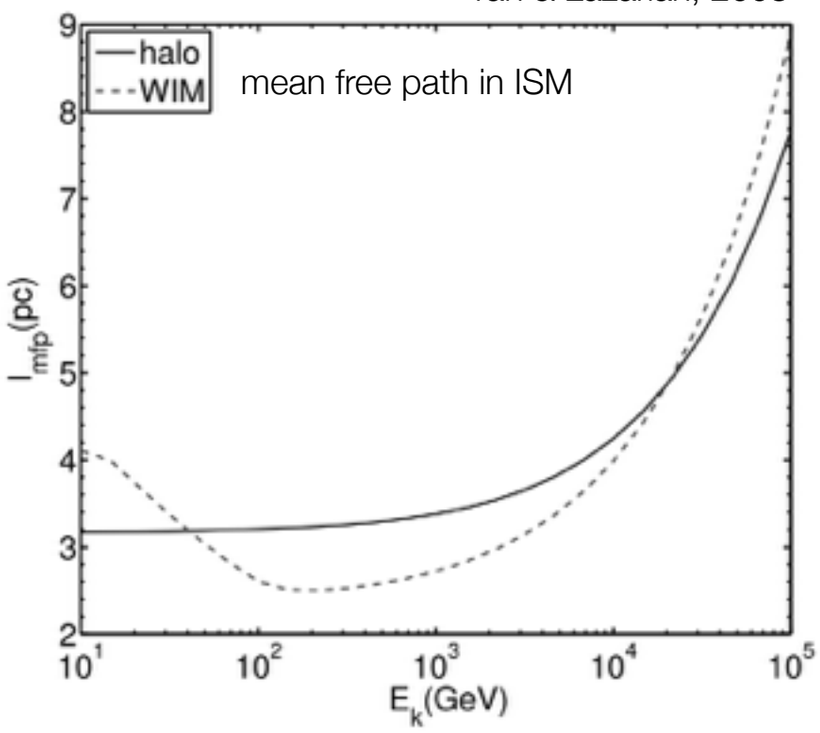

Giacinti & Sigl, 2012

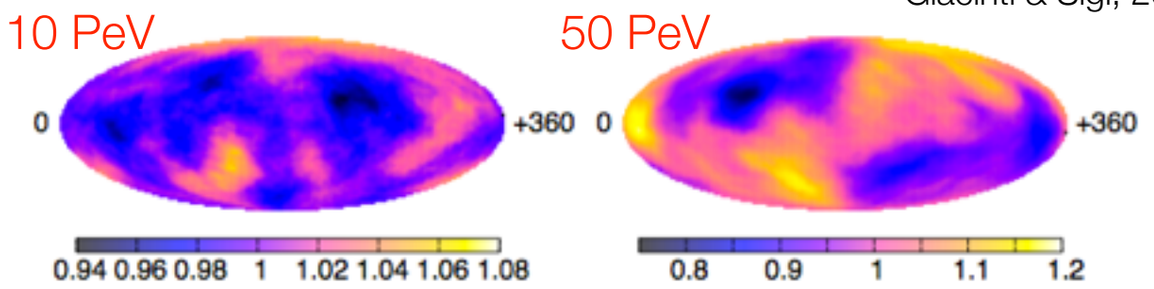

FIG. 1. Renormalized CR flux predicted at Earth for a concrete realization of the turbulent magnetic field, *after subtracting the dipole* and smoothing on 20° radius circles. Primaries with rigidities $p/Z = 10^{16}$ eV (*left panel*) and 5×10^{16} eV (*right panel*). See text for the field parameters and boundary conditions on the sphere of radius $R = 250$ pc.

cosmic ray anisotropy
probing magnetic field turbulence ?

- propagation effect from turbulent realization of interstellar magnetic field within scattering mean free path

Ahlers, 2014

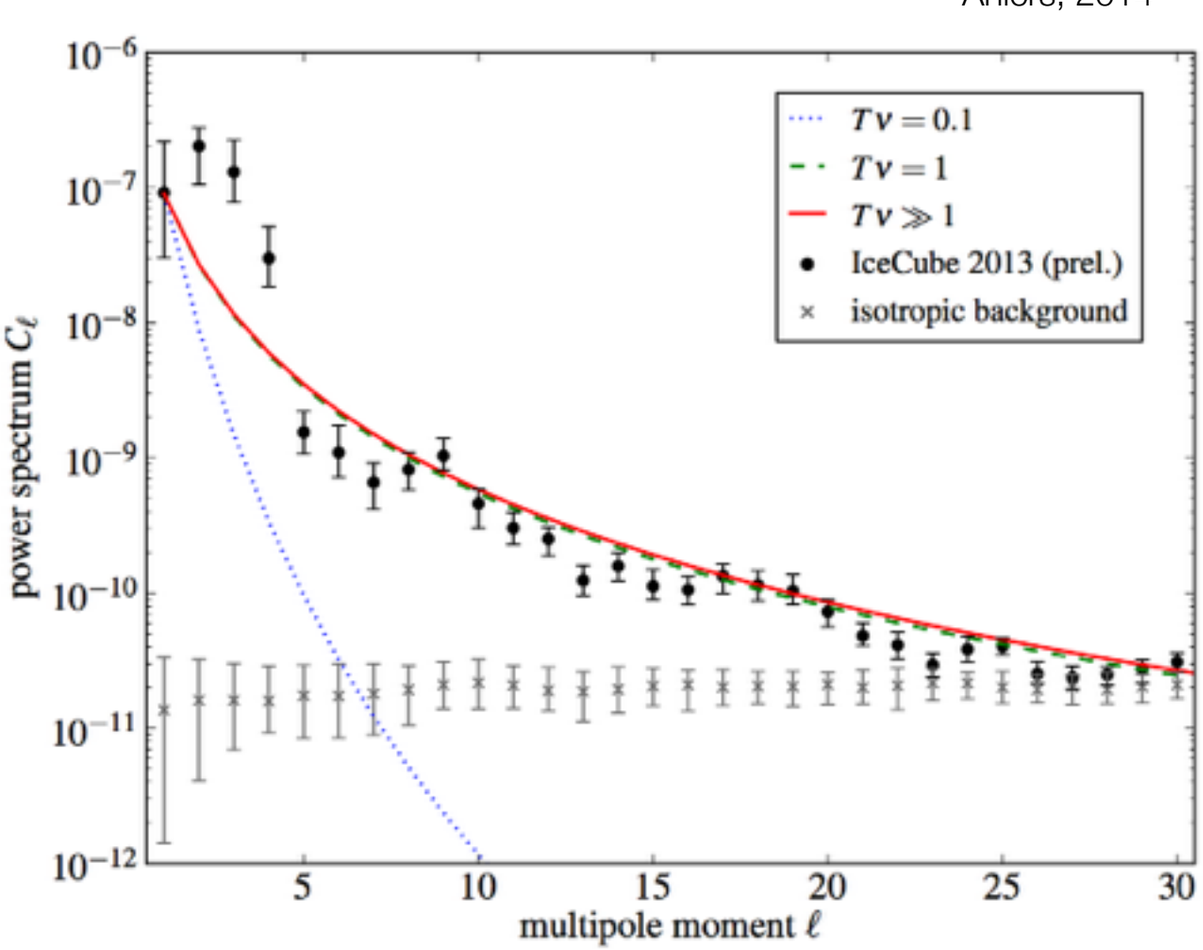

anomalous anisotropy structure spontaneously generated from a global dipole anisotropy as a consequence of Liouville Theorem in the presence of a local turbulent magnetic field

cosmic ray anisotropy
probing diffusion properties

anisotropic diffusion

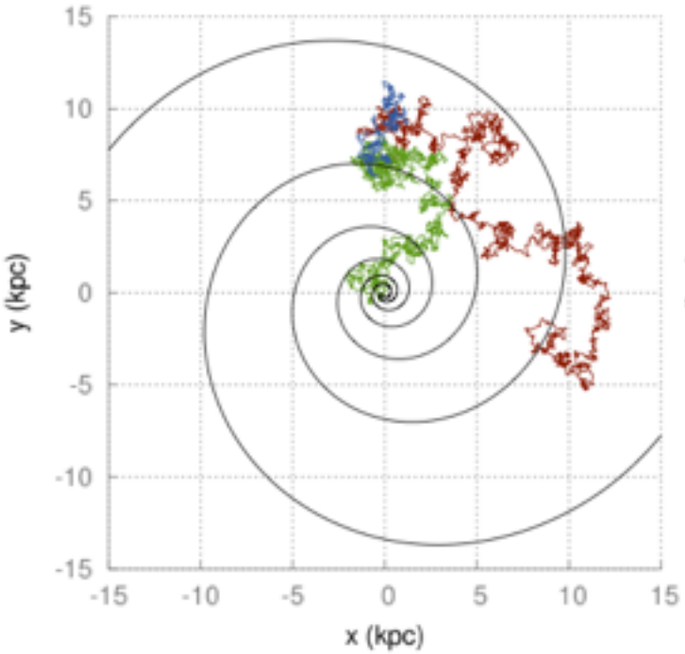

Effenberger+, 2012

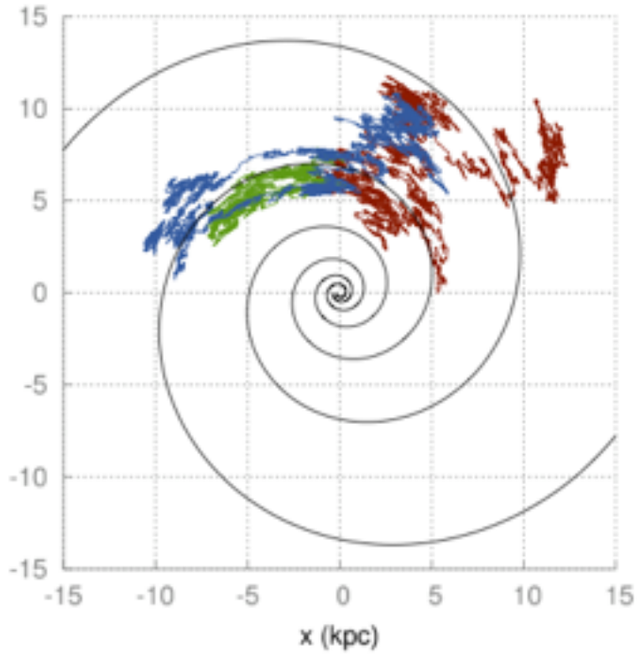

- diffusion coefficient hardly a single power law, homogeneous and isotropic

Kumar & Eichler, 2014

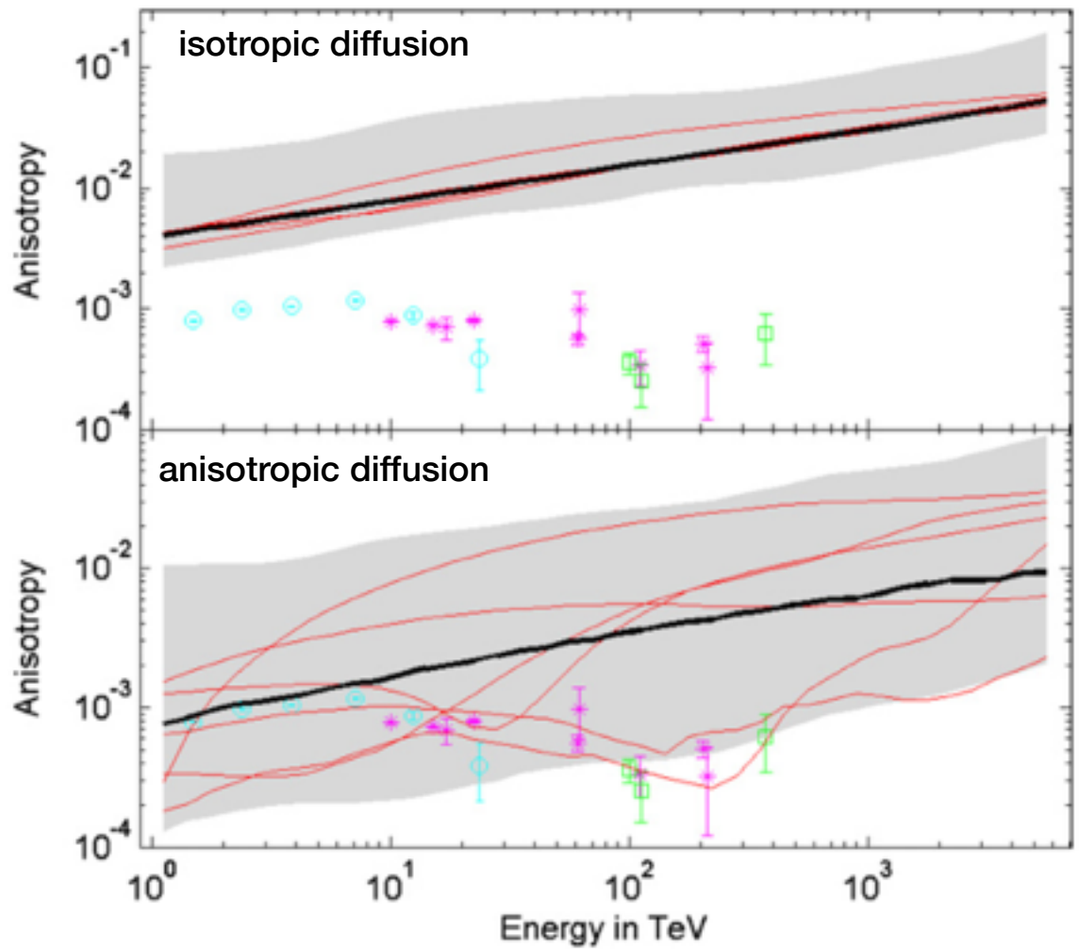

cosmic ray anisotropy
local interstellar medium

local ISMF shaped by LOOP I expansion sub-shell (with center ~60 pc away in Scorpius-Centaurus OB Association)

local cloudlets fragments of the shell moving at similar velocities

14 pc - Frisch+, 2011

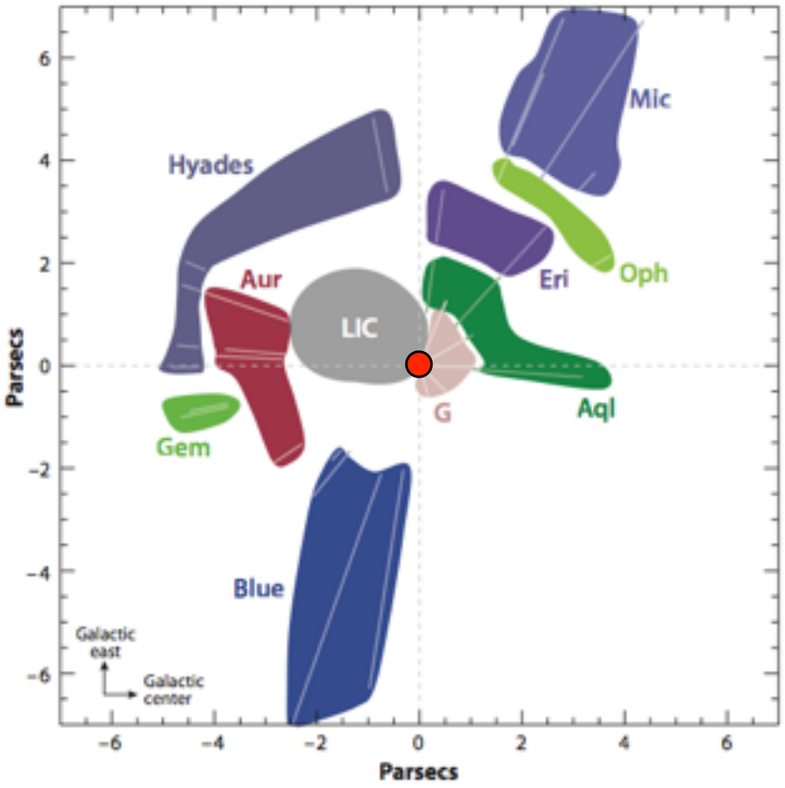

100 pc - Wolleben, 2007

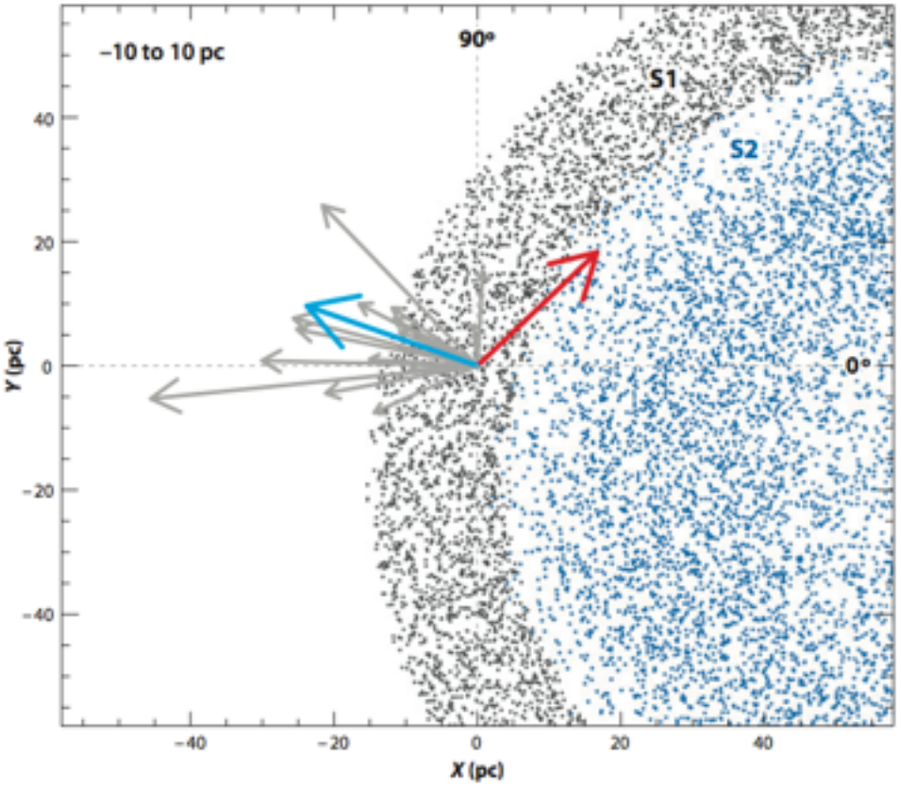

500 pc - (Priscilla Frisch)

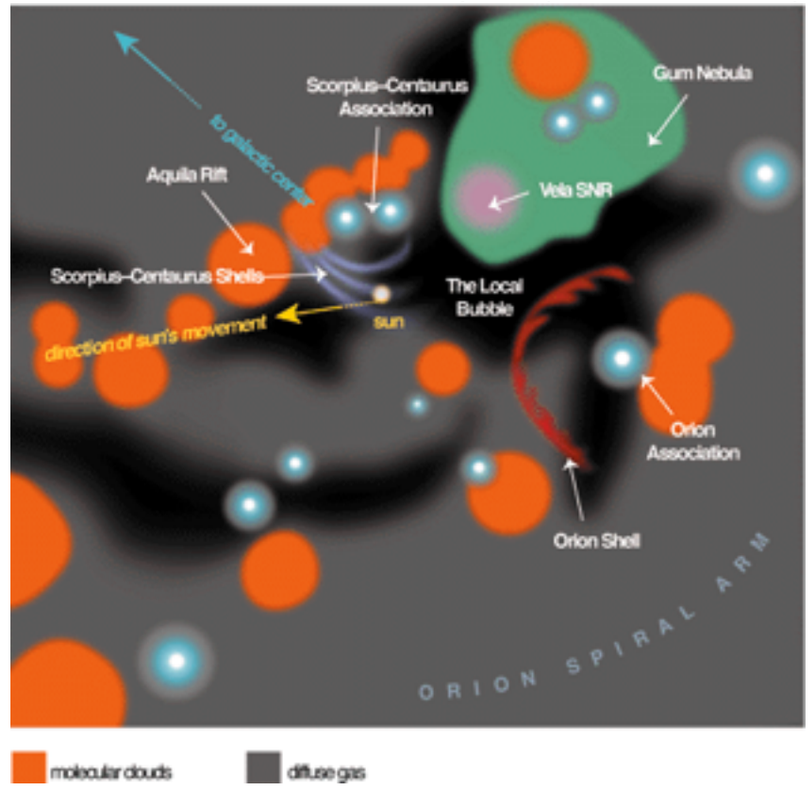

- interstellar magnetic field affected by inhomogeneities — Redfield & Linsky, 2008; Frisch+, 2011
- local ISMF relatively uniform over spacial scales of order 60-100 pc (**inter-arm**) — Frisch+, 2012

cosmic ray anisotropy
heliosphere

$$r_L \approx \frac{200}{Z} \frac{E(TeV)}{B(\mu G)} AU$$

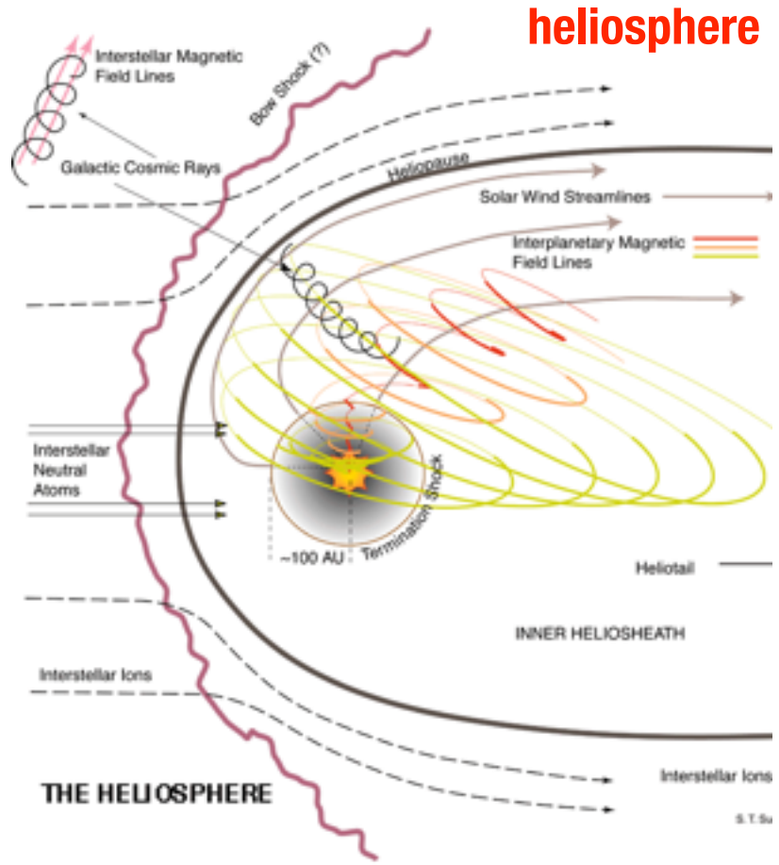

heliotail

local ISMF draping around heliosphere

Pogorelov+ 2011

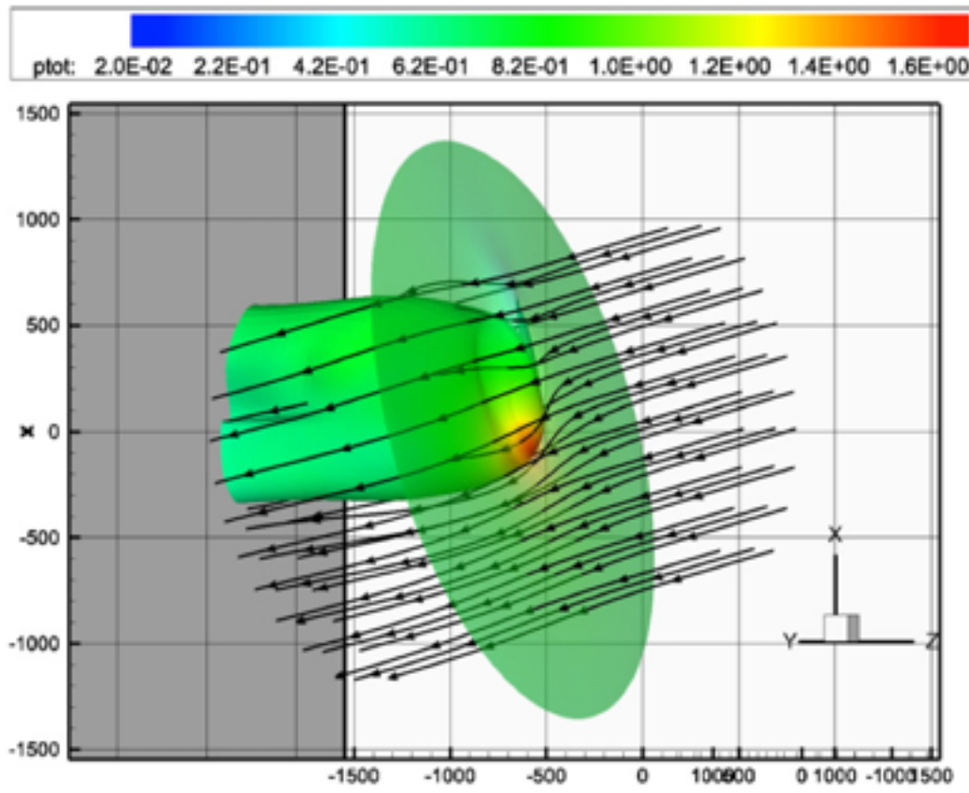

- heliosphere as O(100-1000) AU **magnetic perturbation of local ISMF** PD & Lazarian, 2013
- influence on ≲ 10 TeV protons (R_L ≲ 600 AU)
- cosmic rays >100's TeV influenced by interstellar magnetic field (**change of anisotropy**)

scattering at heliospheric boundary
heuristic model

- resonant scattering to **re-direct** CR distribution
- **back-scattering** @ flanks back from downstream

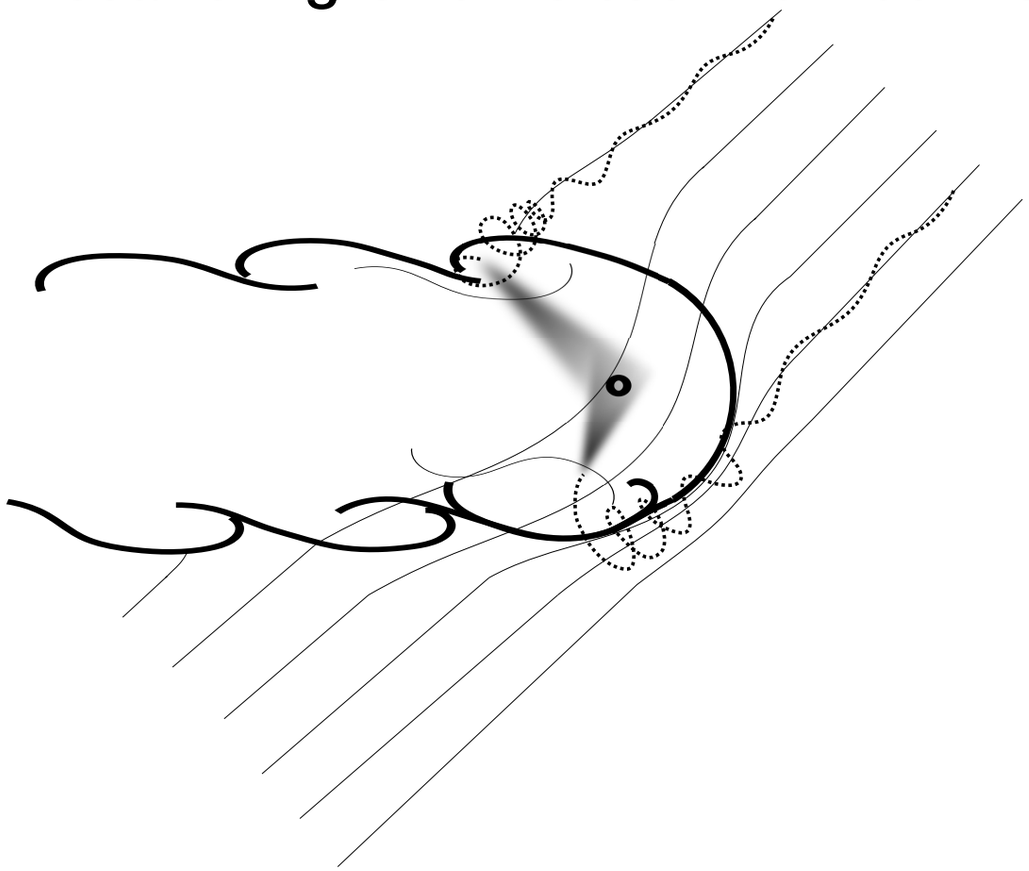

PD & Lazarian 2013

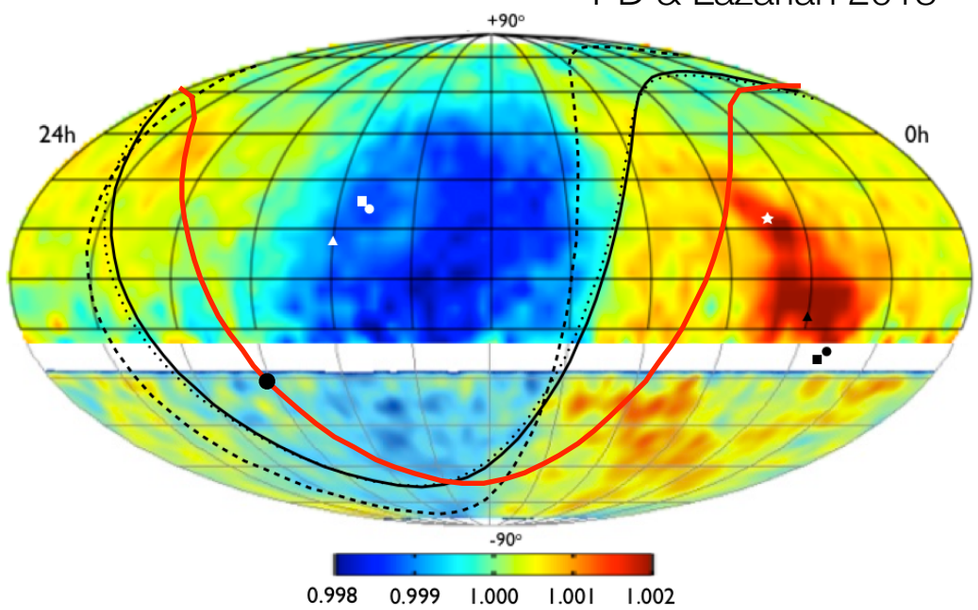

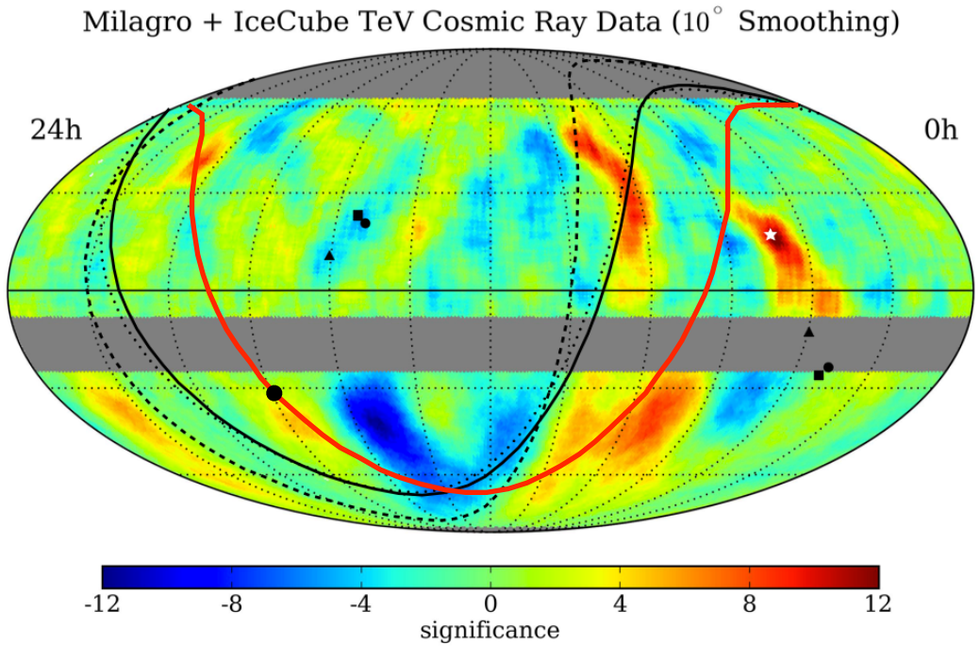

- global anisotropy with **large edge gradients**
- magnetic reconnection

Lazarian & PD 2010
PD & Lazarian 2012

anisotropy and local galactic environment
low to high energy connection

- IBEX observations of keV Energetic Neutral Atoms
- determination of interstellar flow direction
- determination of interstellar magnetic field direction
- investigating the role of heliospheric turbulence

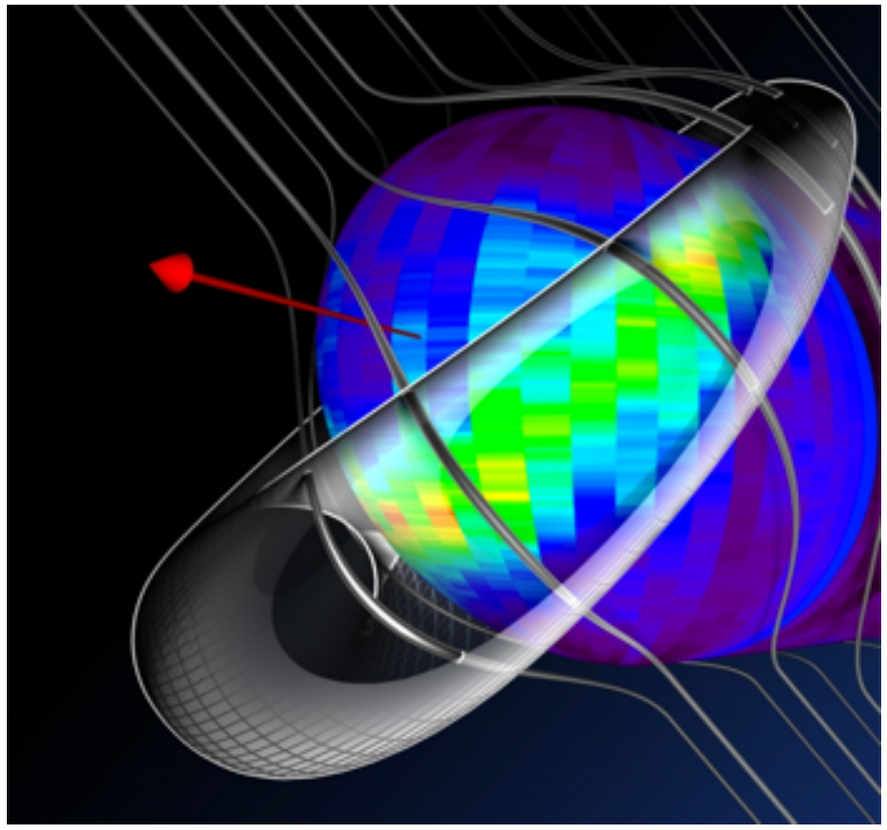

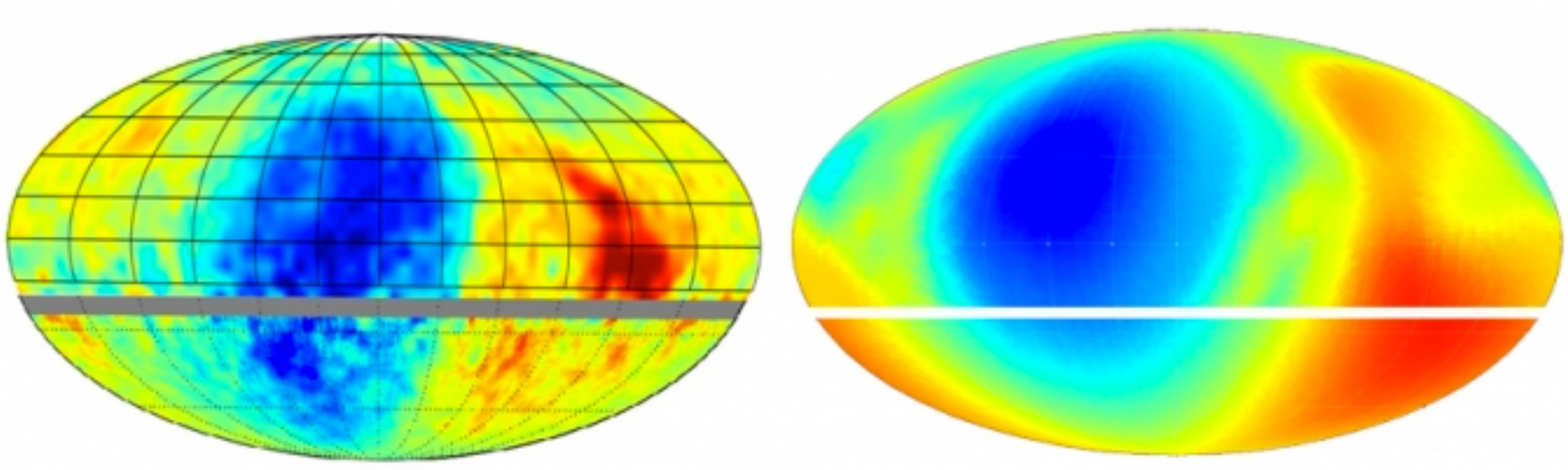

Schwadron, et al., Science, 1245026 (2014)

conclusions

- cosmic ray anisotropy observed **up to PeV scale** & **down to 5º** with IceCube & IceTop
- anisotropy **not a dipole**, **changes topology** with energy and has **complex structure**
- AMANDA & IceCube **global anisotropy stable over one solar cycle** within statistics

➡ study **correlation** between anisotropy & spectral anomalies vs **primary mass**

- high energy cosmic ray anisotropy to probe into their **origin and propagation**
- understanding of **interstellar medium** towards astrophysical scenarios for the observations
- better understand particle **diffusion in magnetic fields**

thanks for your attention

backup slides

IceTop shower reconstruction

Aartsen et al. PRD 88 (2013) 042004

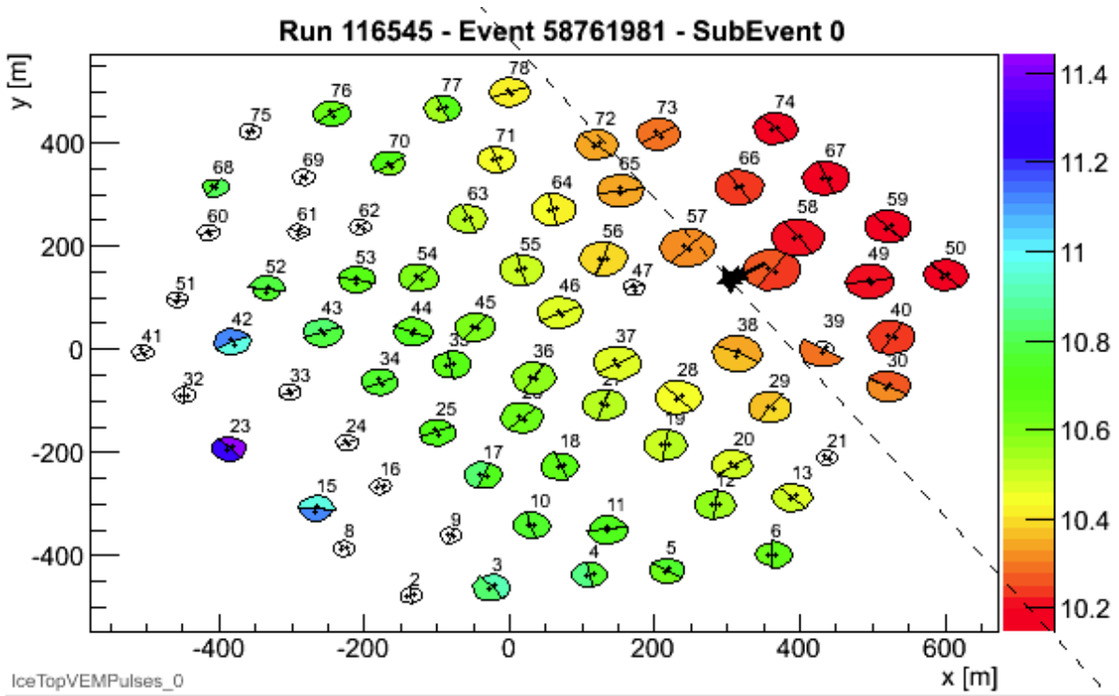

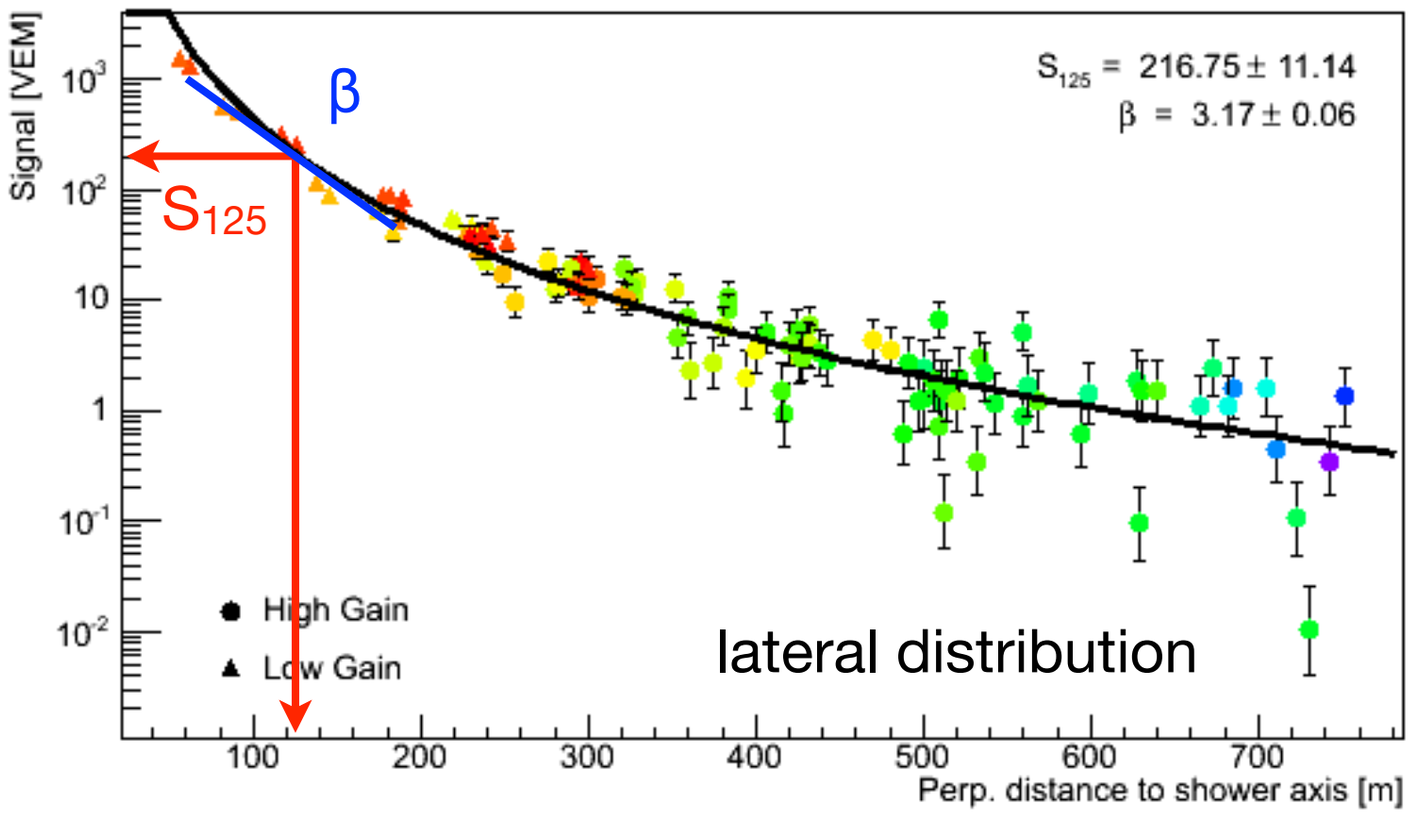

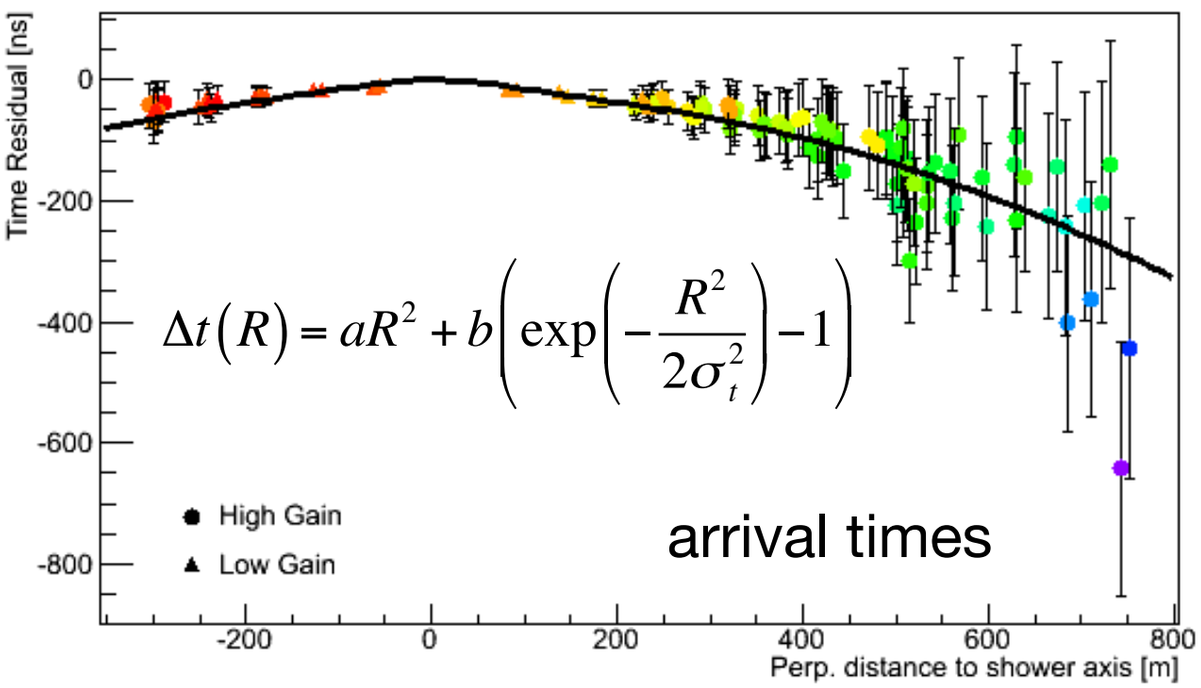

$$S(R) = S_{125}\left(\frac{R}{125m}\right)^{-\beta-\kappa\log(R/125m)}$$

S_{125} : signal at r = 125m

β : slope at r = 125m

κ = 0.303 fixed

IceTop-only all-particle spectrum estimating primary energy

IceTop-73
326 days livetime
Jun 2010 - May 2011

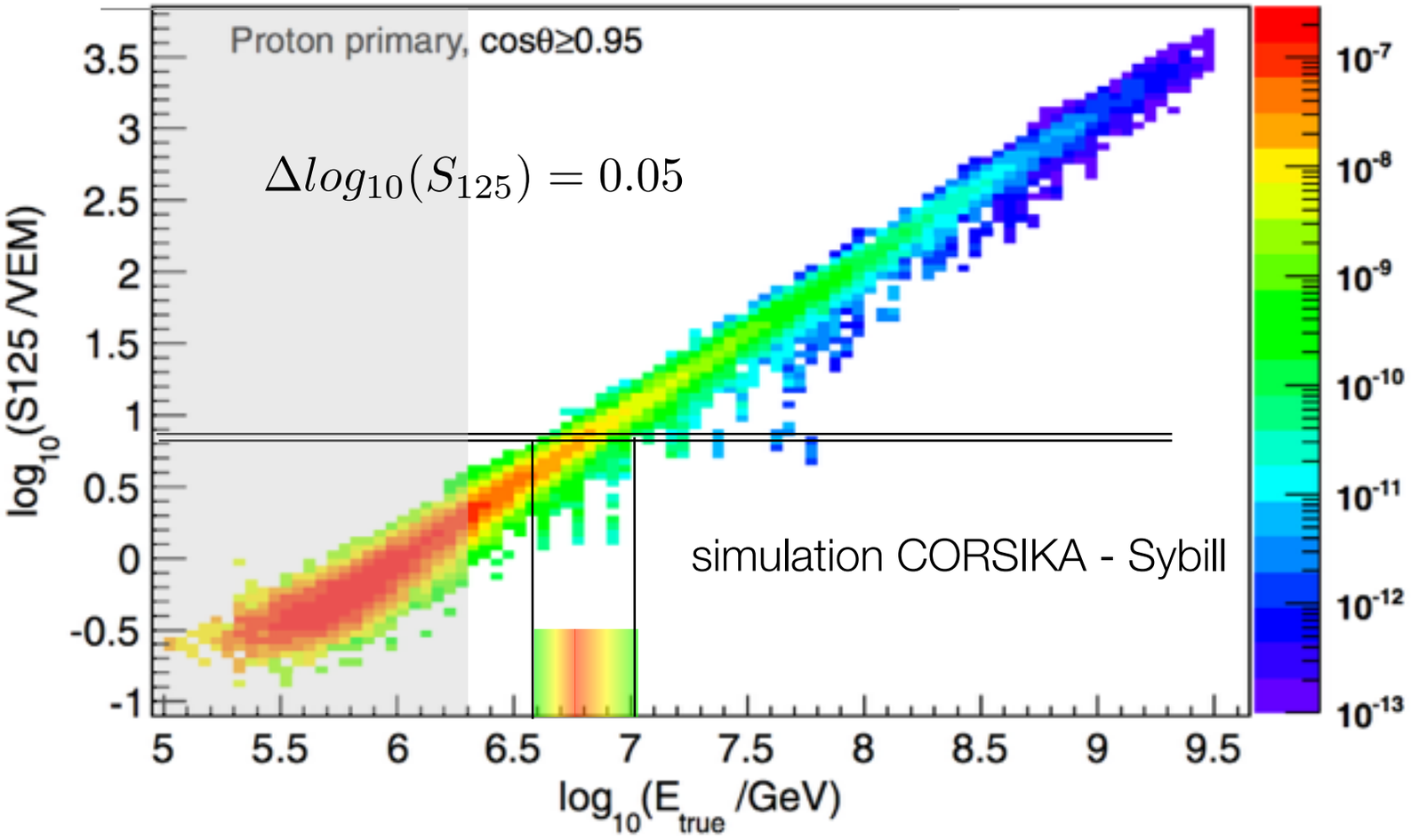

Aartsen et al. PRD 88 (2013) 042004

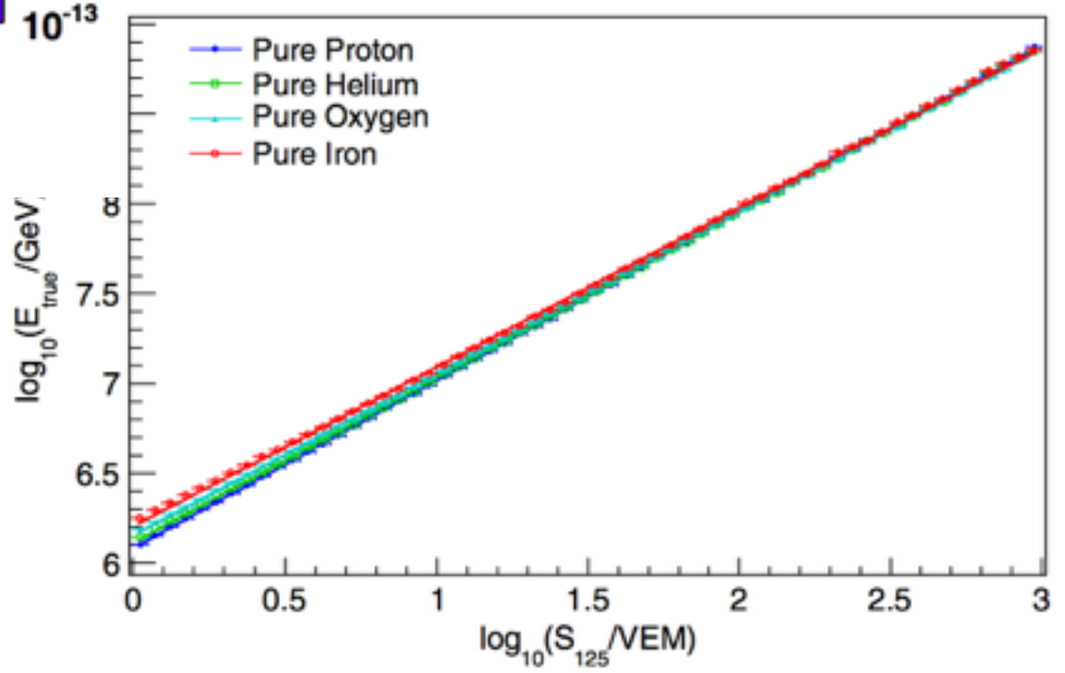

the relationship between S_{125} and primary energy depends on **mass** and **zenith angle**

IceTop-only all-particle spectrum

IceTop-73
326 days livetime
Jun 2010 - May 2011

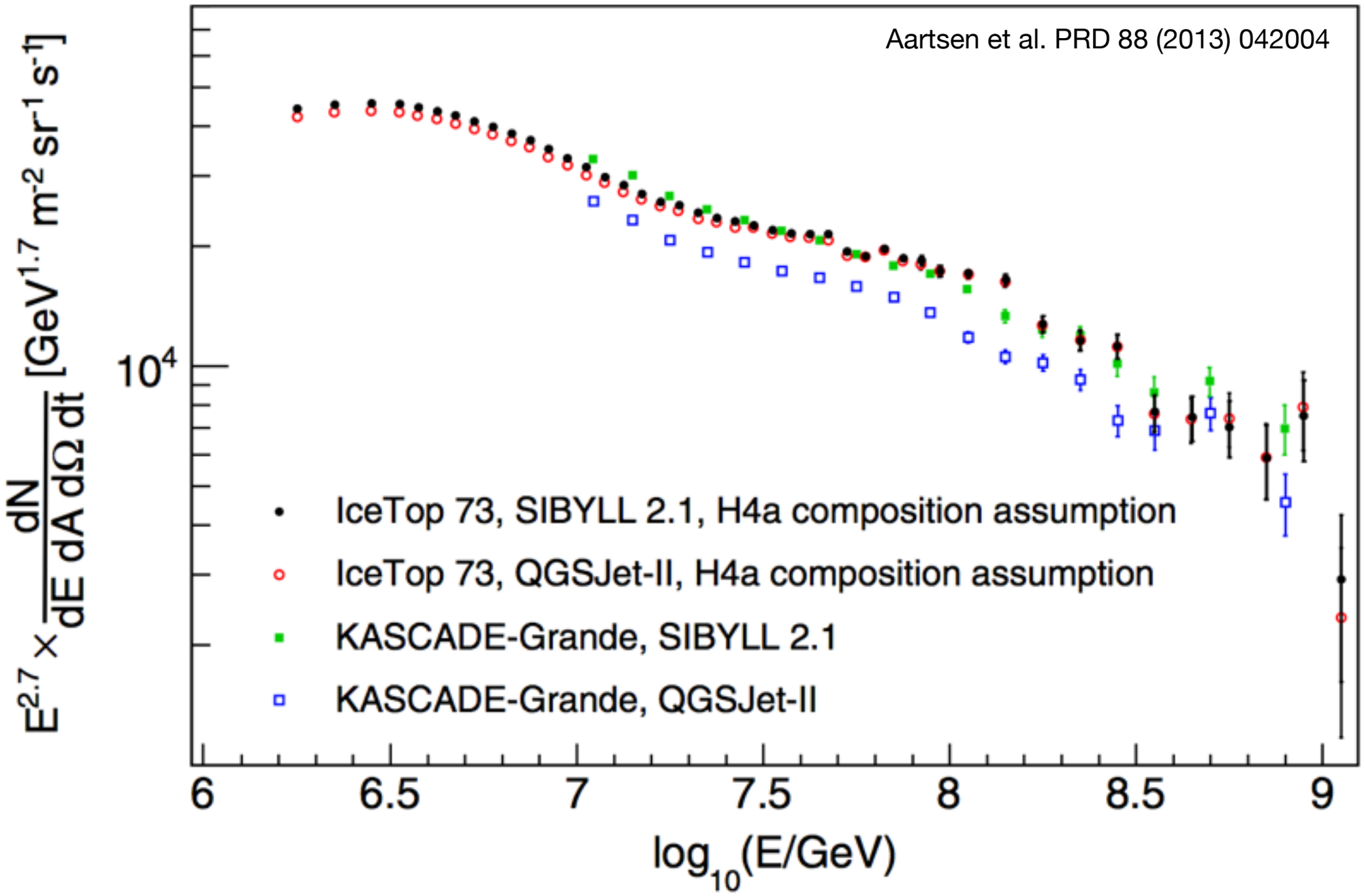

IceTop-only all-particle spectrum

IceTop
2.67 yr livetime
2010 - 2013

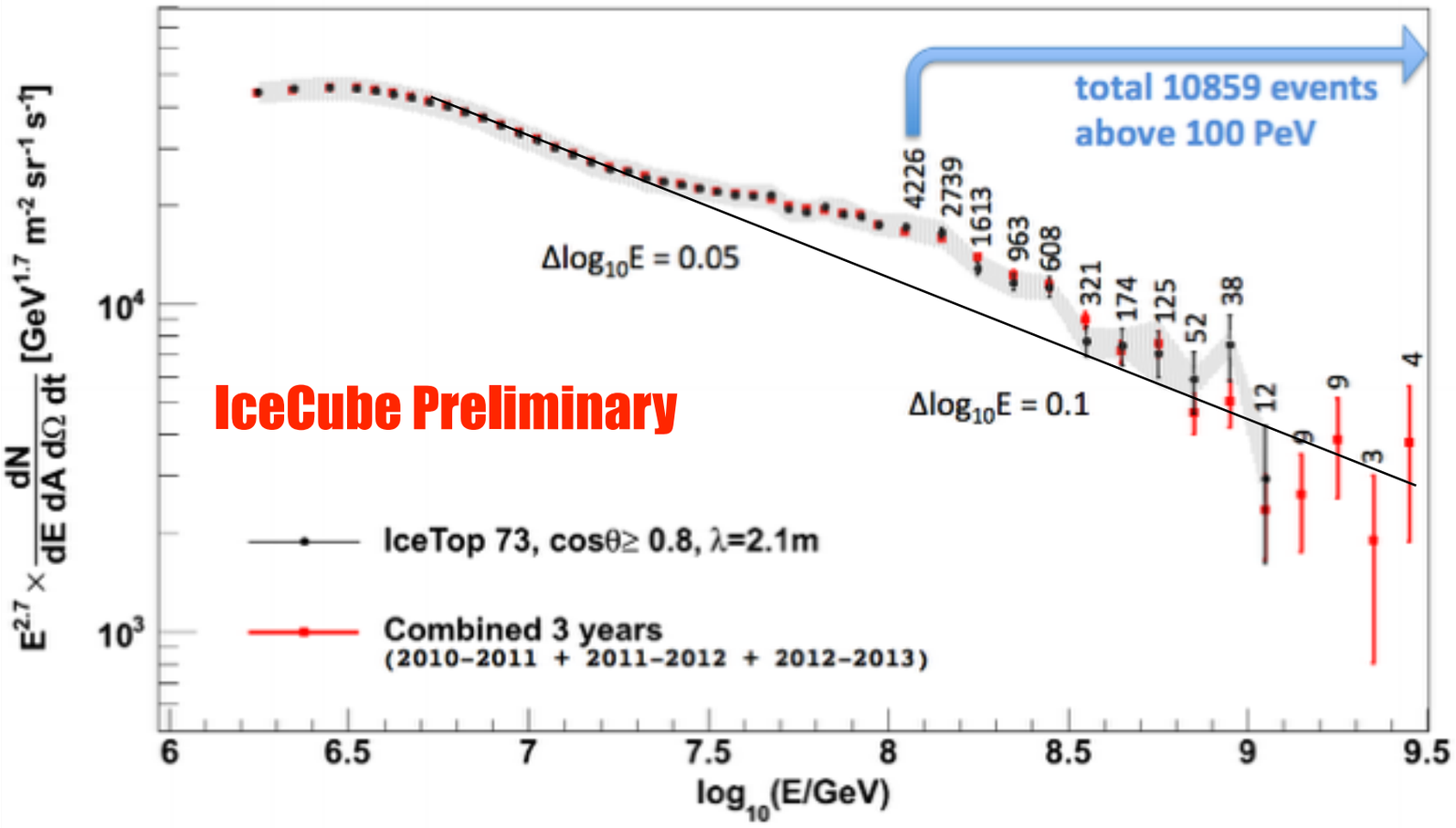

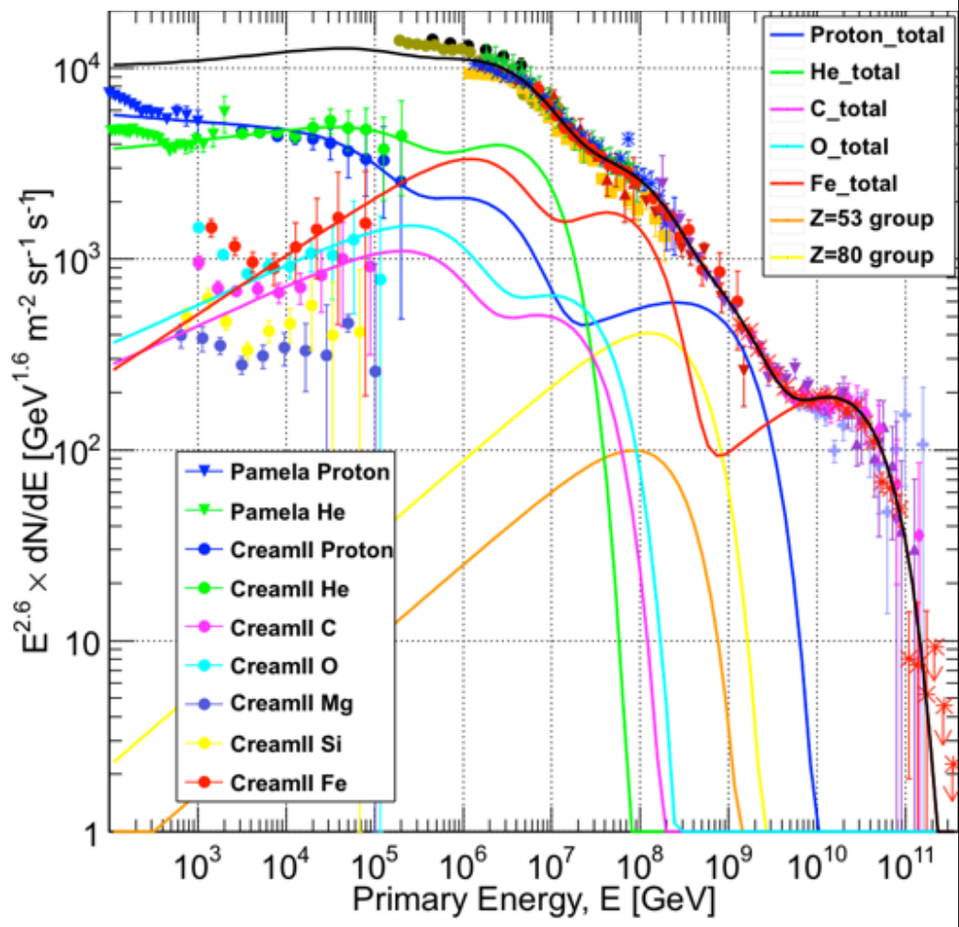

IceTop-only all-particle spectrum

IceTop-73
326 days livetime
Jun 2010 - May 2011

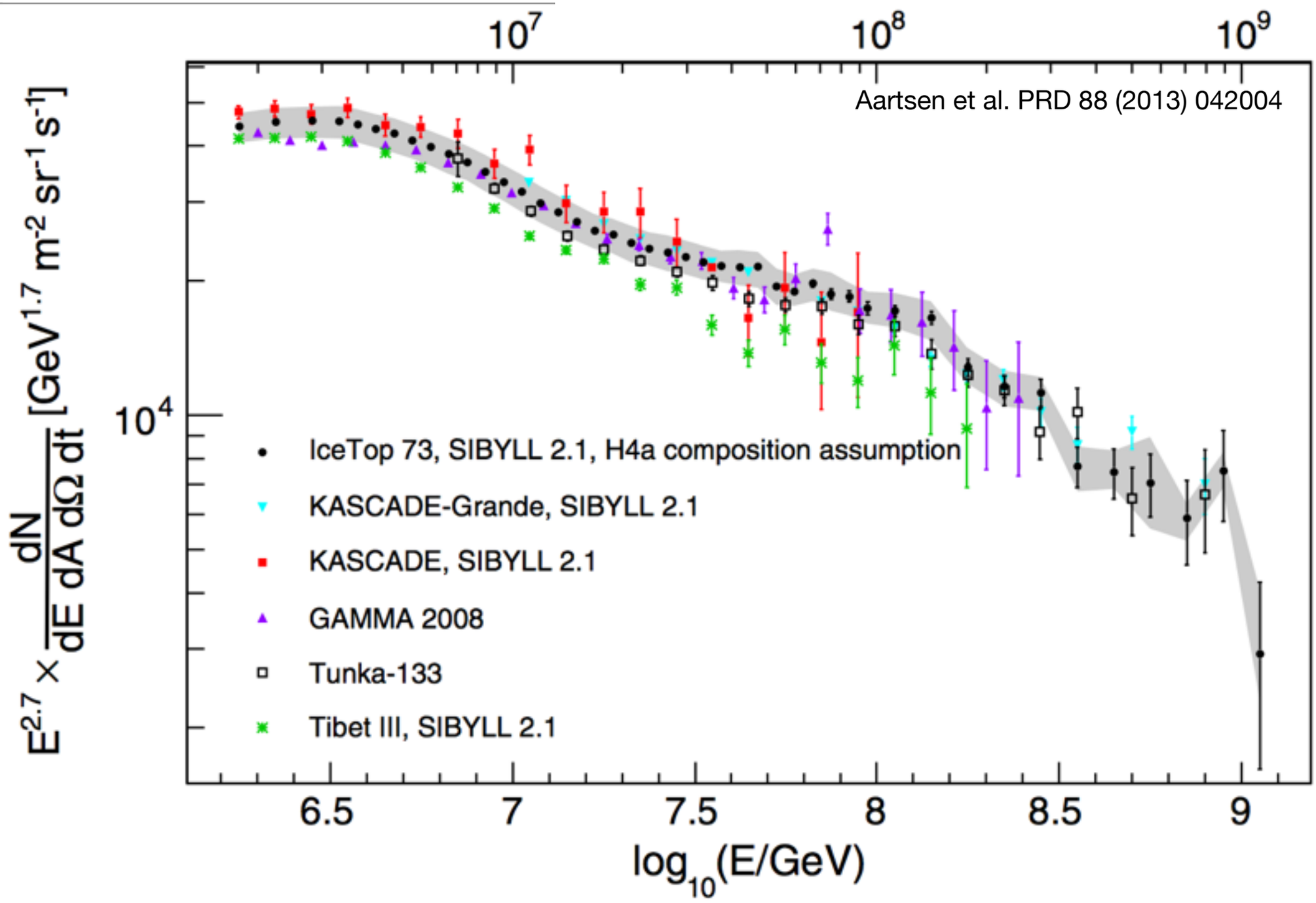

IceTop-only all-particle spectrum

IceTop
2.67 yr livetime
2010 - 2013

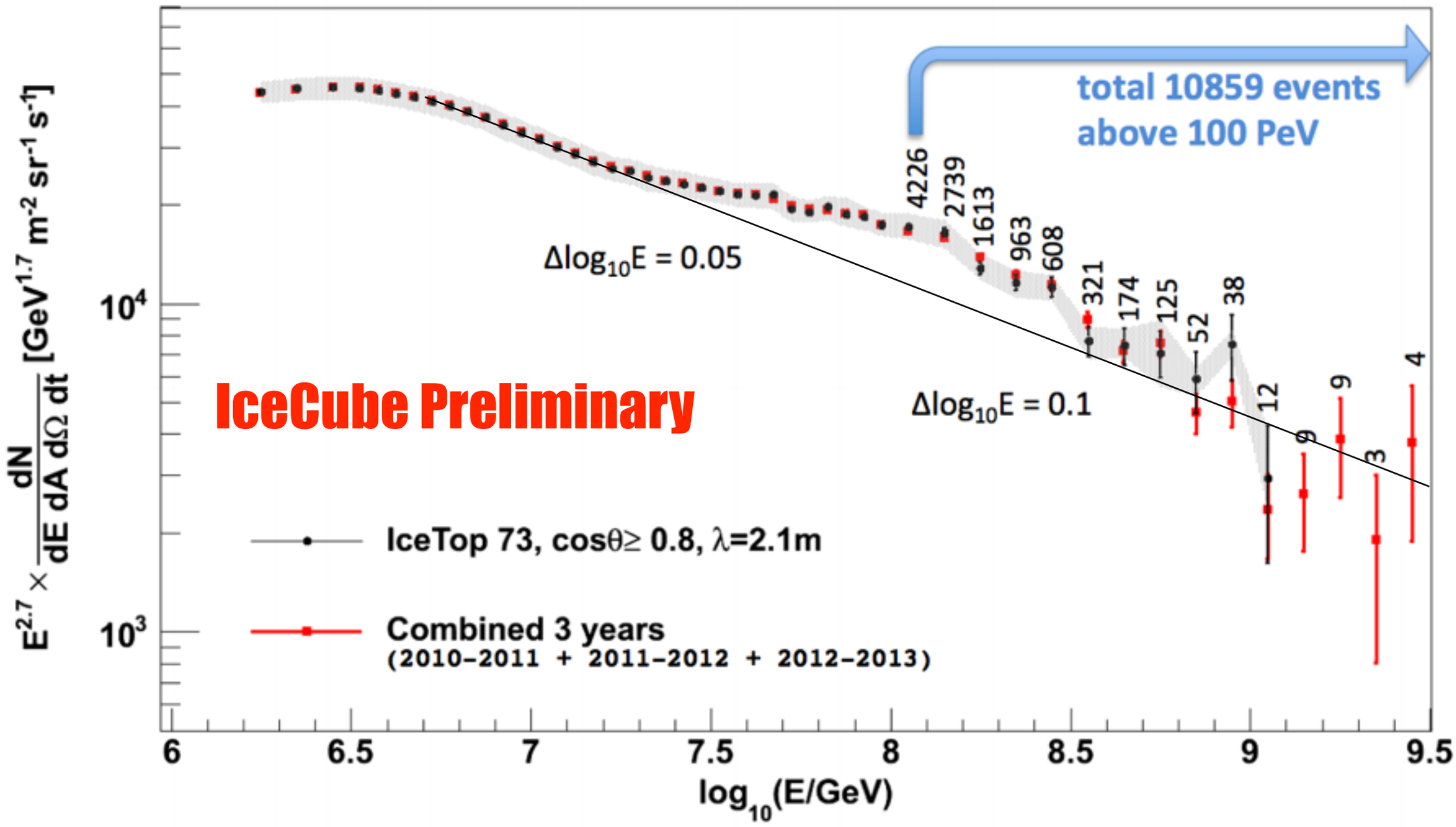

IceTop-only all-particle spectrum

IceTop-73
326 days livetime
Jun 2010 - May 2011

$$\frac{dN}{d\,ln(E)} = \frac{N_{events}\,/\,bin}{\epsilon\,A\,\Delta\Omega\,T\,ln(E_{i+1}/E_i)}$$

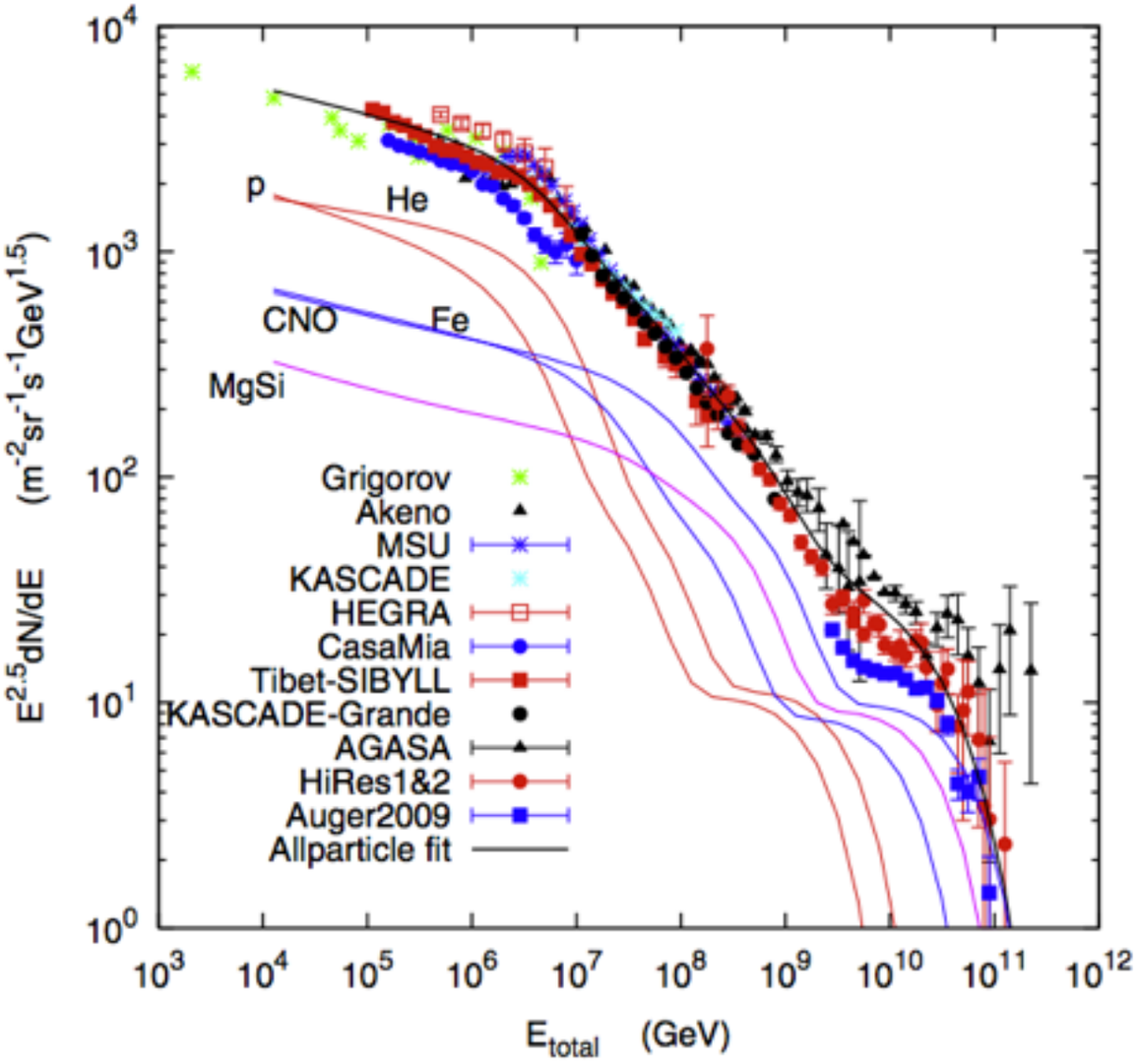

Gaisser, Astropart. Phys. 35 (2012) 801

Aartsen et al. PRD 88 (2013) 042004

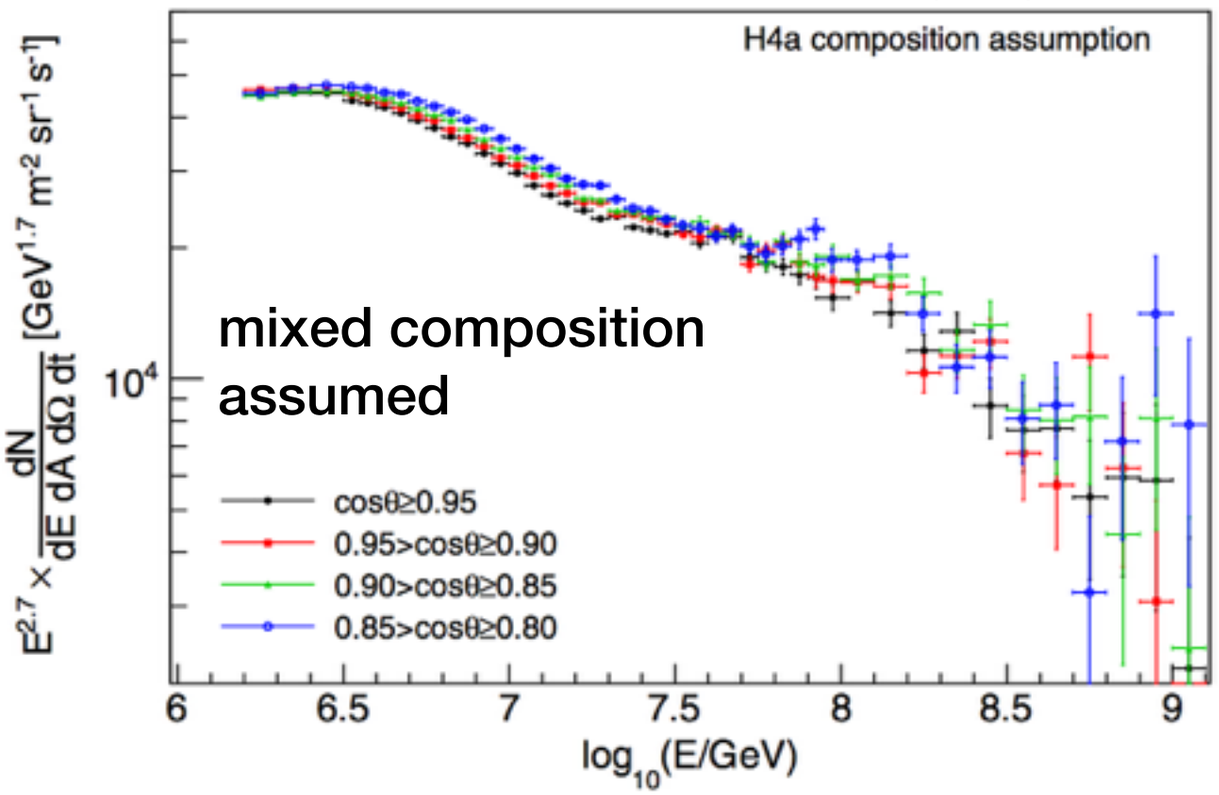

5 nuclear components

3 populations

- galactic (e.g. SNR) - CREAM
- galactic II - Hillas
- extragalactic (p or mixed)

IceTop/IceCube spectrum & composition

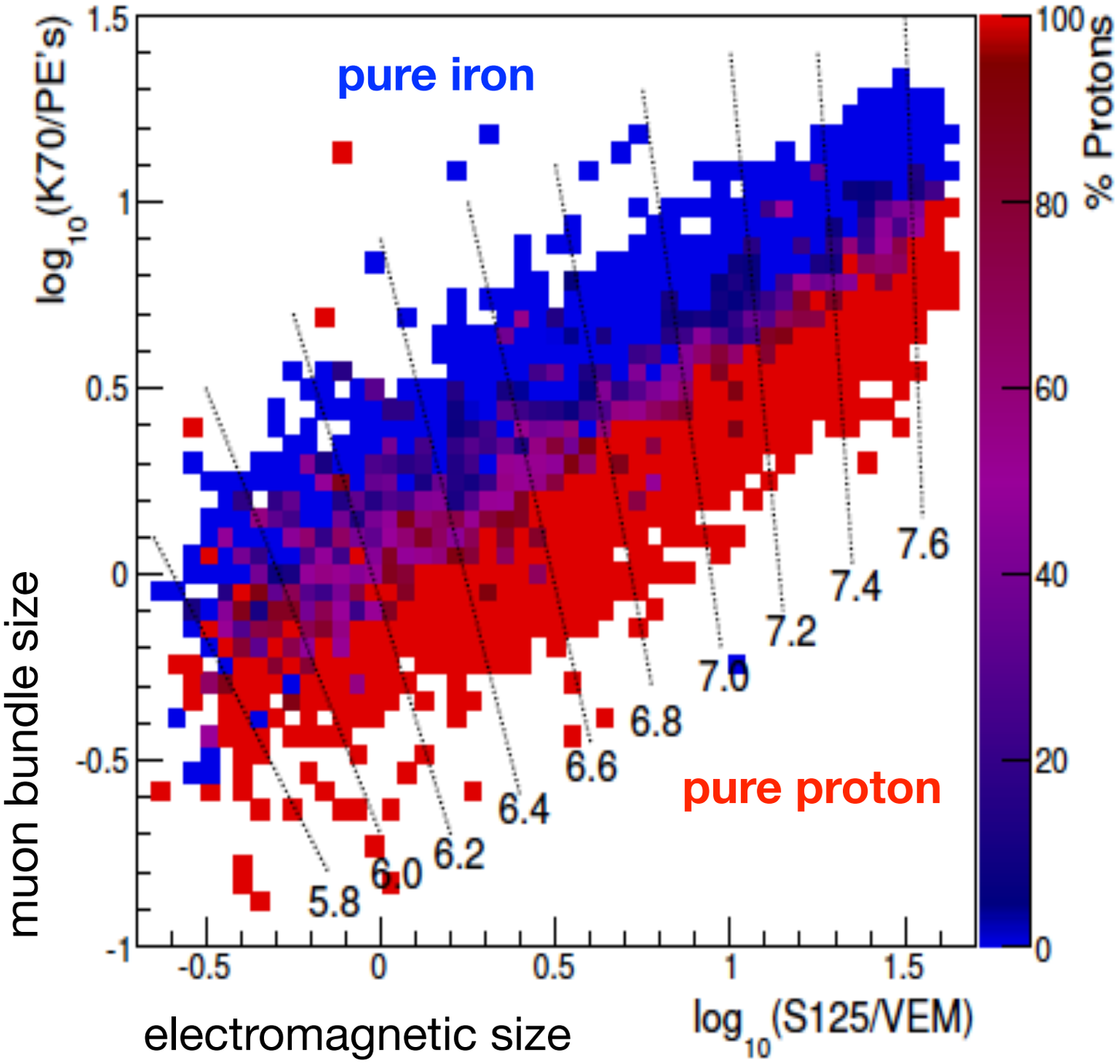

IT-40/IC-40

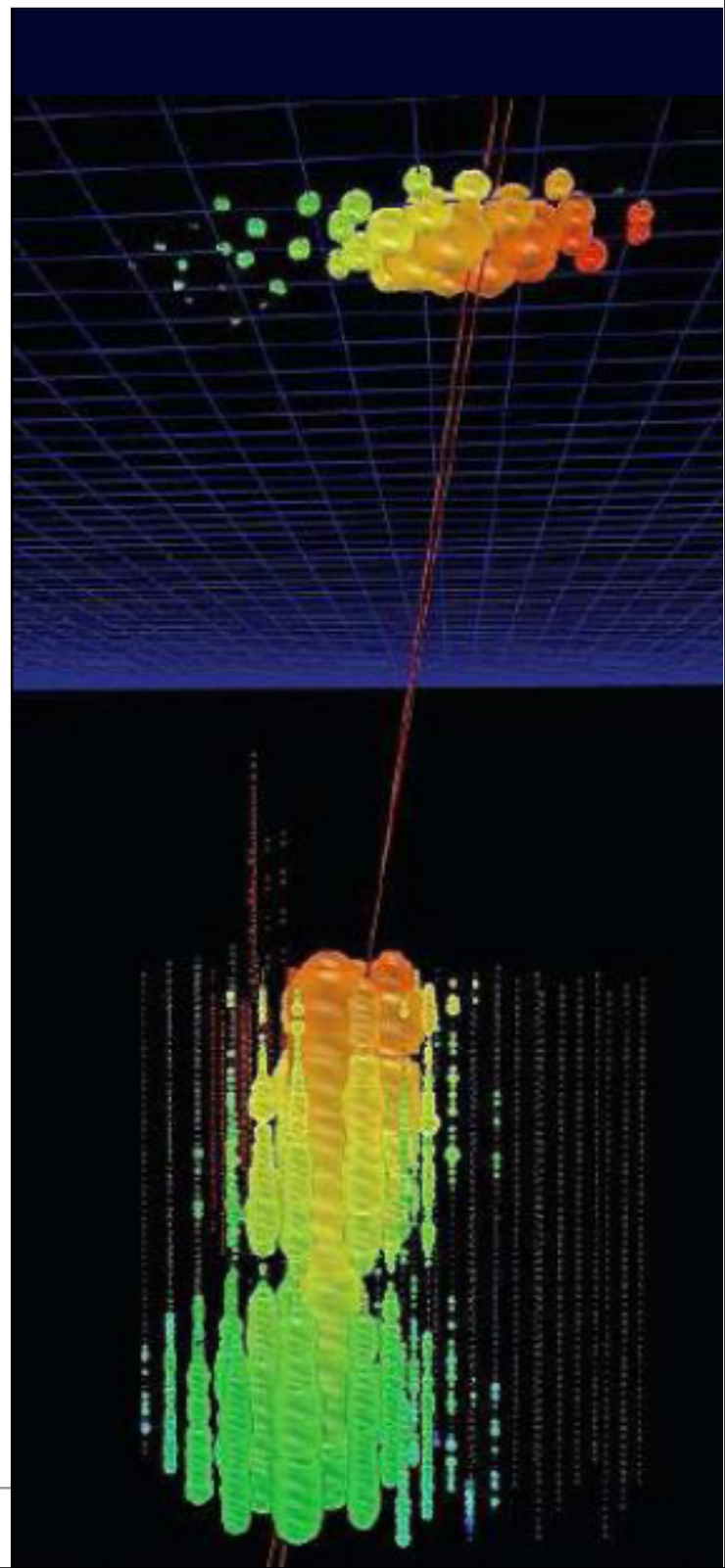

IceTop/IceCube spectrum & composition

IT-40/IC-40

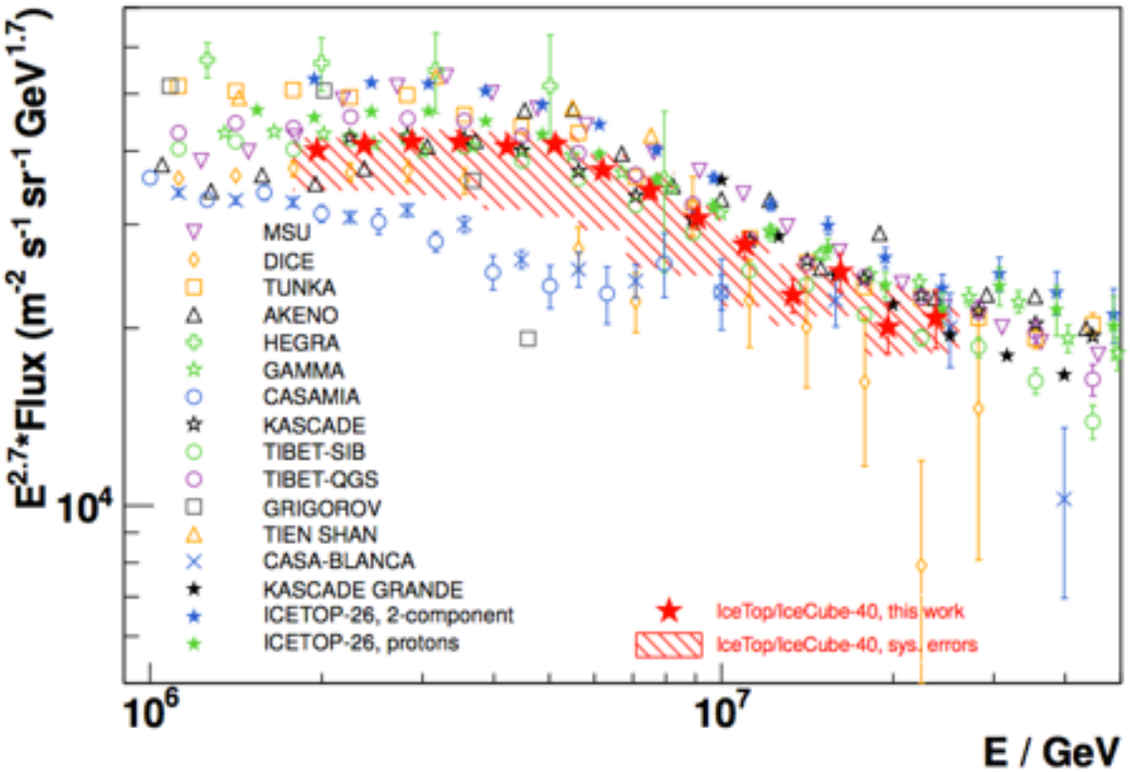

Abbasi et al. Astropart.Phys. 42 (2013) 15

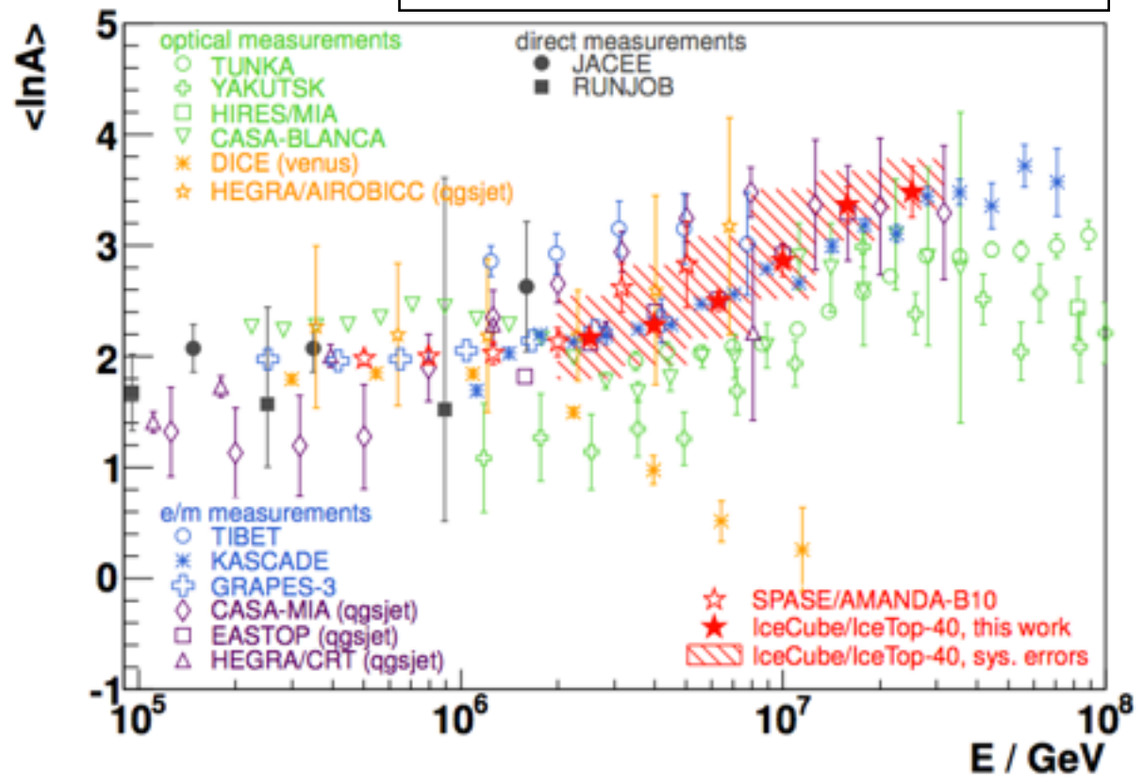

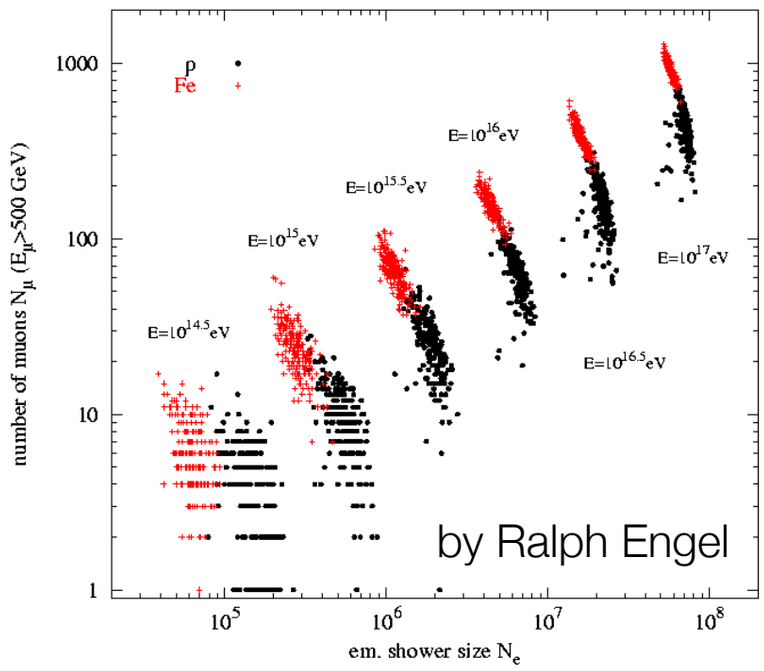

mass-independent primary energy resolution of 0.05 in logE

simultaneous EM and hadronic component measurement for spectrum/mass unfolding

experimental systematic uncertainties important

- **study being extended to IC59/IC59 & IT73/IC79**

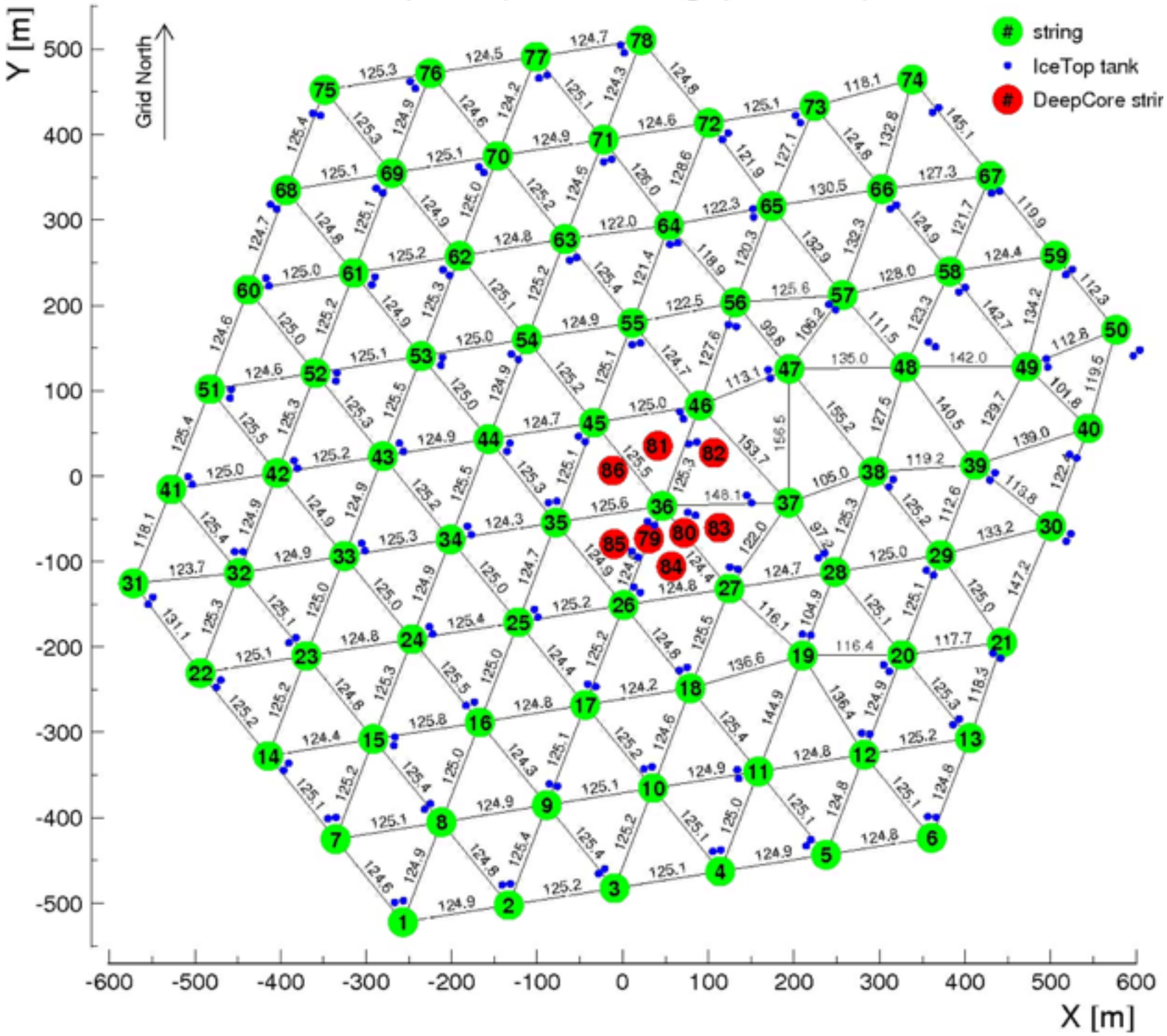

IceCube geometry

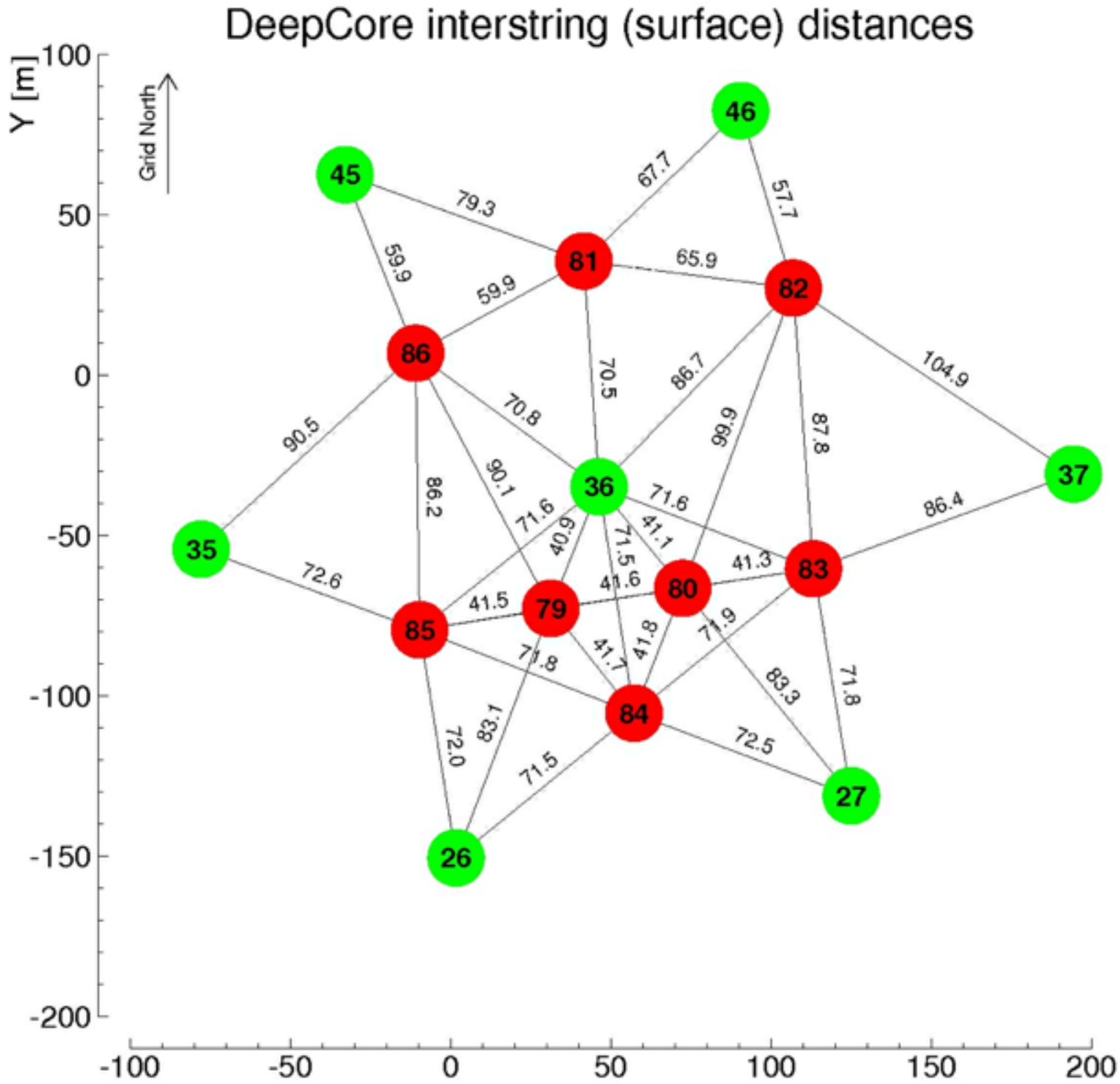

DeepCore geometry

detection principle

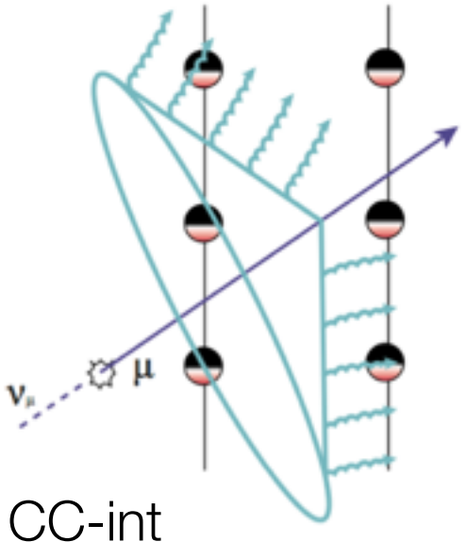

ν_μ CC-int

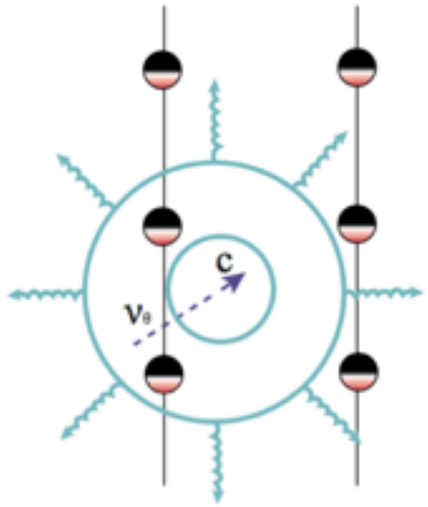

ν_e ν_τ CC-int & ν_i NC-int

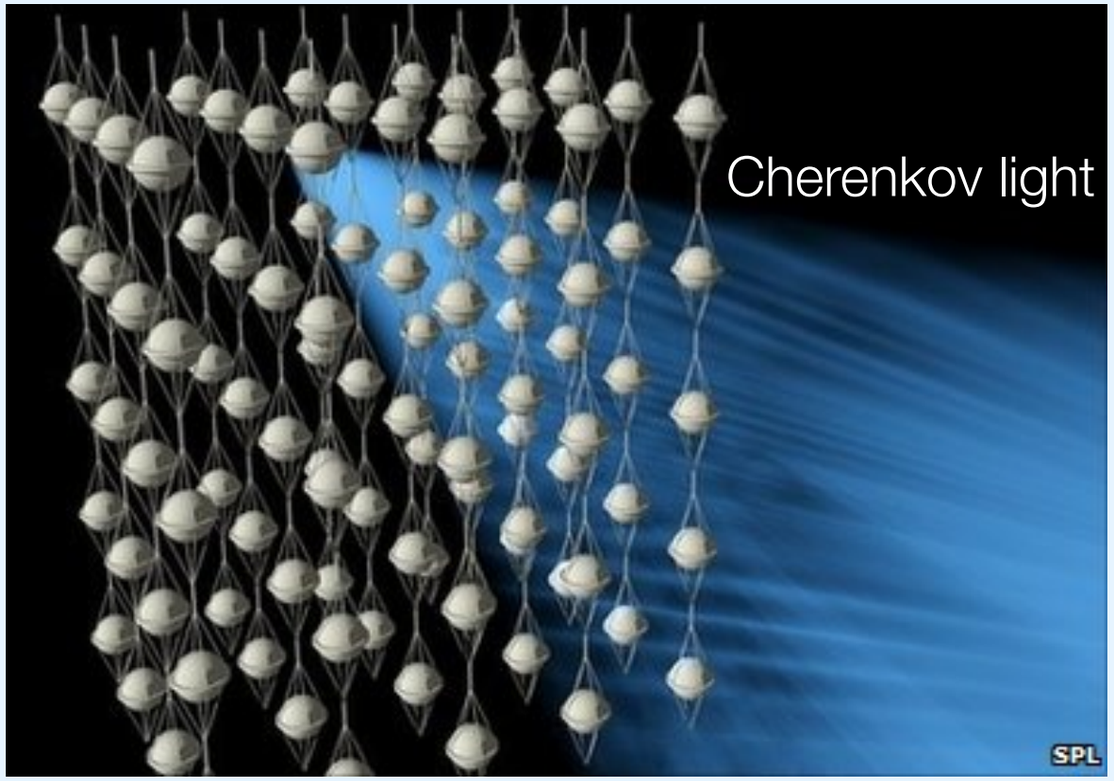

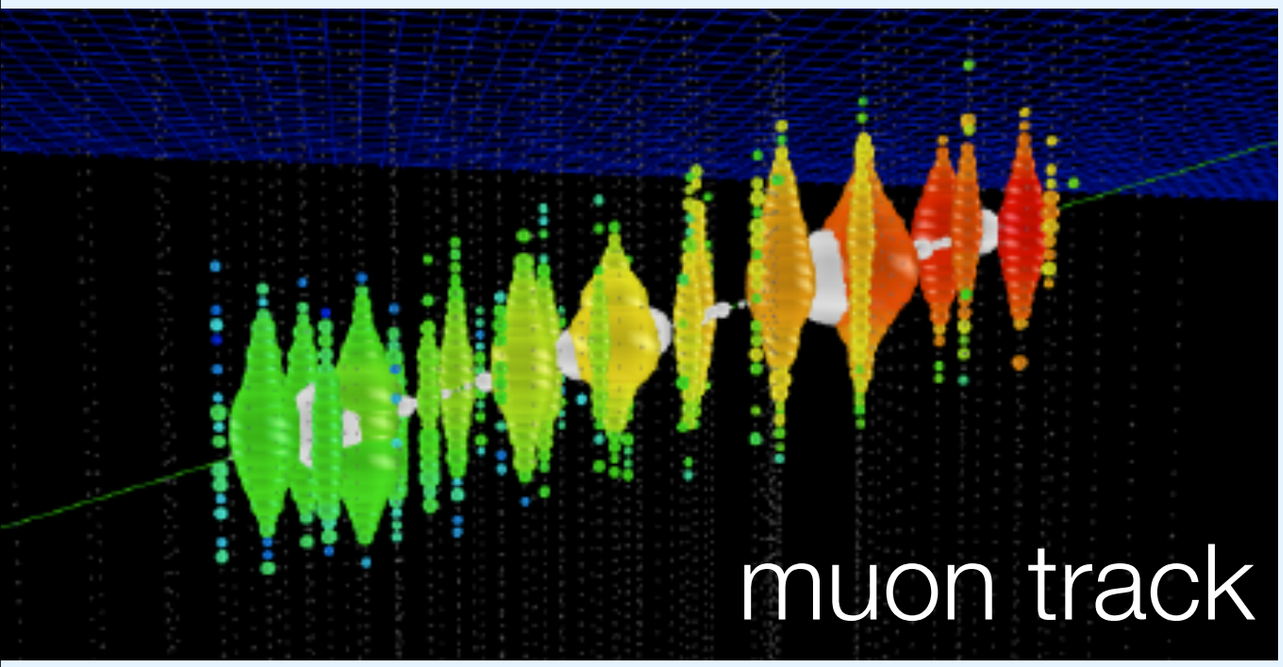

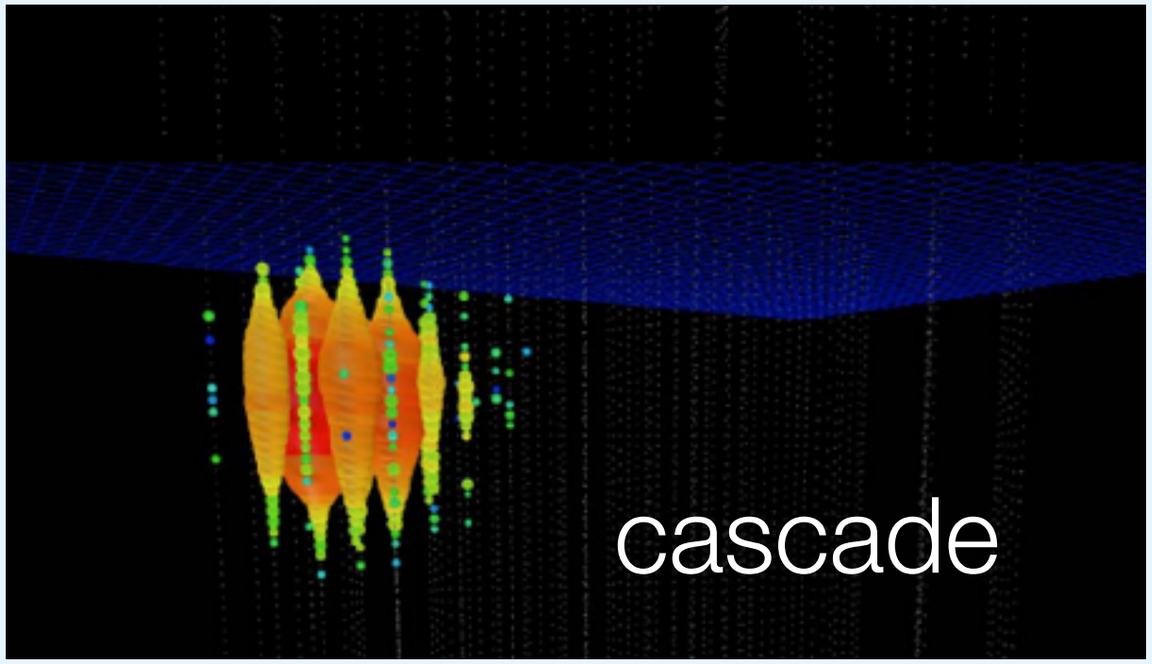

growing IceCube
& event collection

Year	μ rate (SMT8)	CR shower rate (STA3)
2007	500 Hz	13 Hz
2008	1100 Hz	15 Hz
2009	1700 Hz	25 Hz
2010	2000 Hz	30 Hz
2011+	2200 Hz	35 Hz

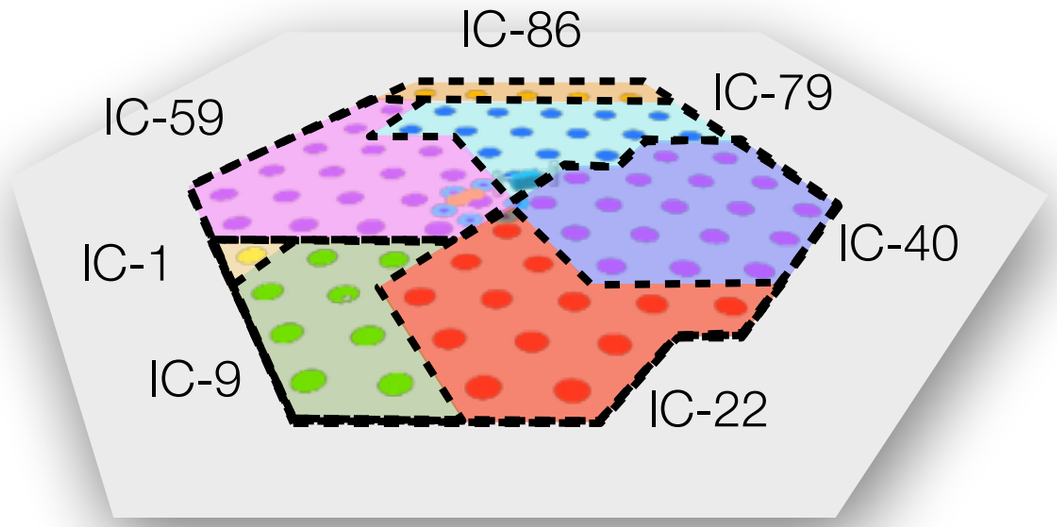

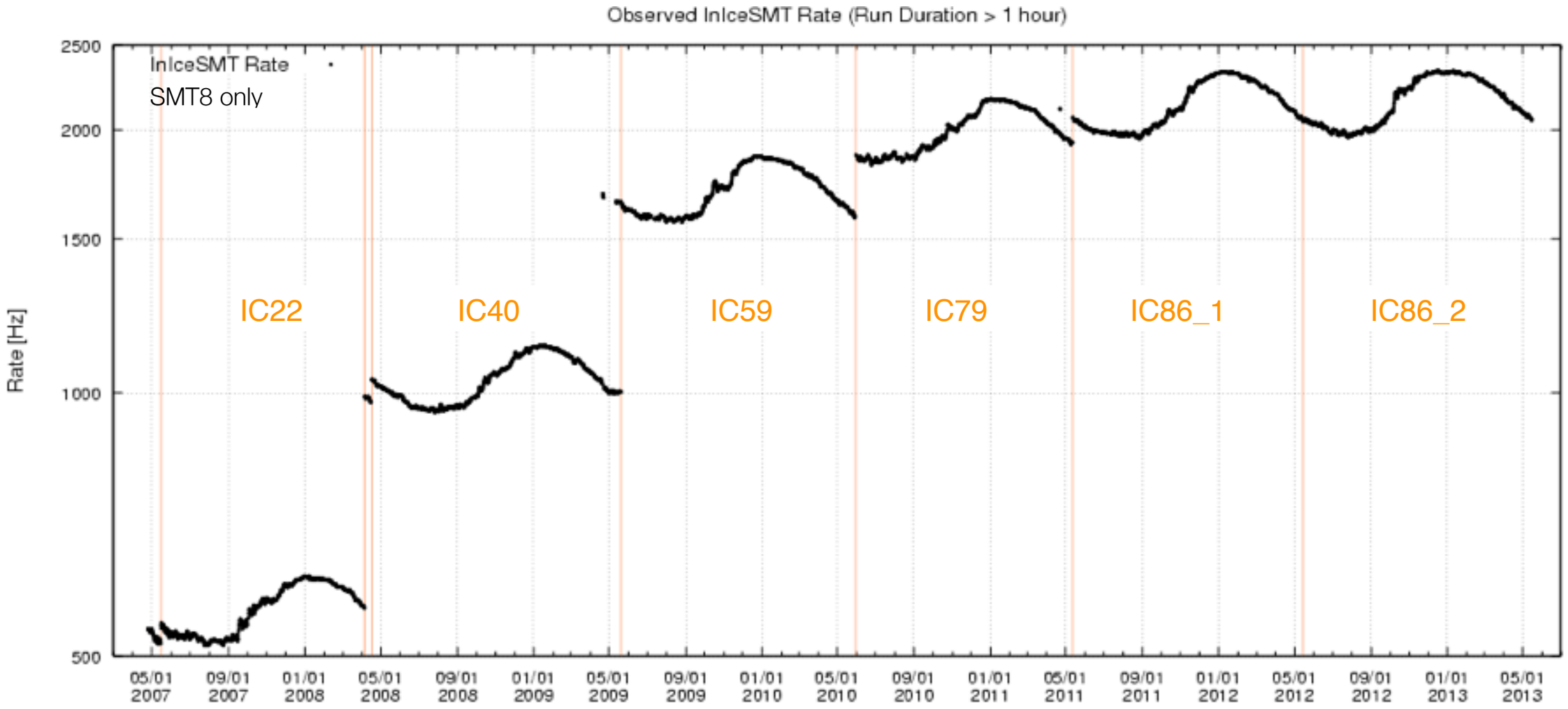

growing IceCube
& event collection

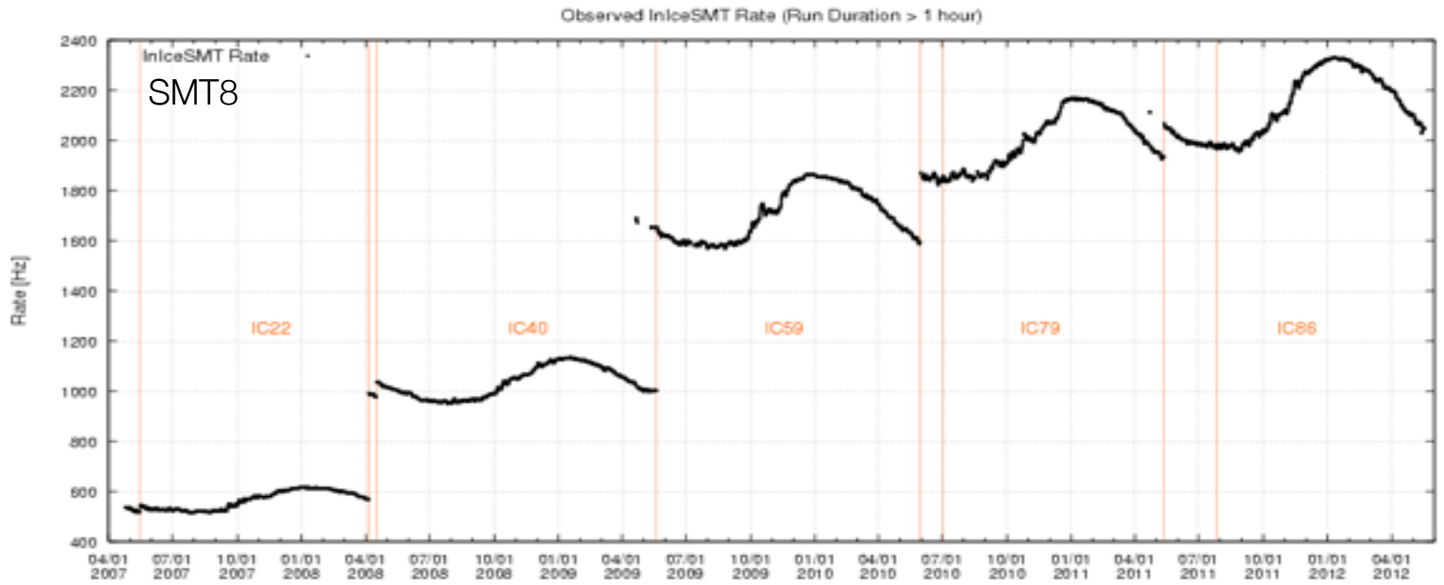

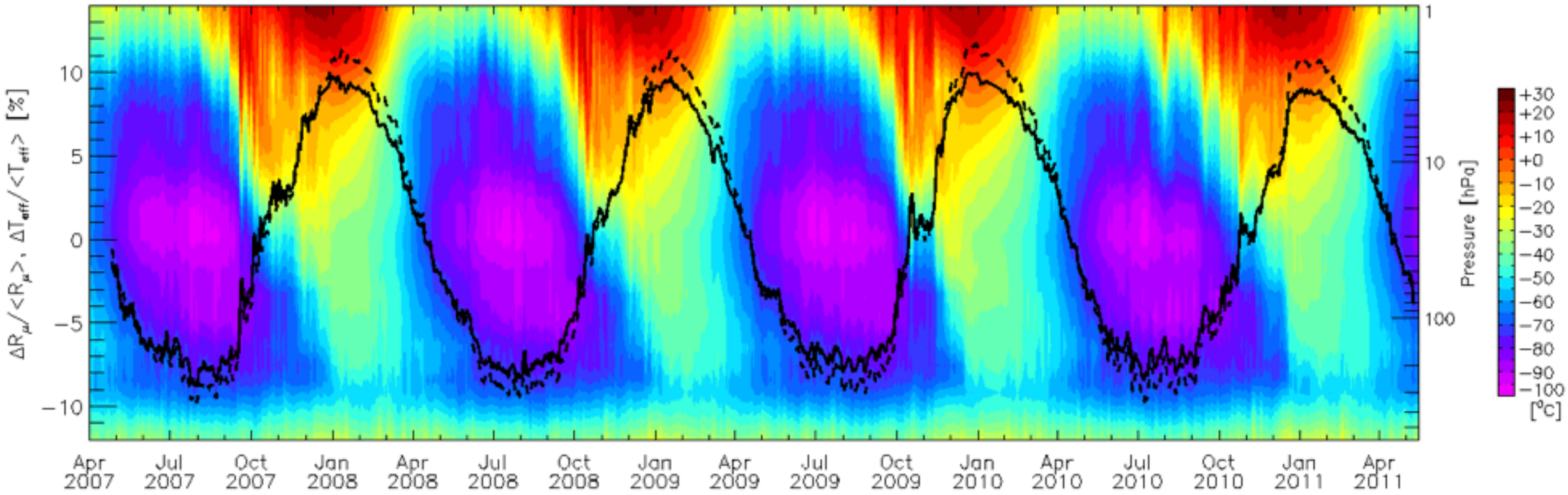

low energy cosmic ray anisotropy in arrival direction

Nagashima+,1998

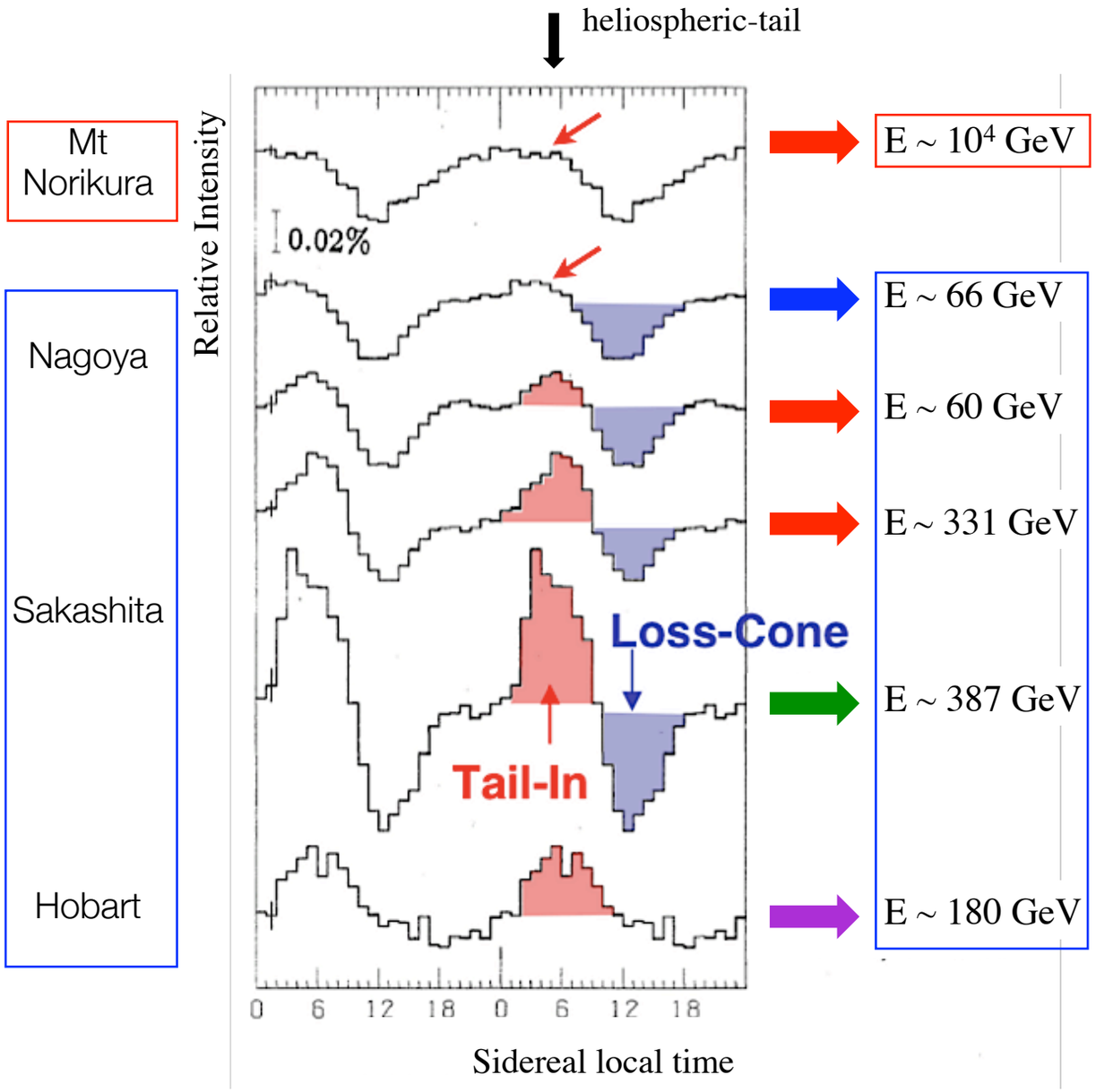

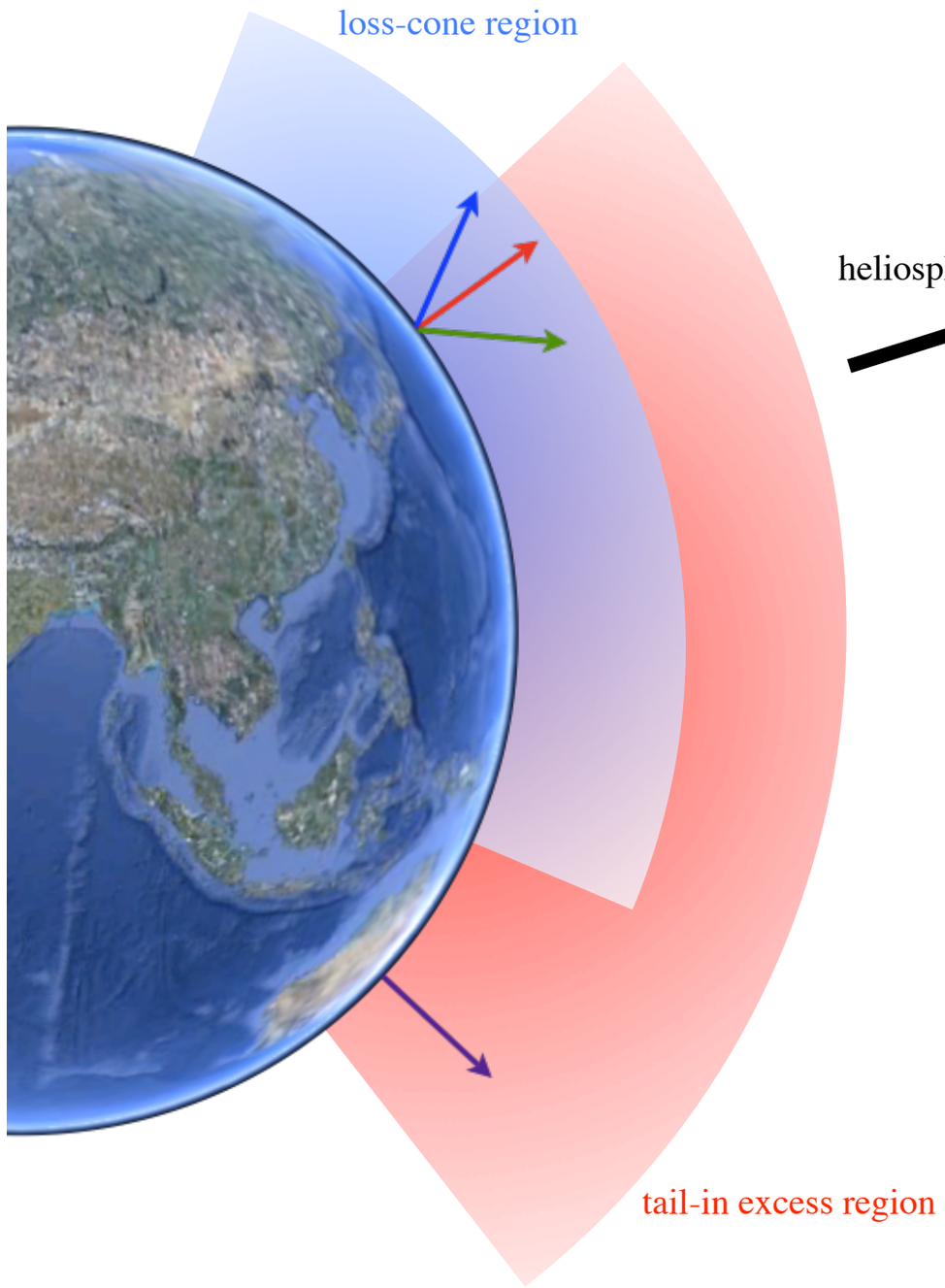

cosmic ray anisotropy vs energy

J.L. Zhang et al., 31st ICRC Łódź - Poland, 2009

ARGO-YBJ

- data from 2008
- 365 days livetime
- $6.5 \cdot 10^{10}$ events
- median CR energy ~ 1.1 TeV

Amenomori et al., Science Vol. 314, pp. 439, 2006

Tibet-III

- data from 1997 to 2005
- 1874 days livetime
- $3.7 \cdot 10^{10}$ events
- angular resolution ~ 0.9°
- modal CR energy ~ 3 TeV

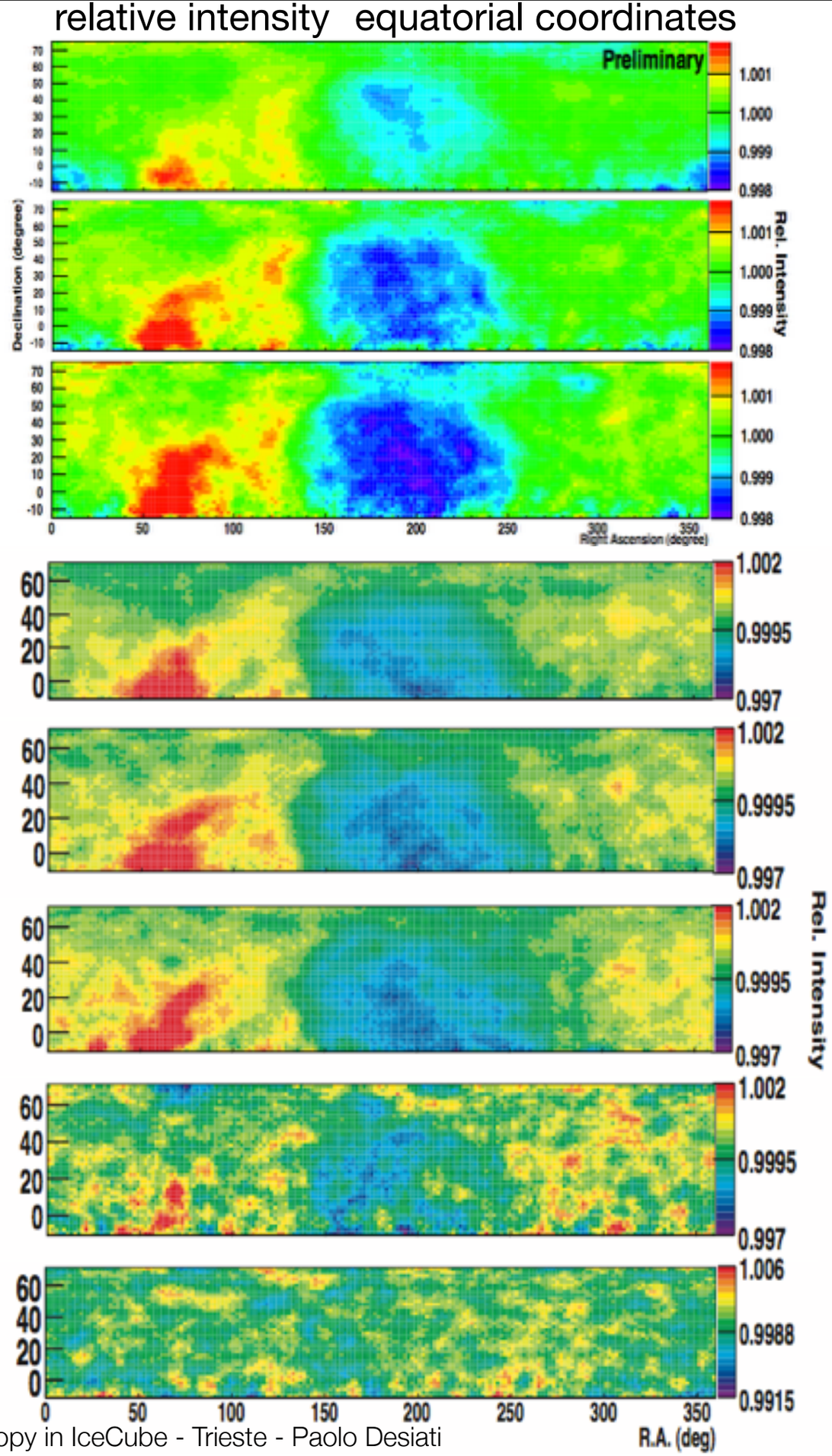

equatorial coordinates

σ

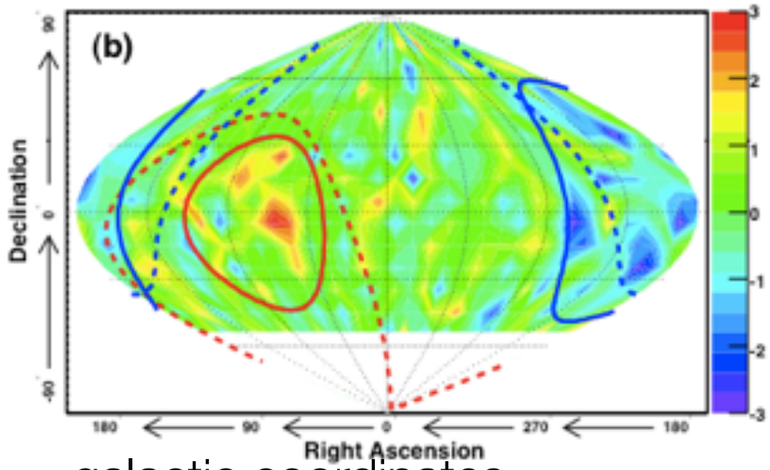

galactic coordinates

σ

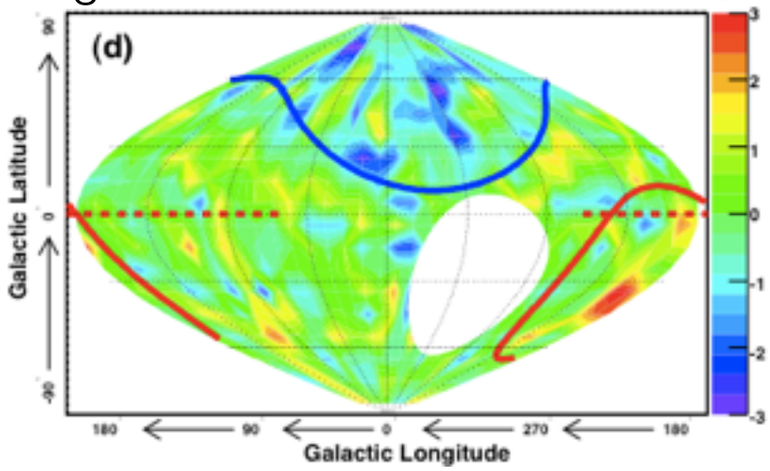

relative intensity

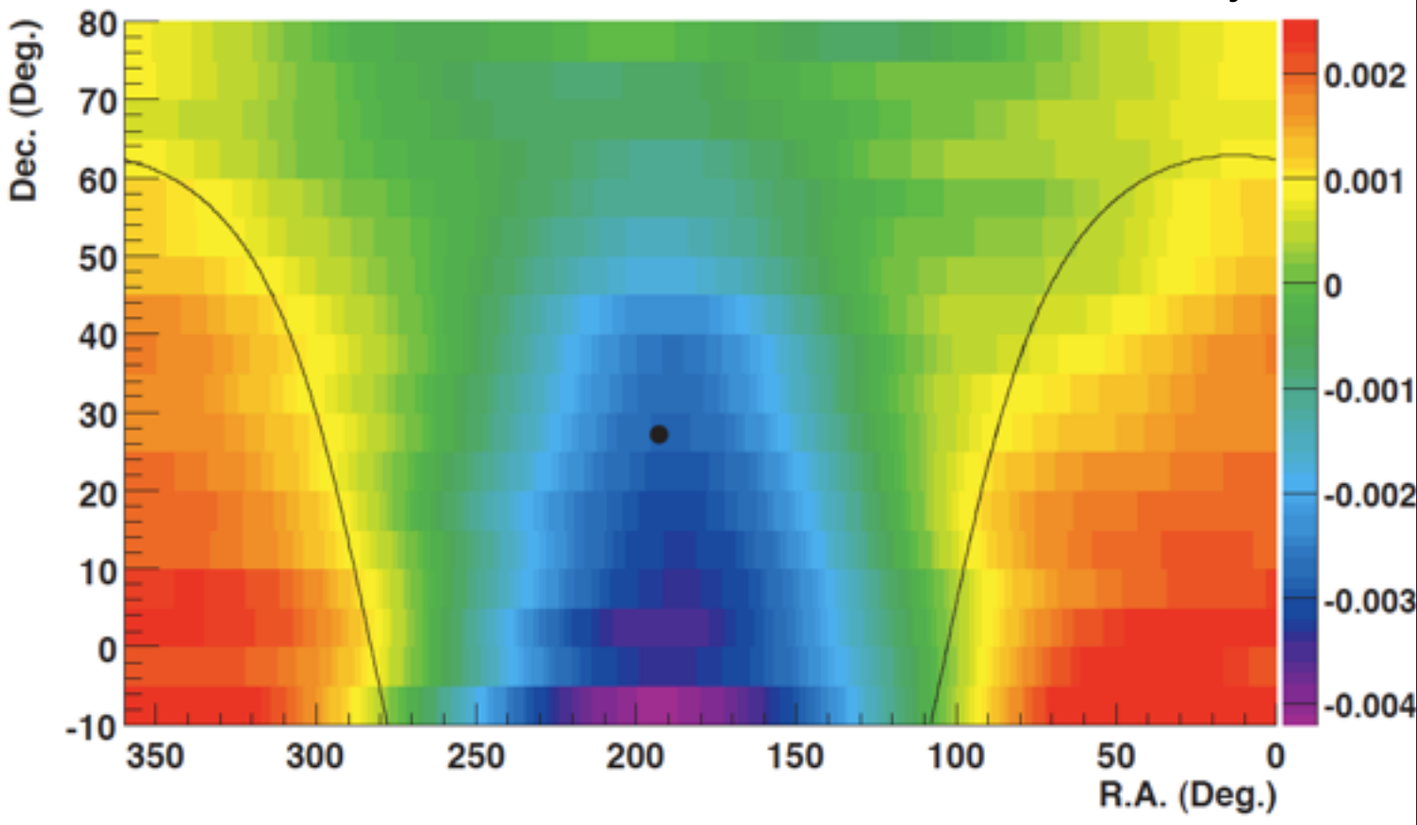

Super-Kamiokande

Guillian et al., Phys Rev D, Vol 75, 063002 (2007)

- data from 1996 to 2001
- 1662 days livetime
- $2.1 \cdot 10^8$ events
- angular resolution < 2°
- median CR energy ~ 10 TeV

Milagro

Abdo et al., ApJ, Vol 698-2, pag 2121 (2009)

- data from 2000 to 2007
- $9.5 \cdot 10^{10}$ events
- angular resolution < 1°
- median CR energy ~ 6 TeV

cosmic ray anisotropy vs energy

300 TeV

Tibet-III

Amenomori et al., Science Vol. 314, pp. 439, 2006

relative intensity

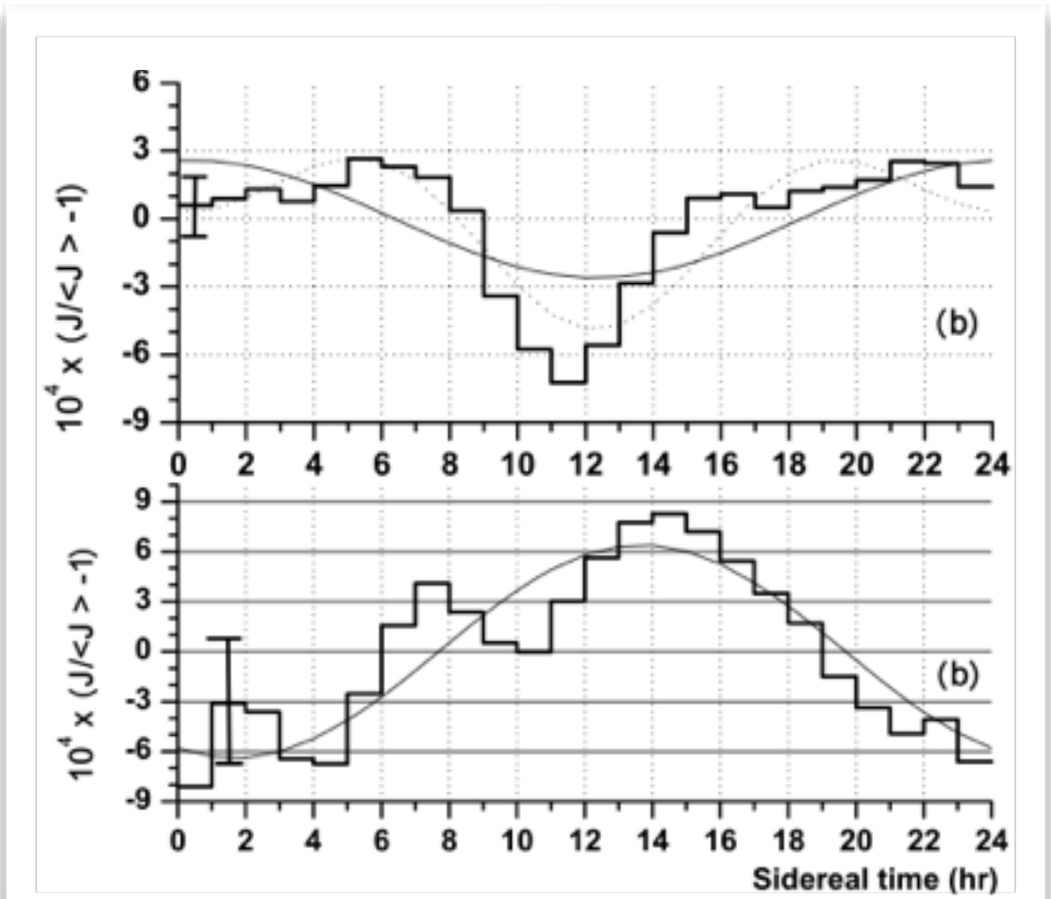

relative intensity equatorial coordinates

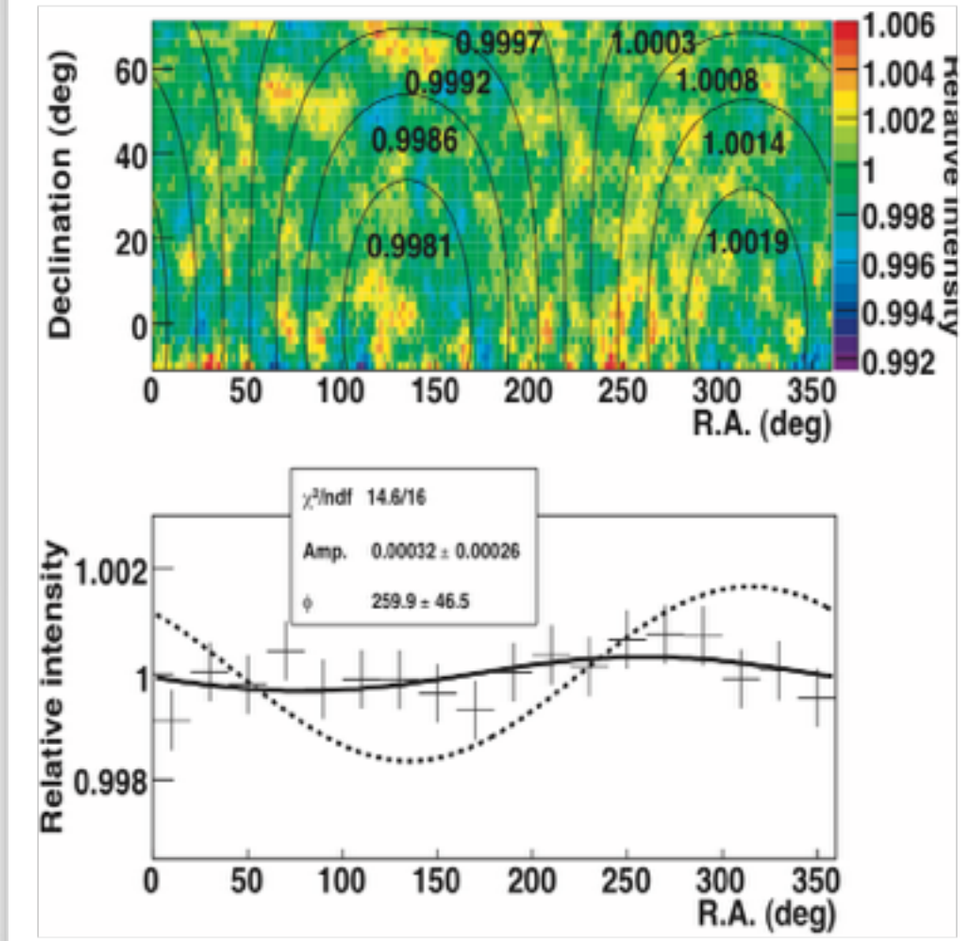

110 TeV

370 TeV

EAS-TOP

Aglietta et al., ApJ 692, L130, 2009

IceCube muon bundle trigger statistics

detector	trigger rate (Hz)	actual time (d)	livetime (d)	number of events
IceCube-22	500	300	226	5.4×10
IceCube-40	1,100	358	324	19×10
IceCube-59	1,700	367	334.5	34×10
IceCube-79	2,000	365	337	40×10
IceCube-86	2,500	365 × 2	365 × 2	50×10

(*) number of events with LLH reconstruction from online-filter collected by DST

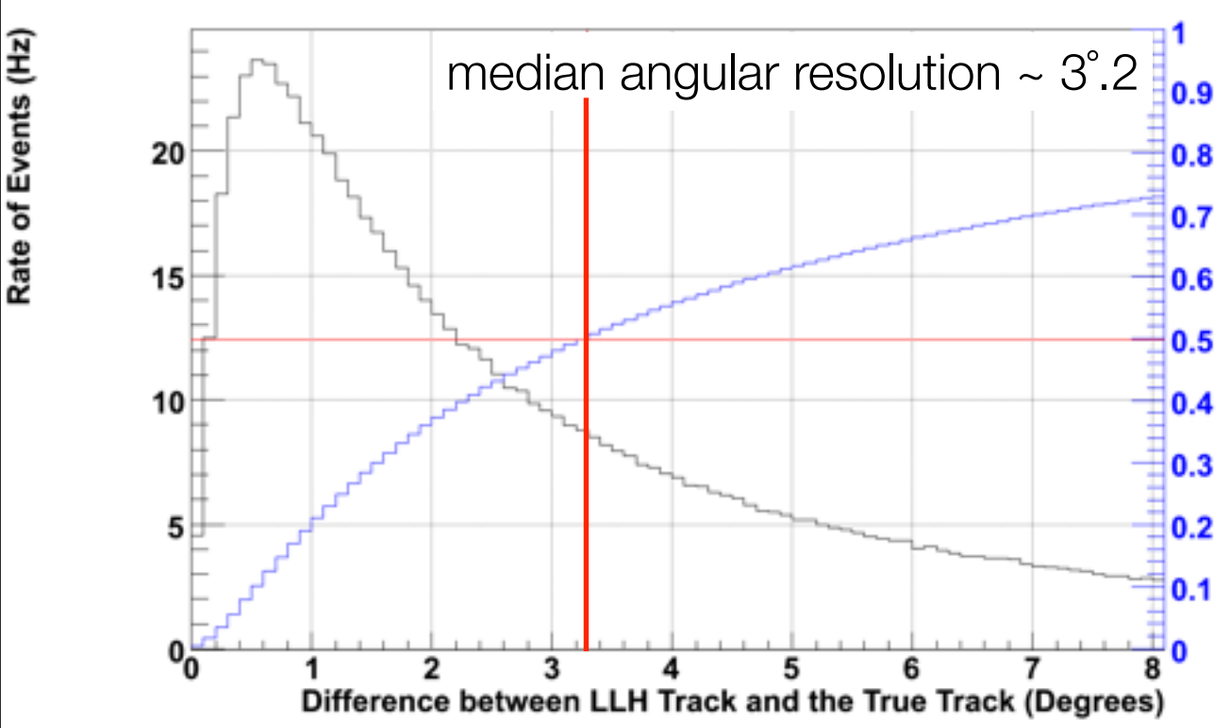

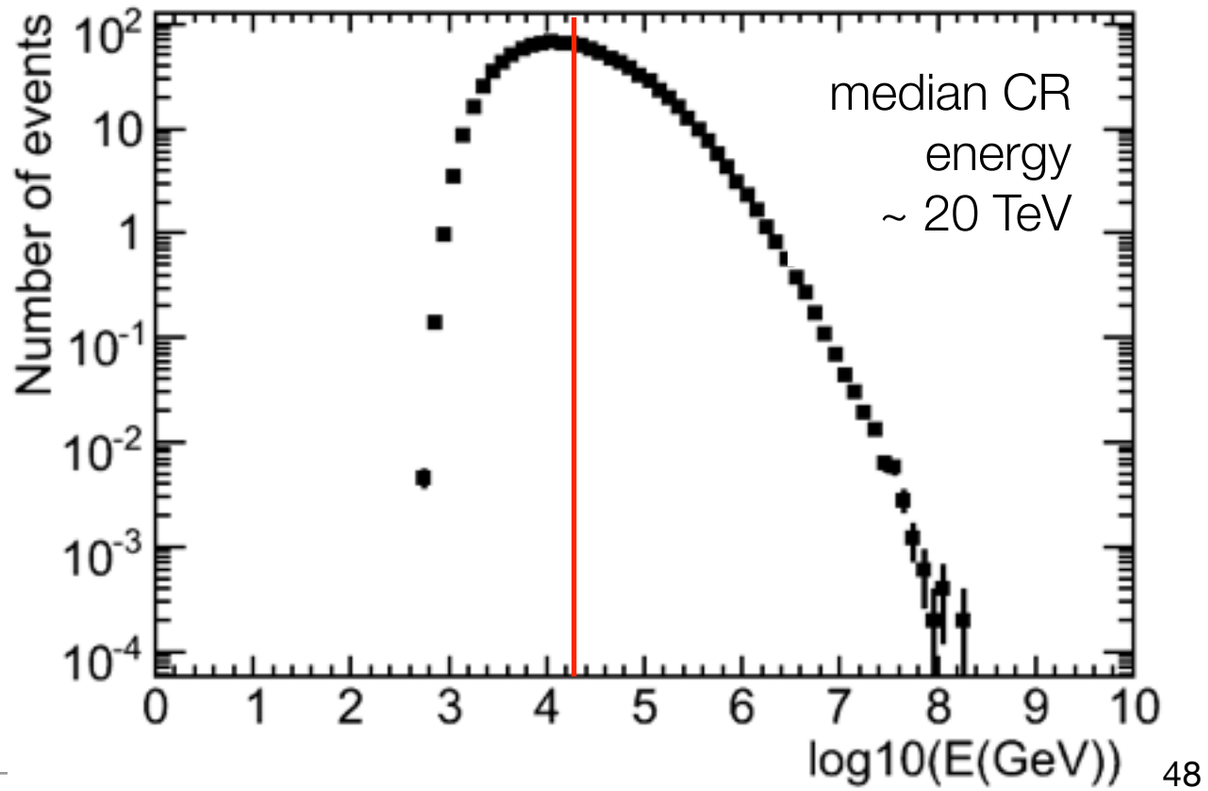

cosmic ray anisotropy analysis technique

raw map of events in equatorial coordinates $(\alpha,\delta)_i$

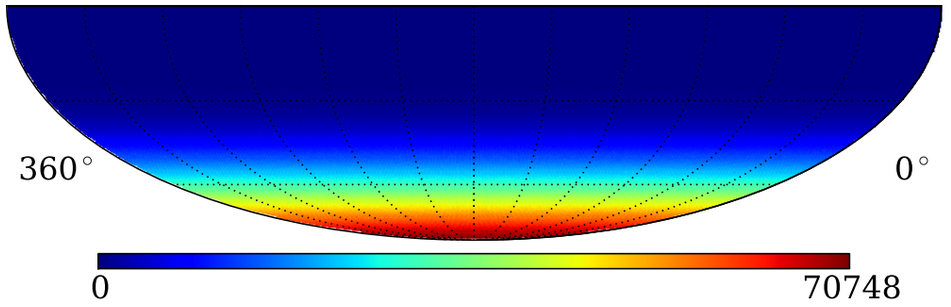

reference map from events scrambled over 24hr in α (or time)

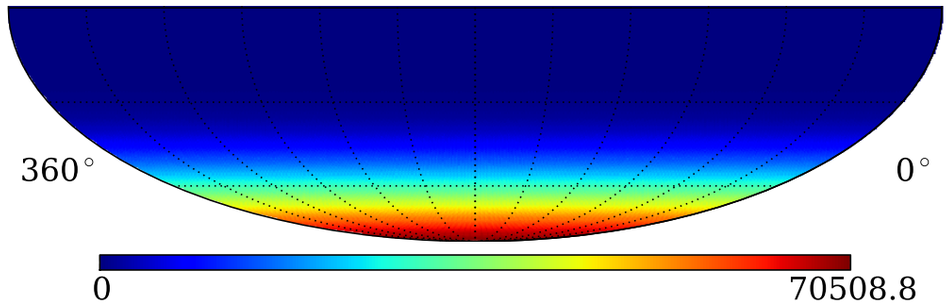

rebin raw and reference maps to enhance inter-bin correlations

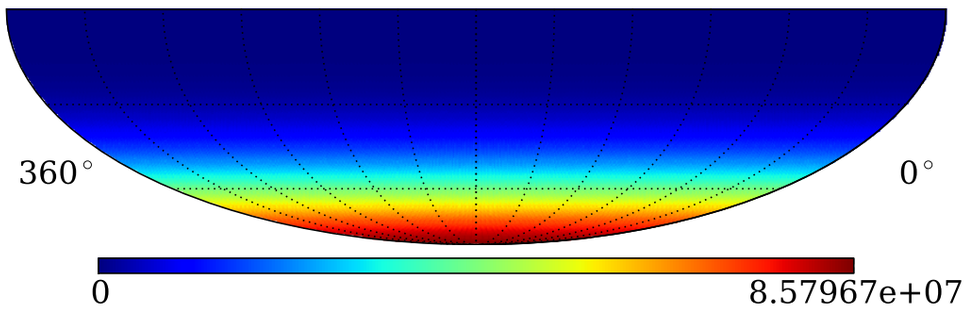

subtract reference map from raw map to determine the residual *relative intensity* map

$$\frac{\Delta I}{\langle I \rangle} \equiv \frac{N_i - \langle N \rangle}{\langle N \rangle}$$

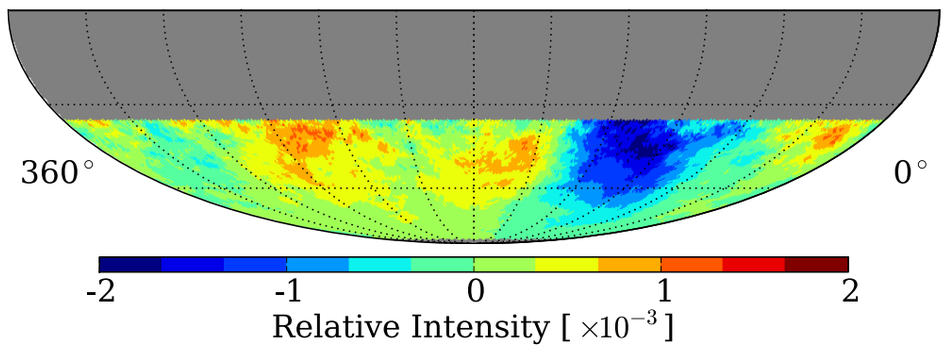

cosmic ray anisotropy energy selection

IceCube

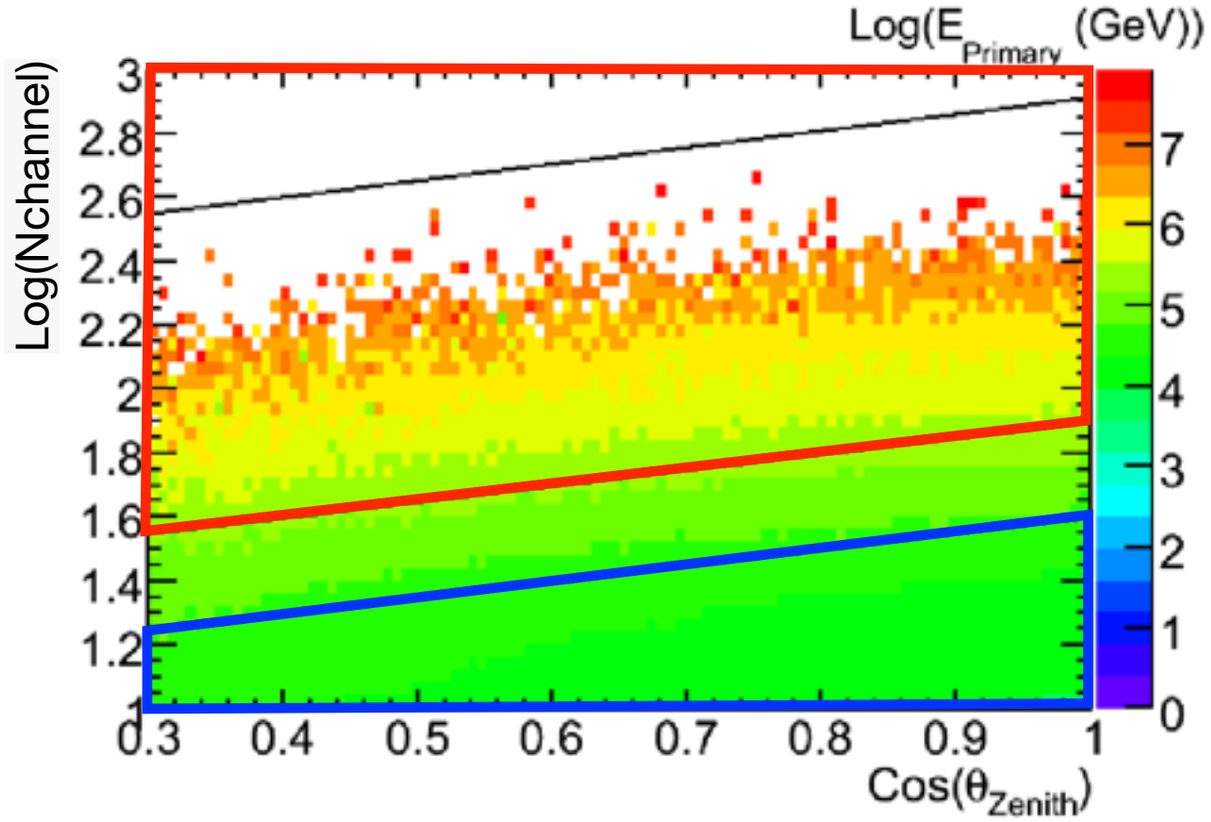

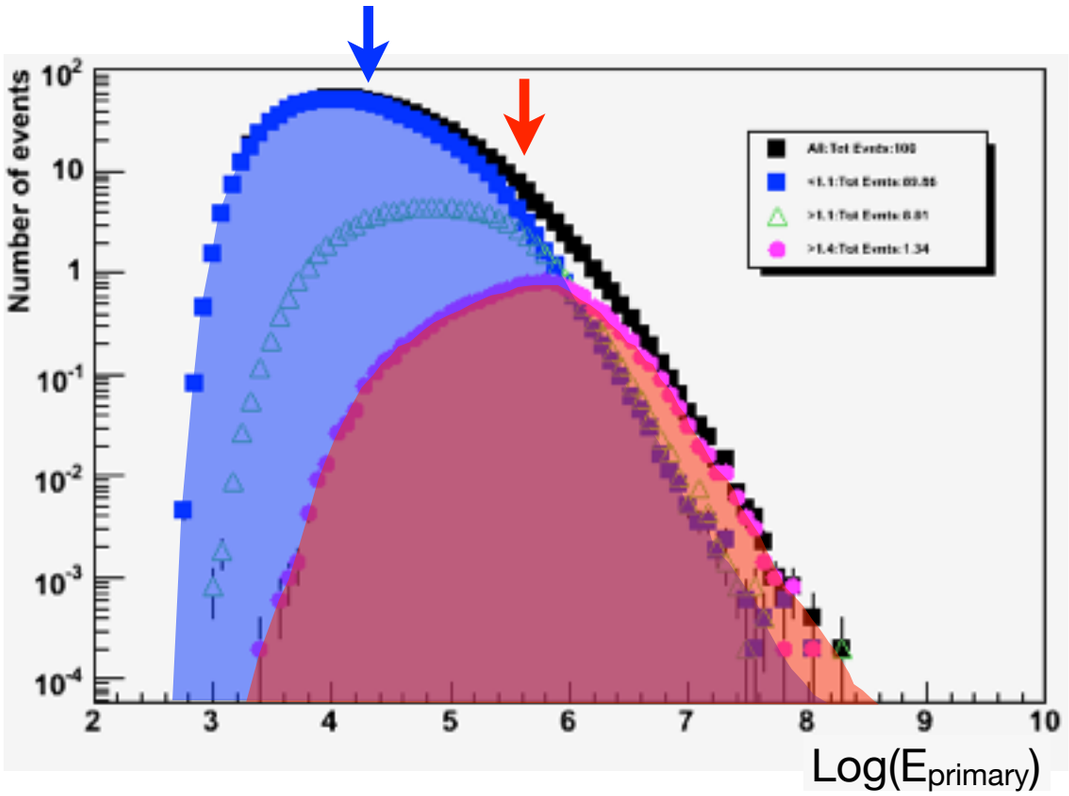

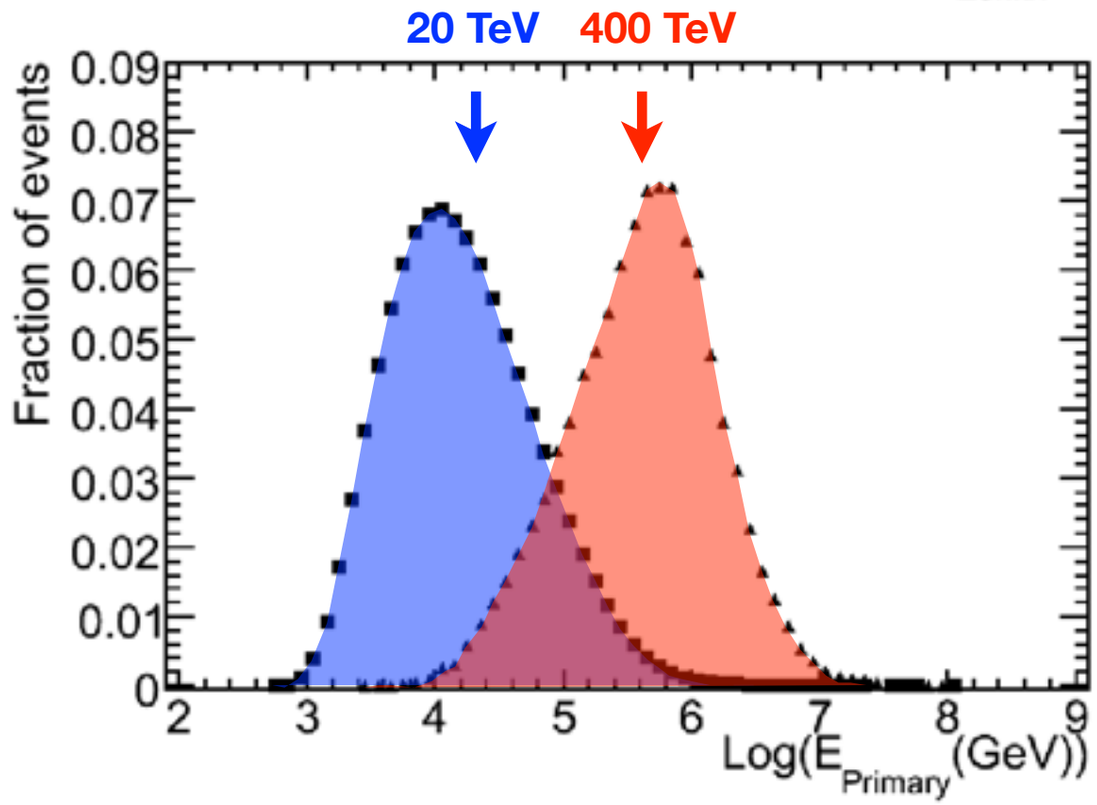

cosmic ray anisotropy vs energy in IceCube-59

EAS-TOP

370 TeV

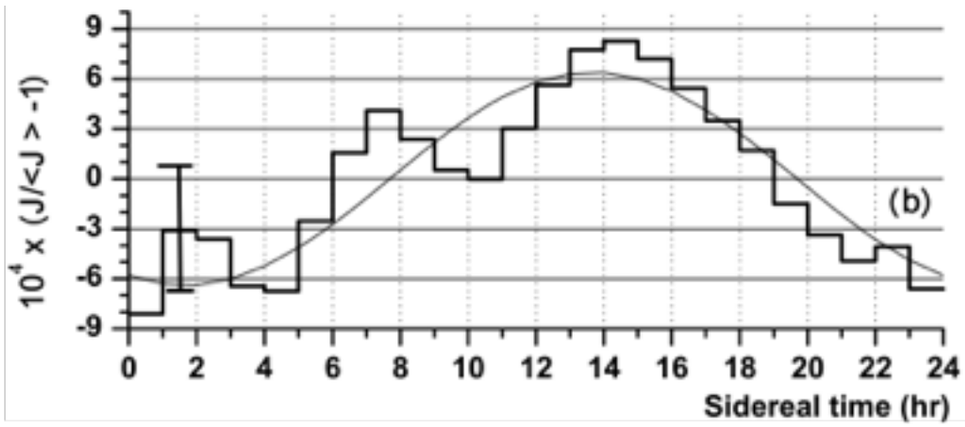

Tibet-III

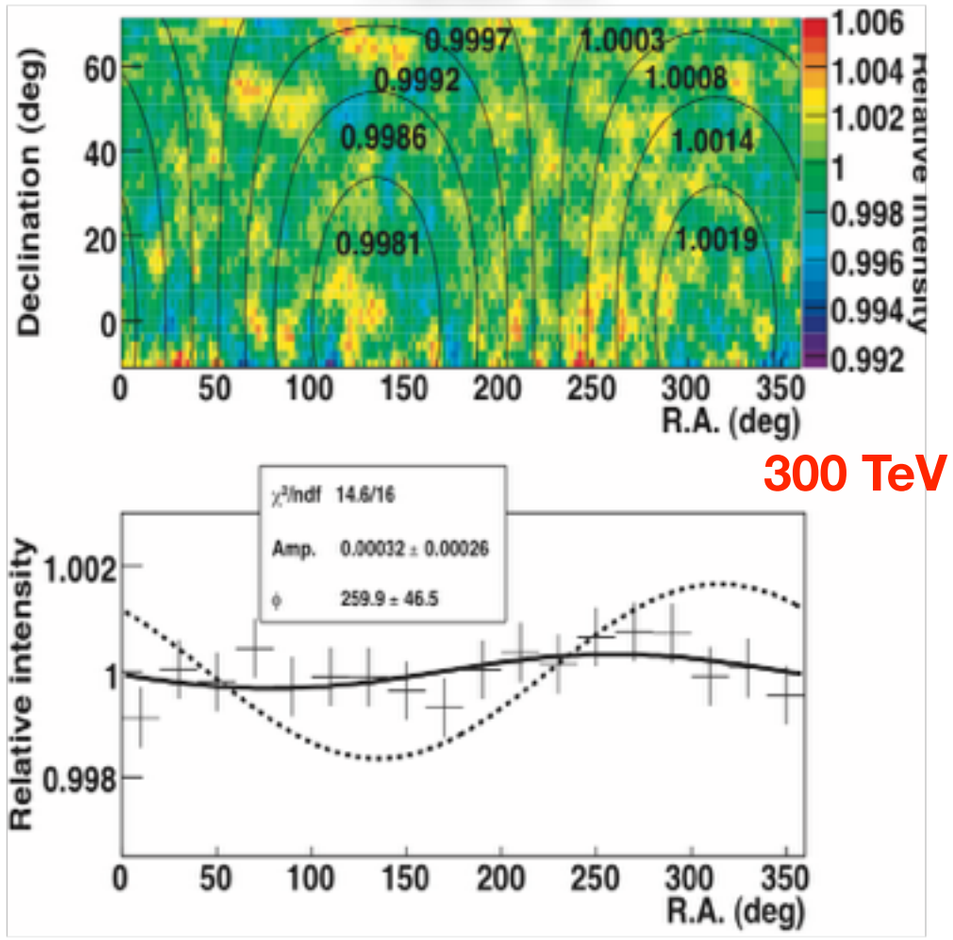

Abbasi et al., ApJ, **746**, 33, 2012

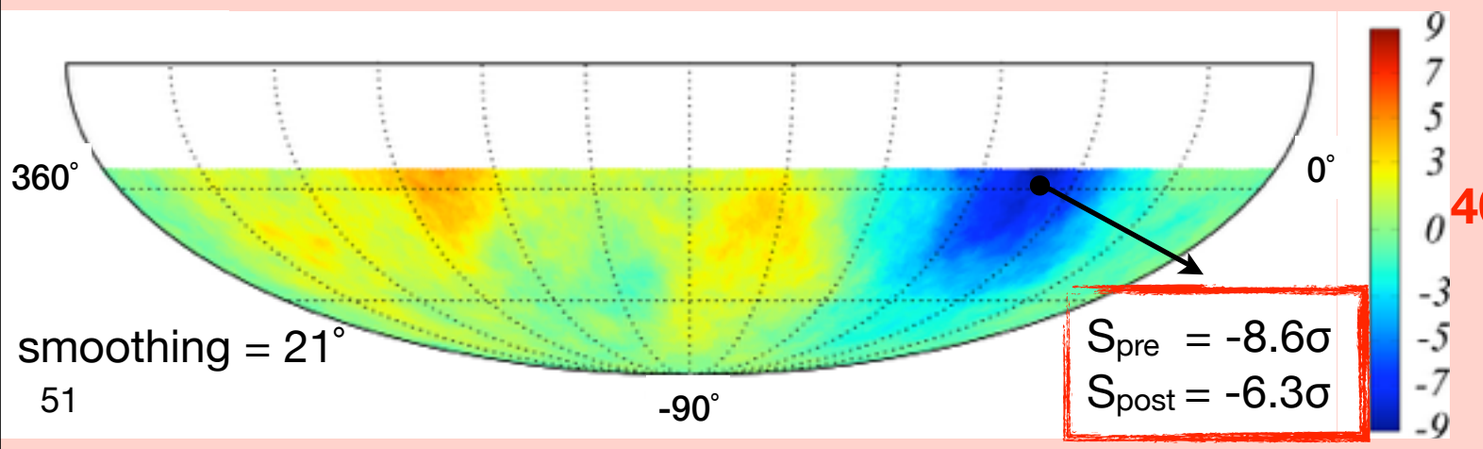

400 TeV

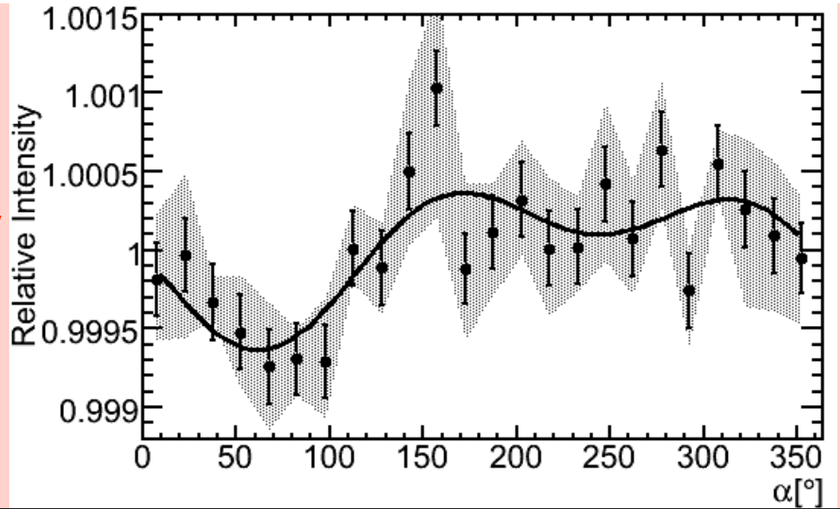

cosmic ray anisotropy large scale
IceCube

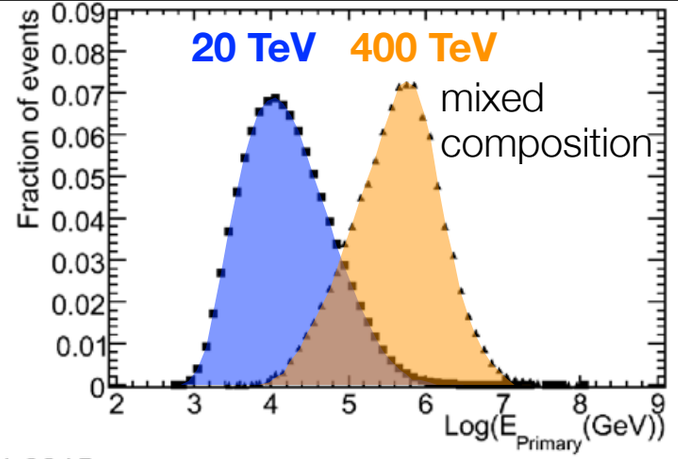

relative intensity equatorial coordinates

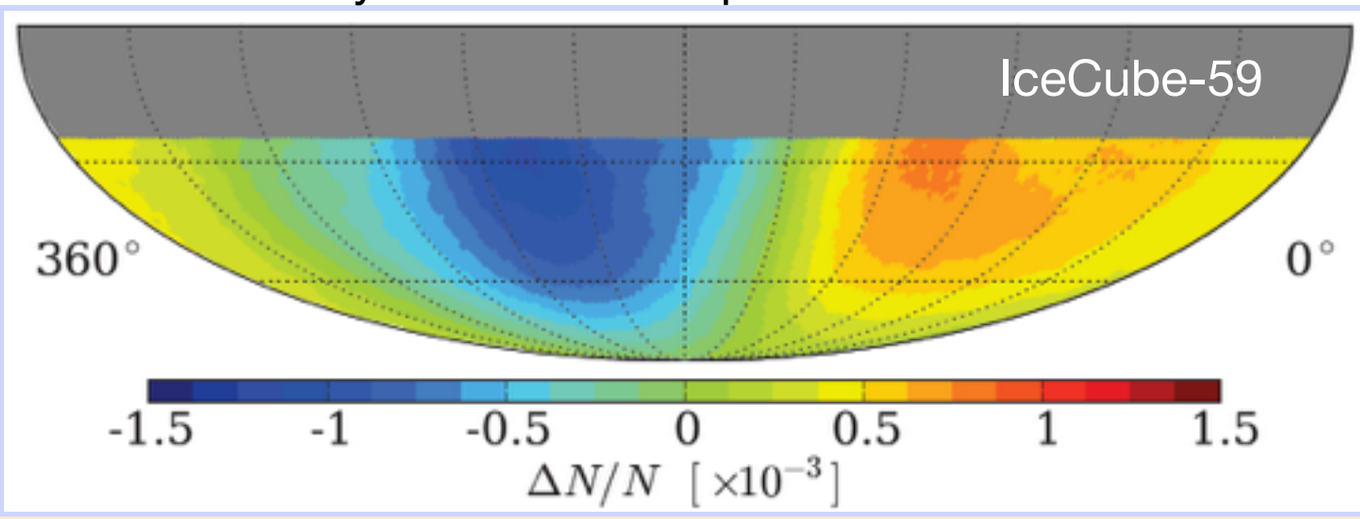

20 TeV

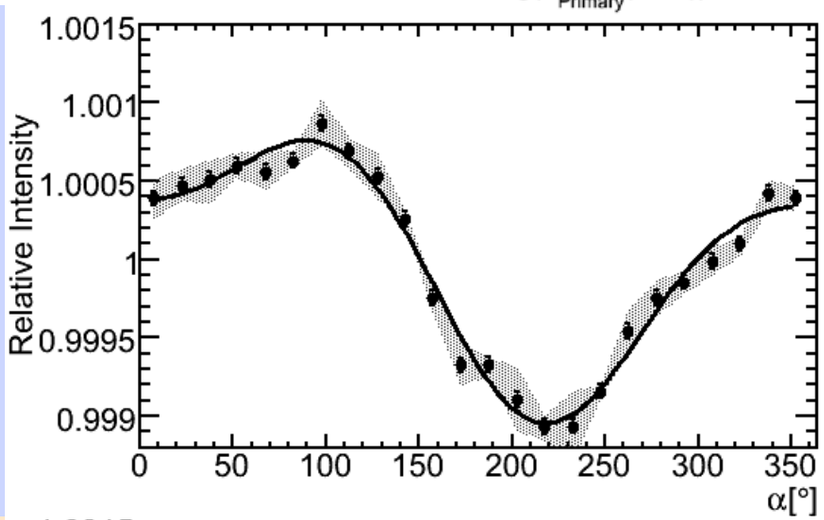

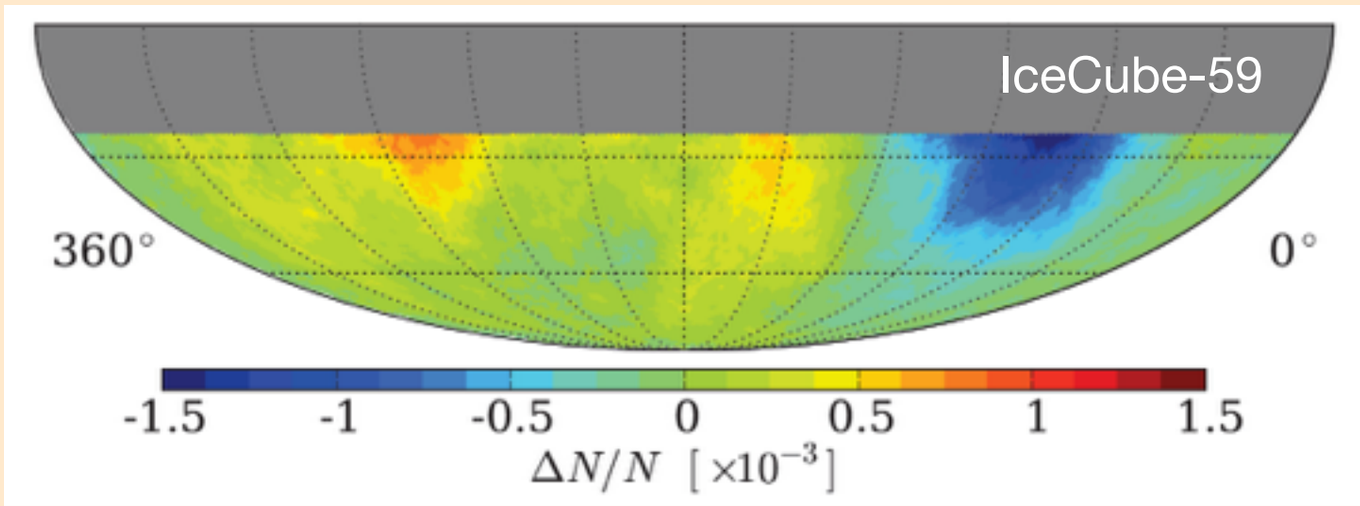

400 TeV

deficit
6.3 σ_{post}

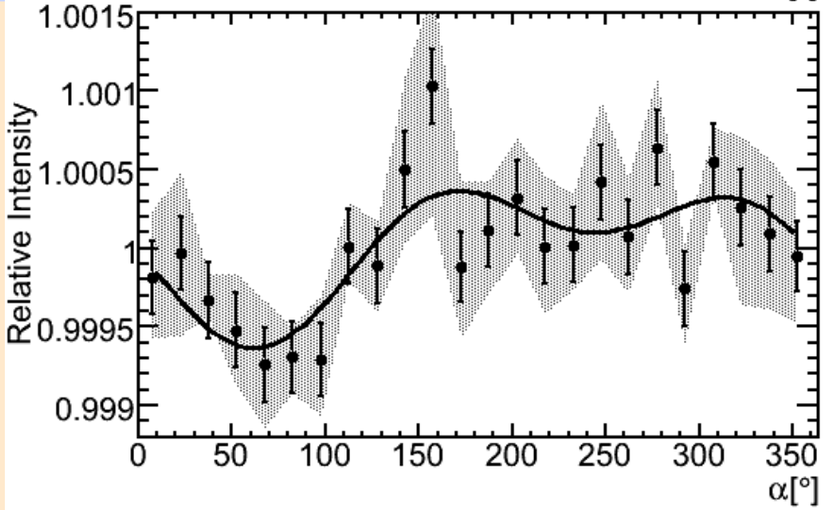

NOTE: anisotropy is not a dipole
topology changes at high energy

IC59 Abbasi et al., ApJ, **746**, 33, 2012

IC22 Abbasi et al., ApJ, **718**, L194, 2010

cosmic ray anisotropy large scale
IceCube

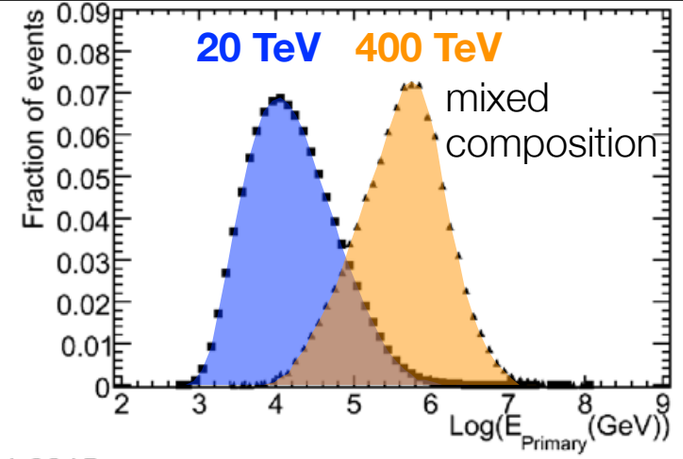

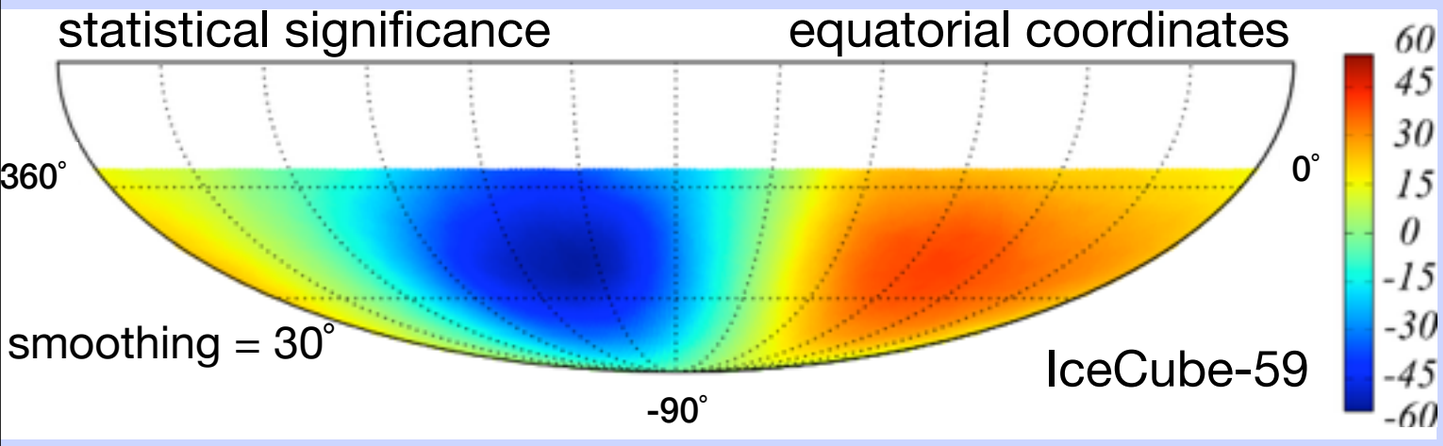

20 TeV

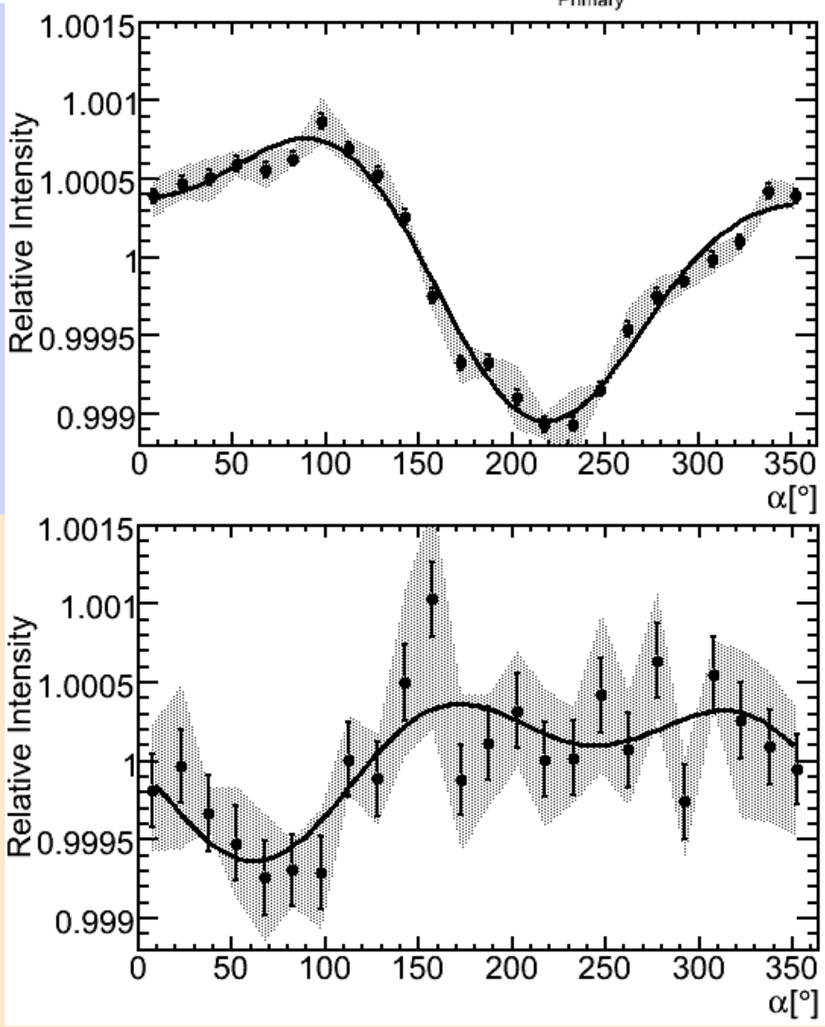

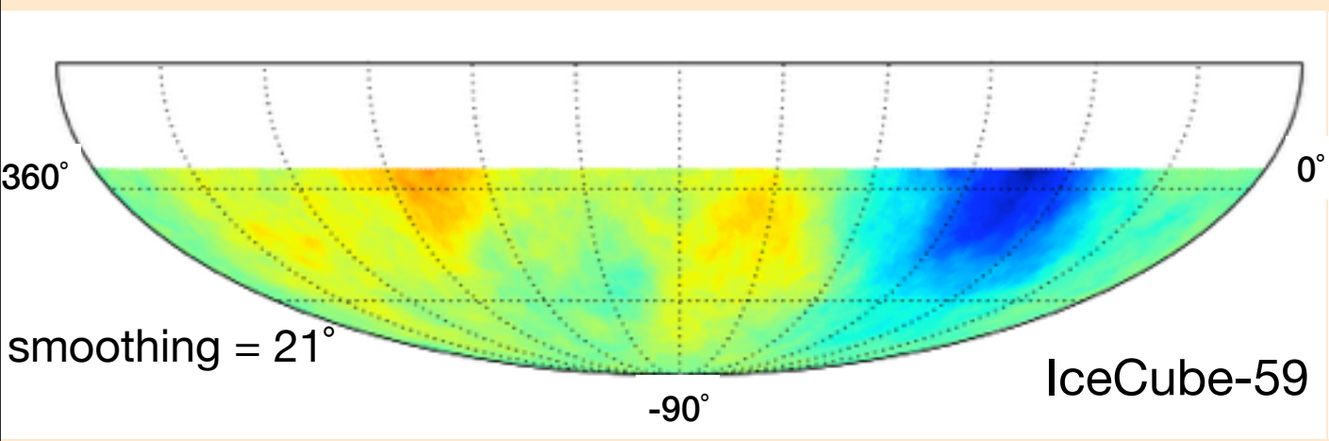

400 TeV

deficit

6.3 σ_{post}

NOTE: anisotropy is not a dipole
topology changes at high energy

IC59 Abbasi et al., ApJ, **746**, 33, 2012

IC22 Abbasi et al., ApJ, **718**, L194, 2010

cosmic ray anisotropy vs energy in IceCube-59

energy

- reference map derived from data with time scrambling
- smoothing radius optimized on highest significance in excess/deficit region

$$s = \sqrt{2}\left\{ N_{\rm on} \ln\left[\frac{1+\alpha}{\alpha}\left(\frac{N_{\rm on}}{N_{\rm on}+N_{\rm off}}\right)\right] + N_{\rm off} \ln\left[(1+\alpha)\left(\frac{N_{\rm off}}{N_{\rm on}+N_{\rm off}}\right)\right]\right\}^{1/2} \qquad \alpha = 1/20$$

Li, T., & Ma, Y. 1983, ApJ, 272, 317

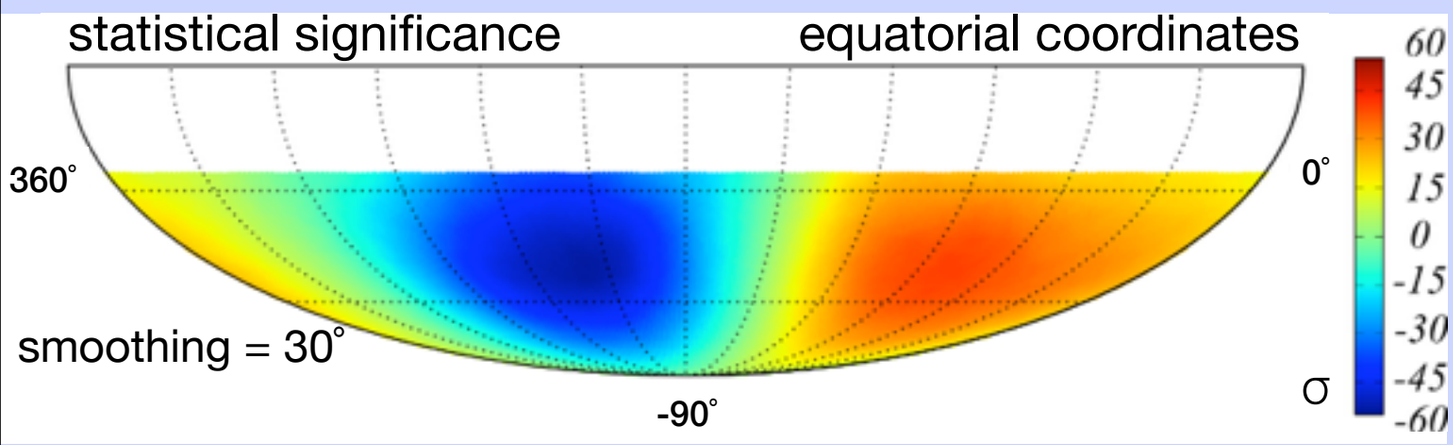

20 TeV

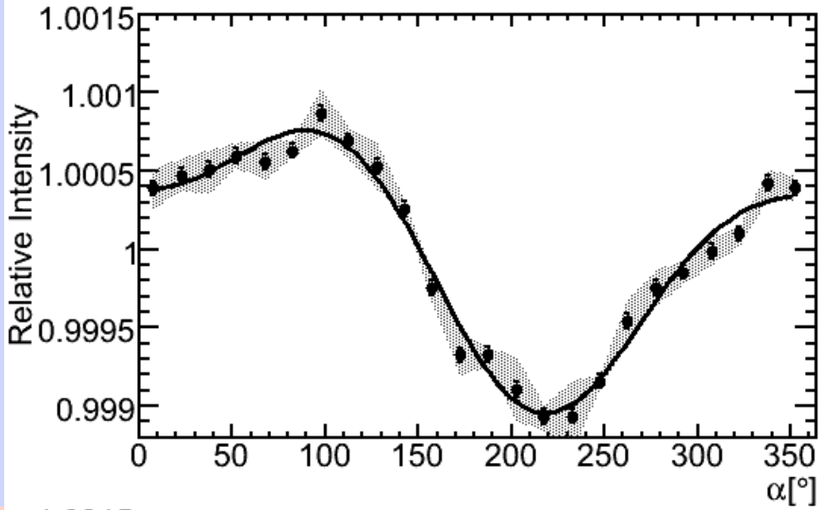

Abbasi et al., ApJ, **746**, 33, 2012

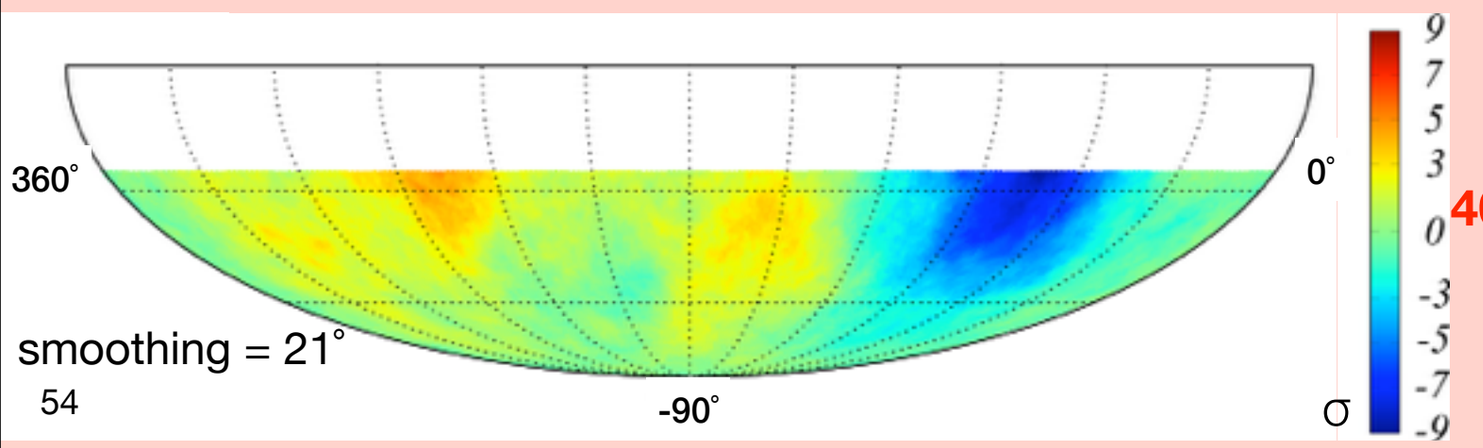

400 TeV

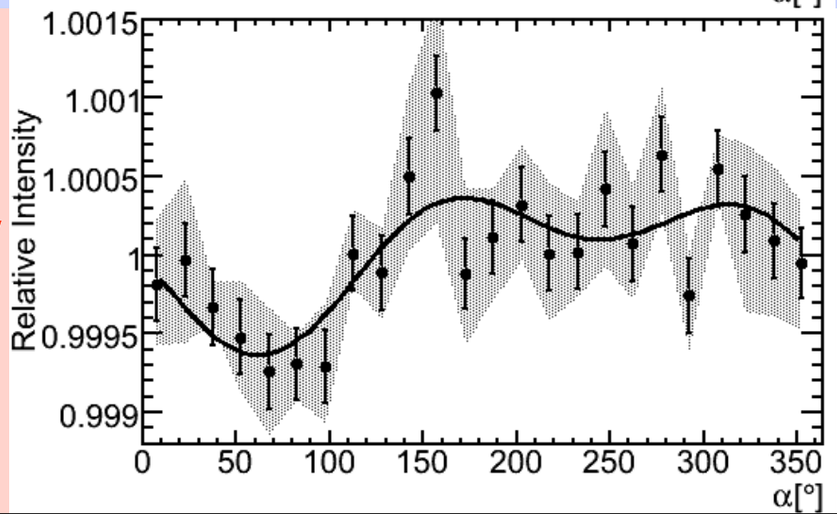

cosmic ray anisotropy large scale
IceTop

relative intensity equatorial coordinates

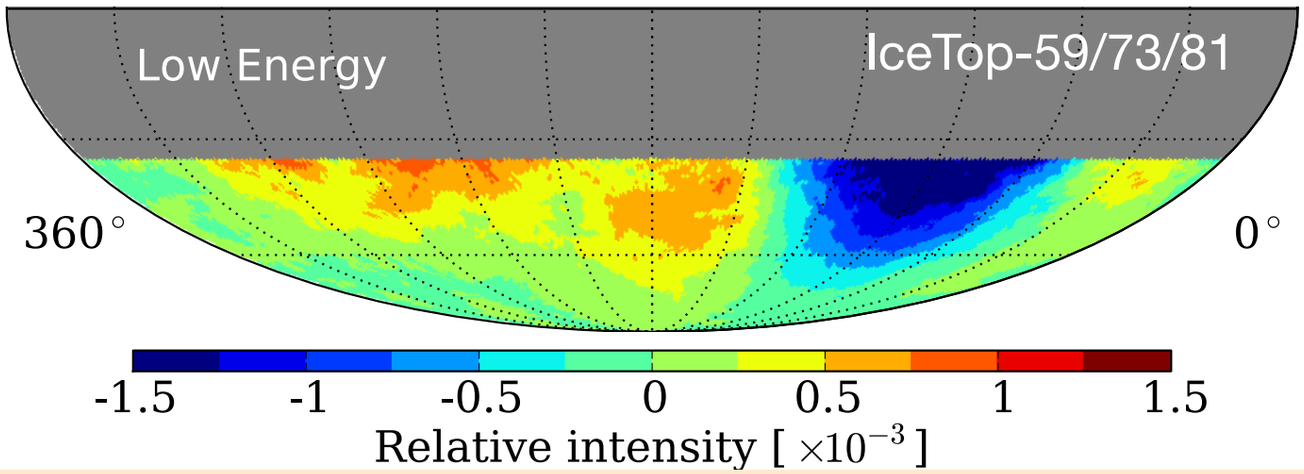

deficit
7 σ_{post}

400 TeV

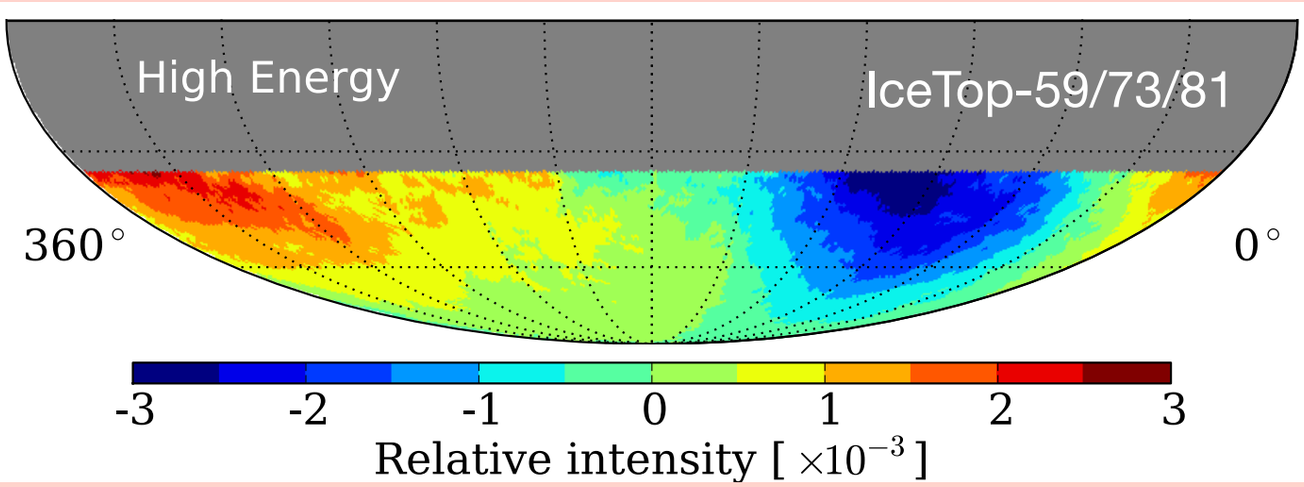

2 PeV

Aartsen et al., ApJ, **765**, 55, 2013

NOTE: global topology does not change

deficit amplitude increases with energy

cosmic ray anisotropy large scale
IceCube & IceTop

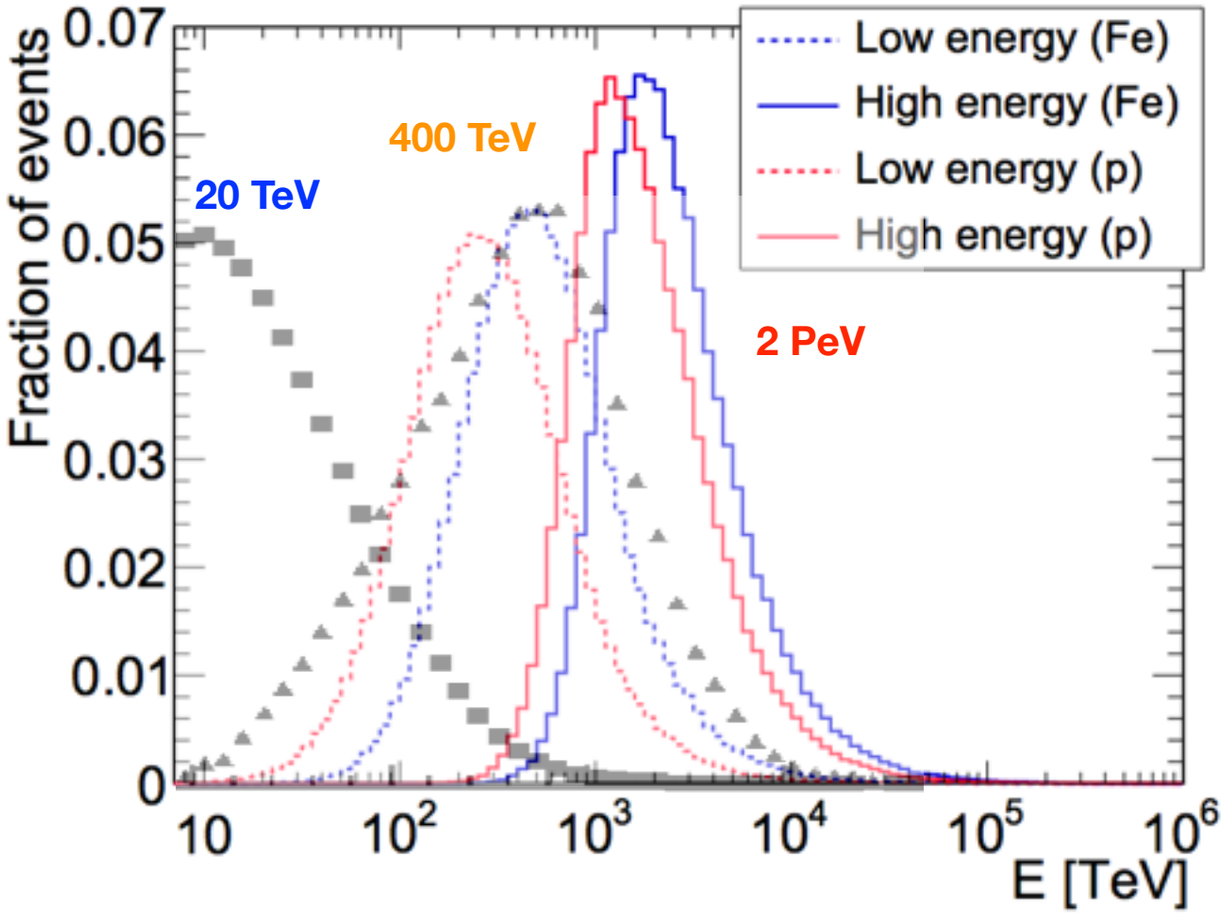

Aartsen et al., ApJ, **765**, 55, 2013

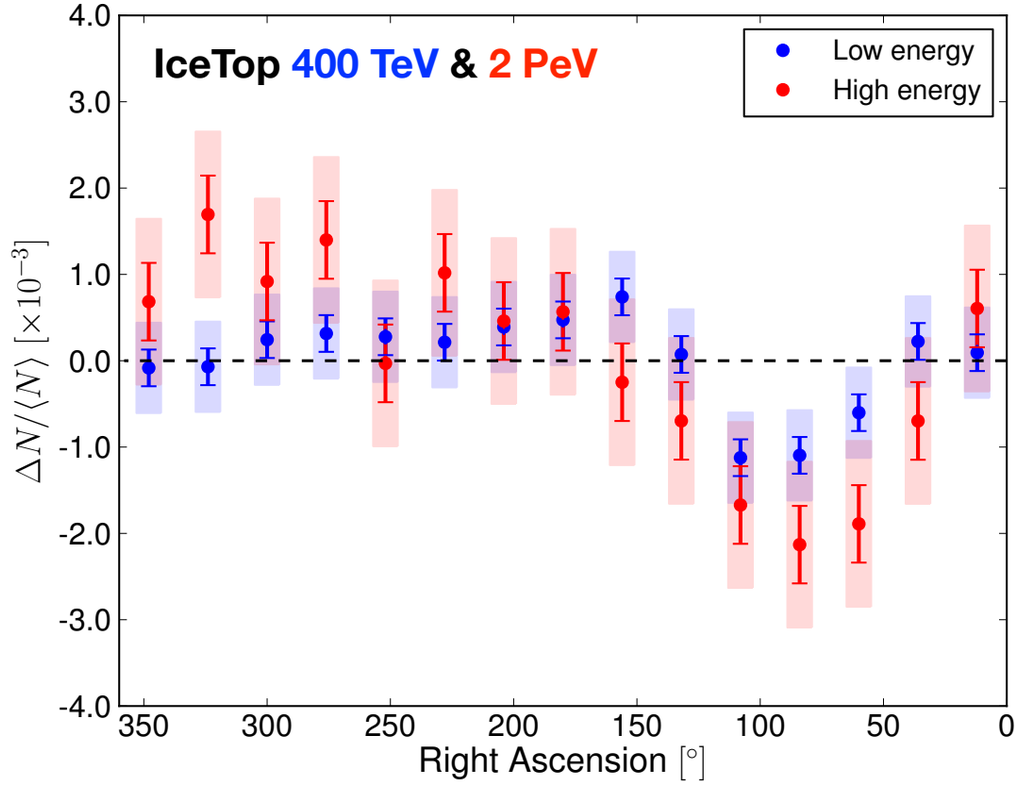

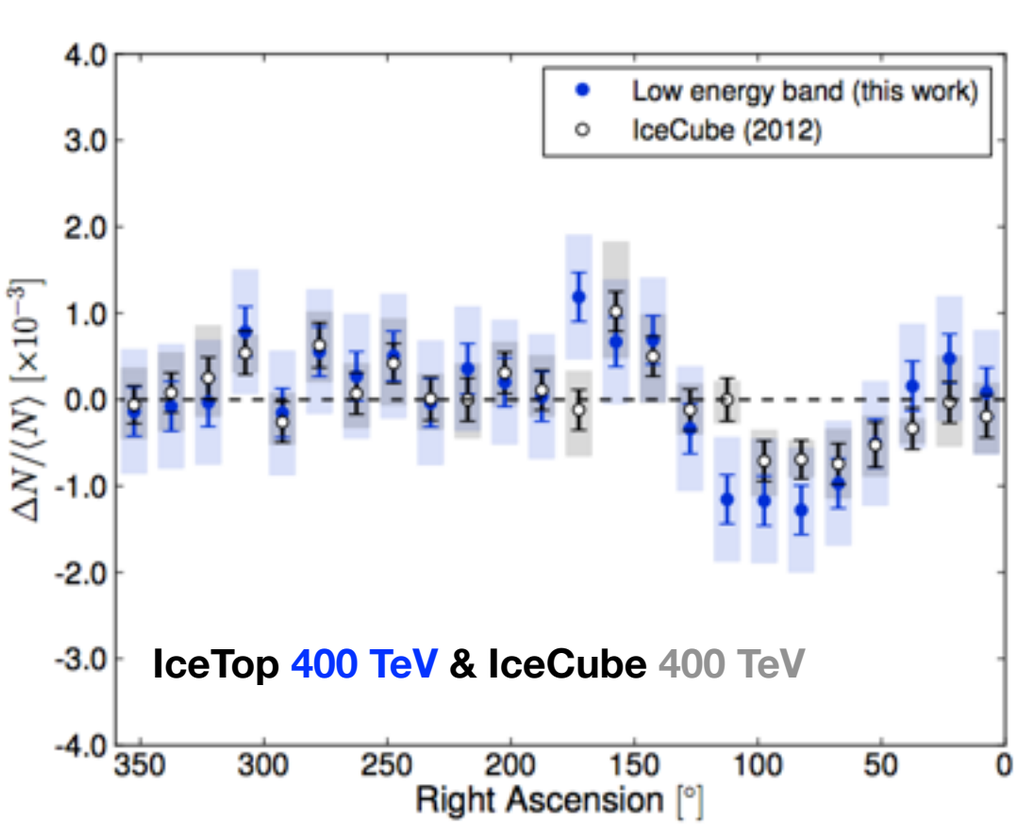

NOTE: different energy response distribution

IceTop with *sharper* low energy threshold

might explain IC/IT amplitude differences

cosmic ray anisotropy large scale
IceTop

relative intensity — equatorial coordinates

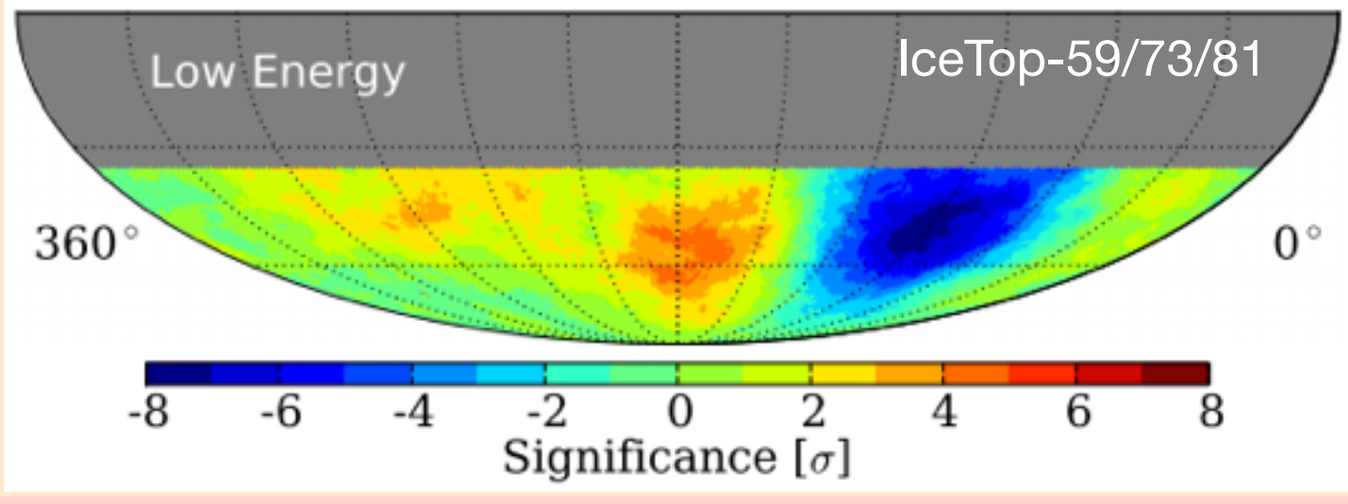

deficit
7 σ_{post}

400 TeV

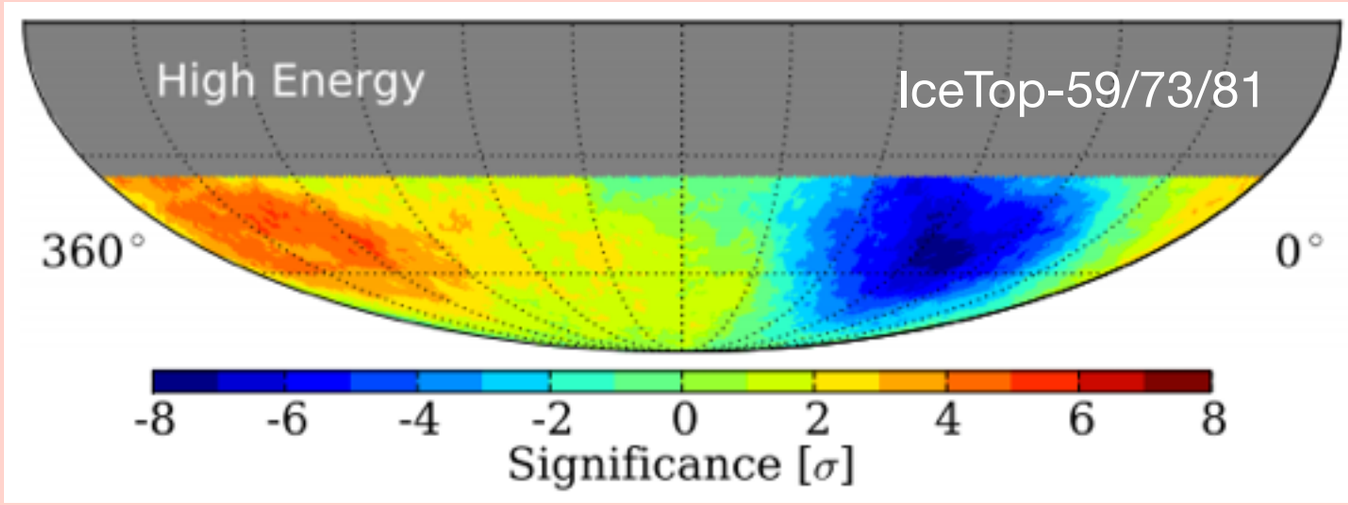

2 PeV

Aartsen et al., ApJ, **765**, 55, 2013

NOTE: global topology does not change

deficit amplitude increases with energy

cosmic ray anisotropy

large scale

IceCube

20 TeV

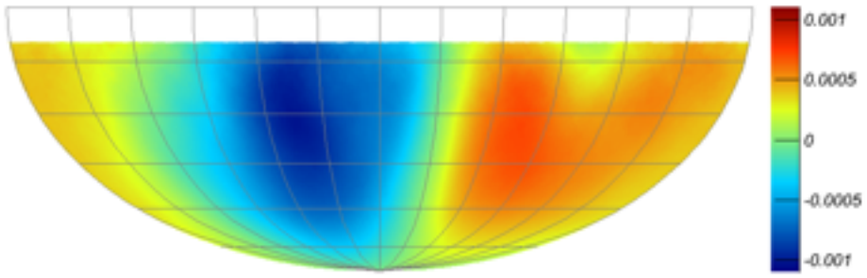

400 TeV

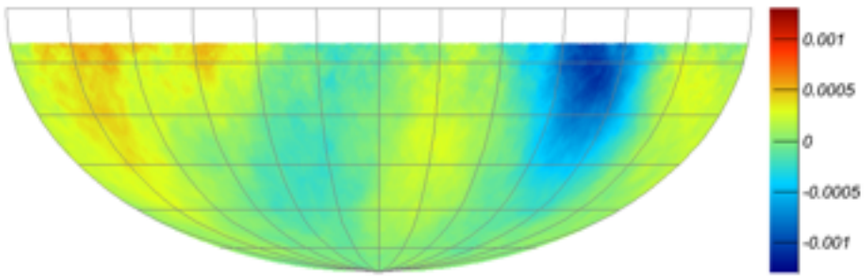

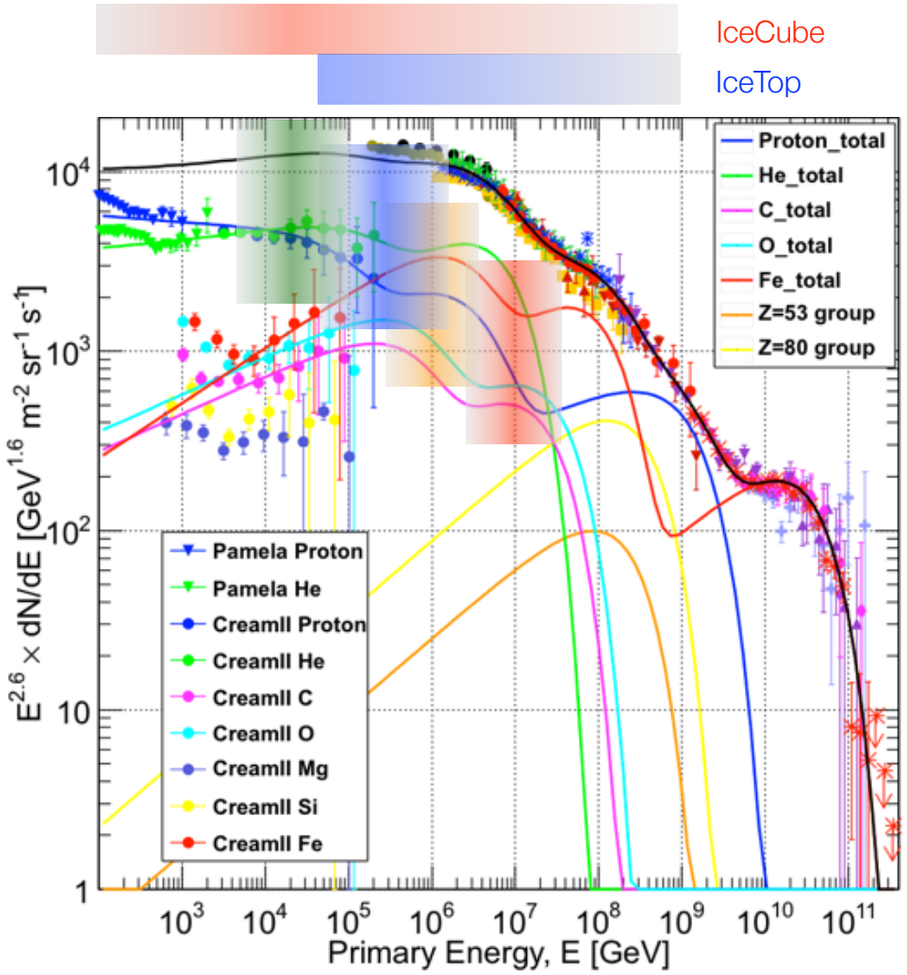

1 PeV

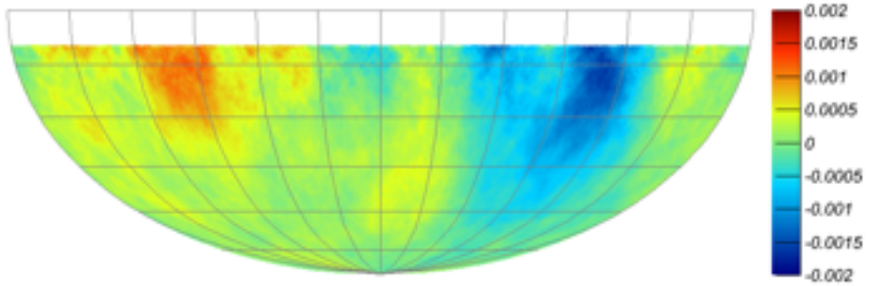

PRELIMINARY

10 PeV

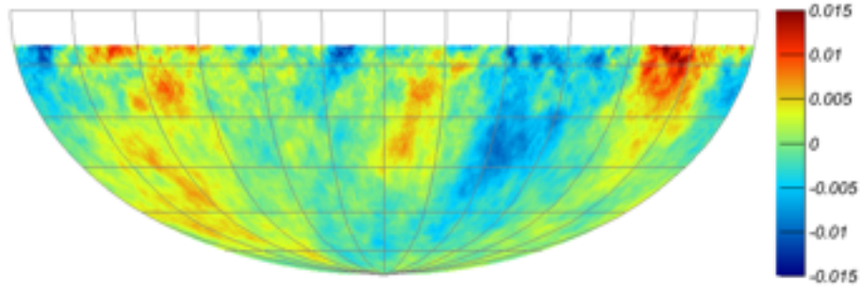

PRELIMINARY

cosmic ray anisotropy large scale energy dependency

Tibet ASγ Amenomori et al., ApJ. 626, L29, 2005

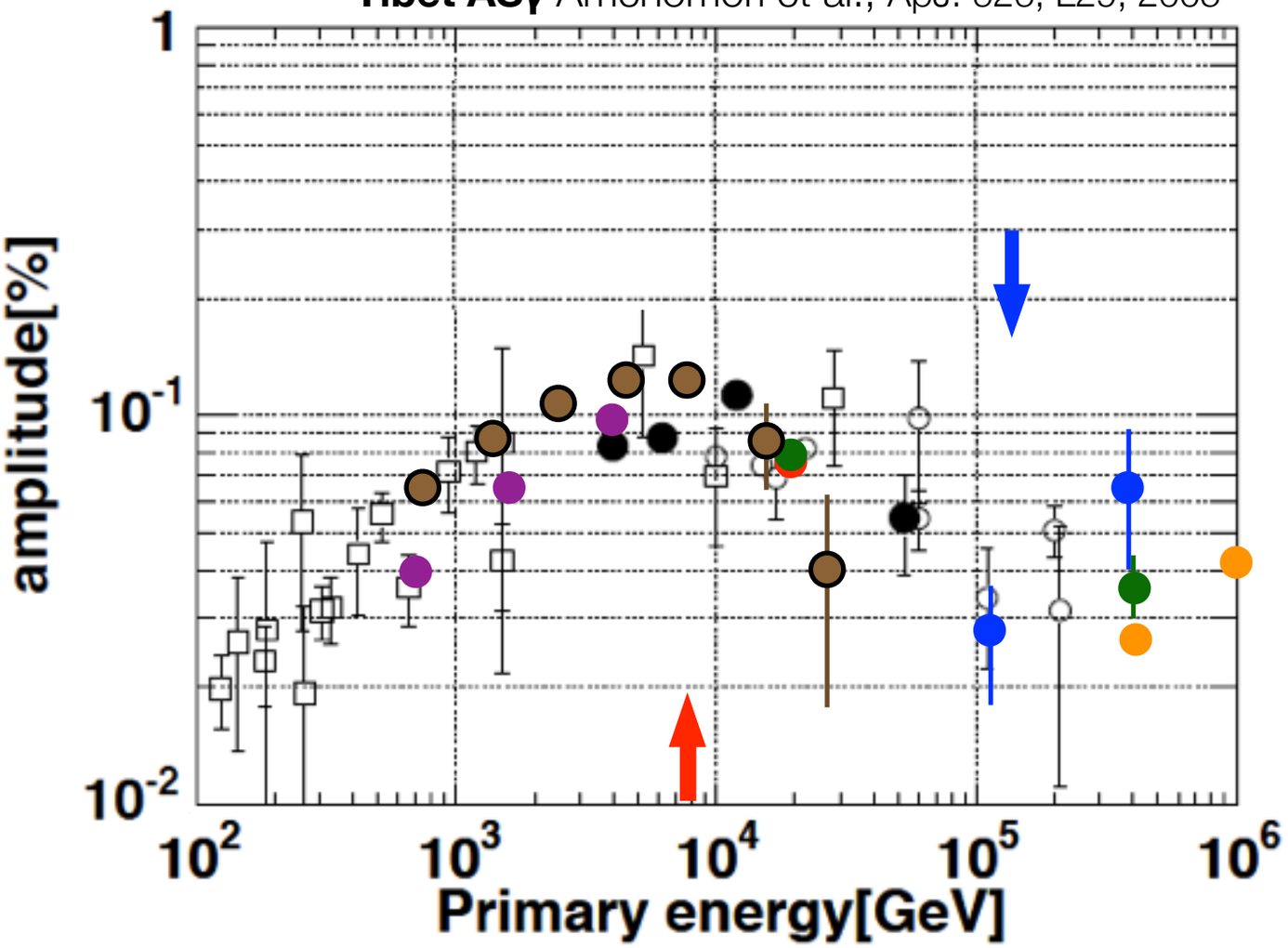

dipole component
- **IceCube-22** Abbasi et al., ApJ, 718, L194, 2010
- **IceCube-59** Abbasi et al., ApJ, 746, 33, 2012
- **EAS-TOP** Aglietta et al., ApJ, 692, L130, 2009
- **ARGO-YBJ** Zhang 31st ICRC Łódź-Poland,2009
- **ARGO-YBJ** 32nd ICRC Beijng China,2011

gaussian fit
- **IceTop** Aartsen et al., ApJ, 765, 55, 2013

- modulation in amplitude of **dipole component**
- corresponds to **transition** in **anisotropy topology**

cosmic ray anisotropy large scale energy dependency

Tibet ASγ Amenomori et al., ApJ. 626, L29, 2005

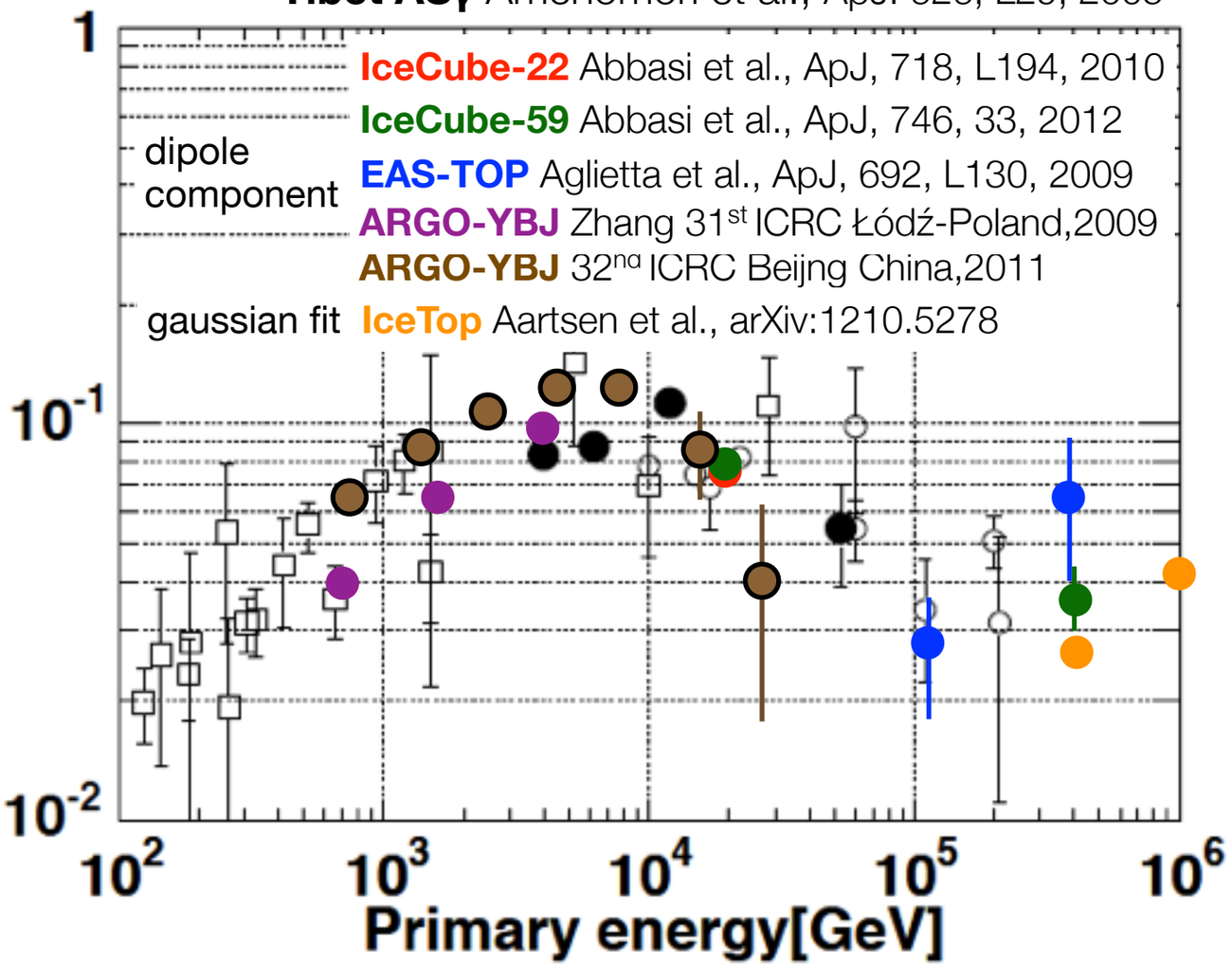

ICRC 2013

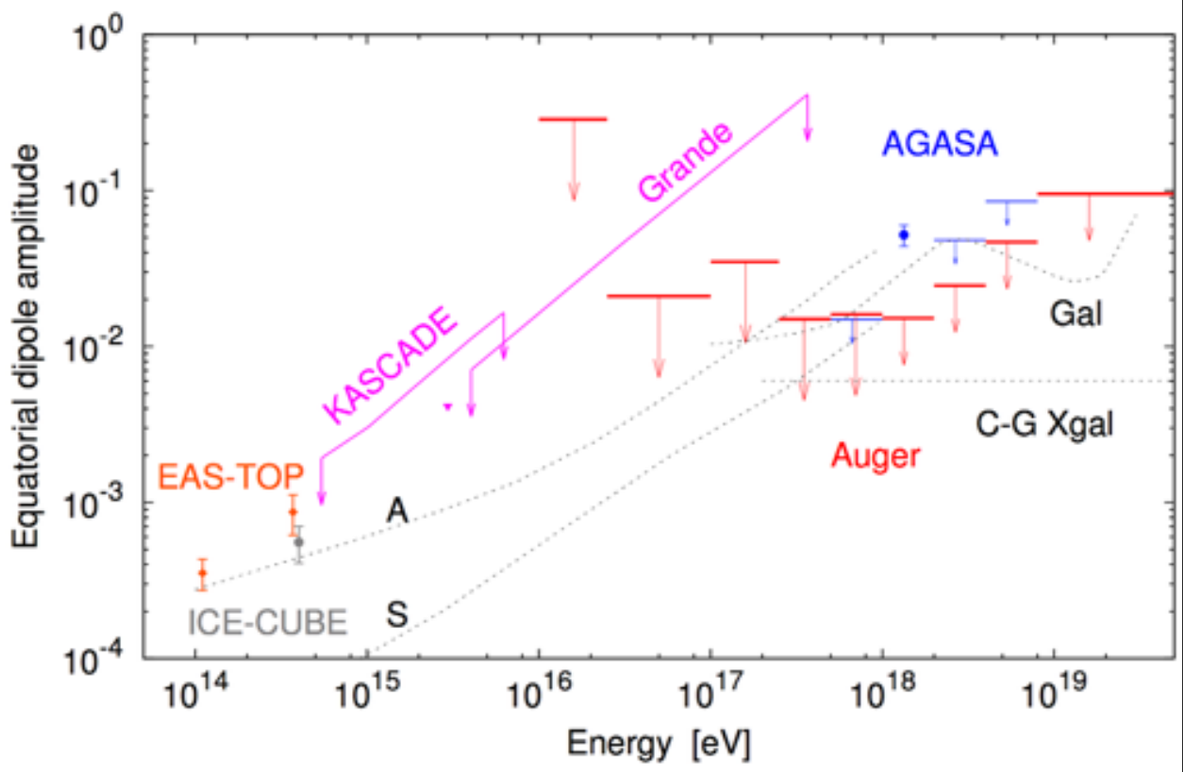

a known anisotropy

Earth's motion around the Sun

Compton & Getting, Phys. Rev. 47, 817 (1935)
Gleeson, & Axford, Ap&SS, 2, 43 (1968)

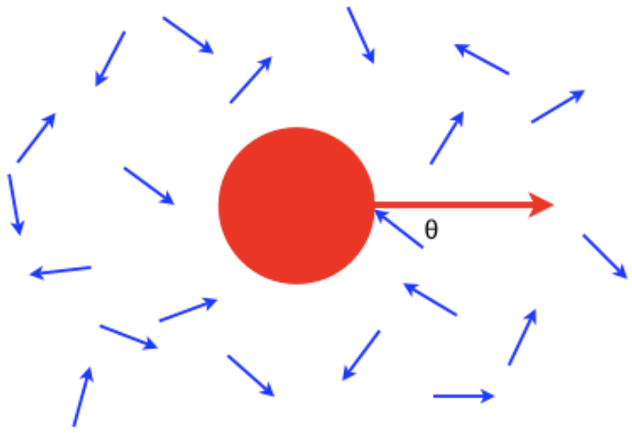

v = 29.8 ± 0.5 km/s

$$\frac{\Delta I}{I} = (\gamma + 2)\frac{v}{c}\cos\theta$$

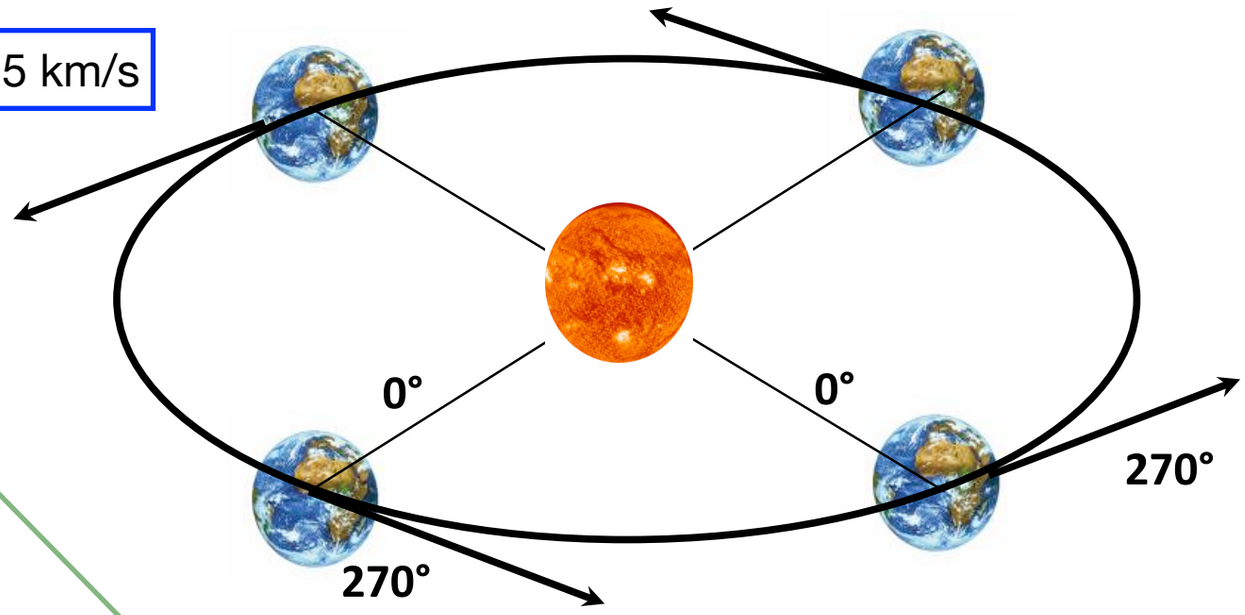

Hörandel, Astrop. Phys. 19, 193, 2003

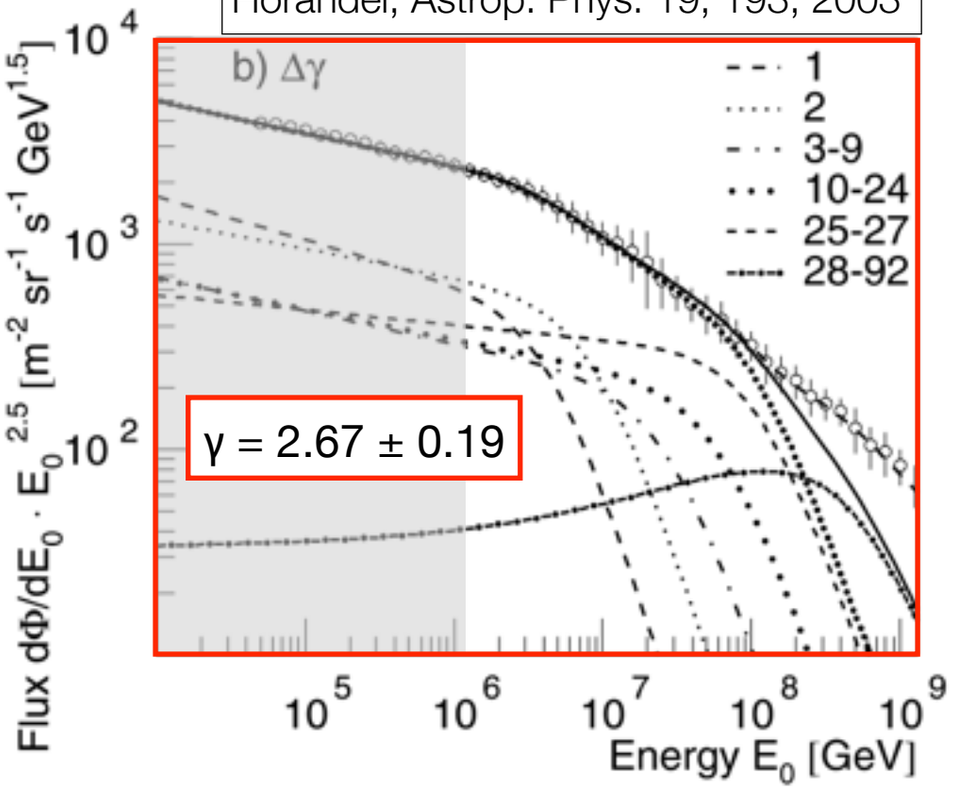

point spread function

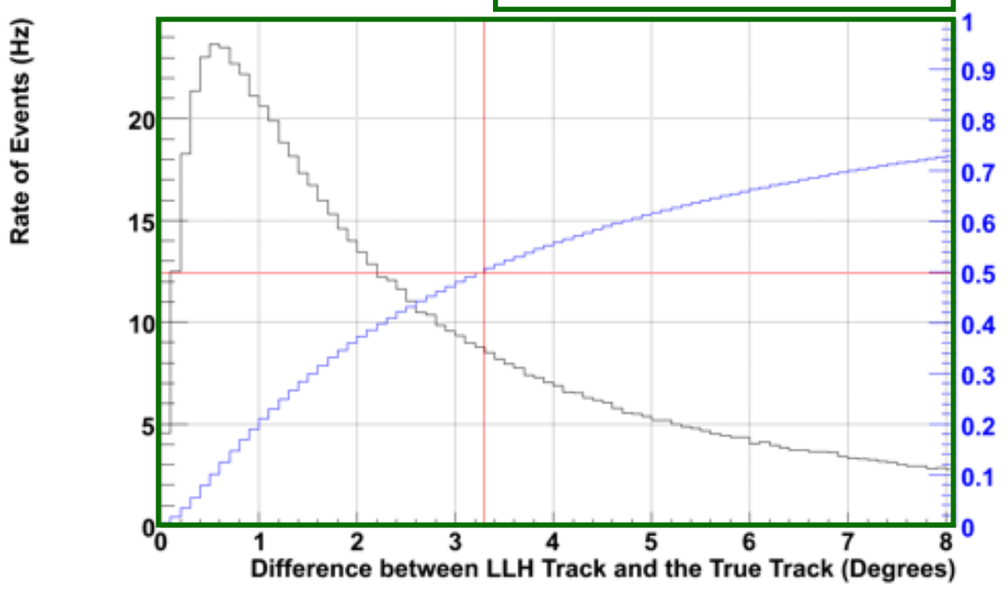

a known anisotropy

Earth's motion around the Sun

- the observation of the **solar dipole** supports the observation of the sidereal anisotropy in cosmic ray arrival direction

- **NO Compton-Getting Effect** signature from galactic rotation observed

relative intensity

α [°] - α_{SUN} [°]

IC59 Abbasi et al., ApJ, **746**, 33, 2012

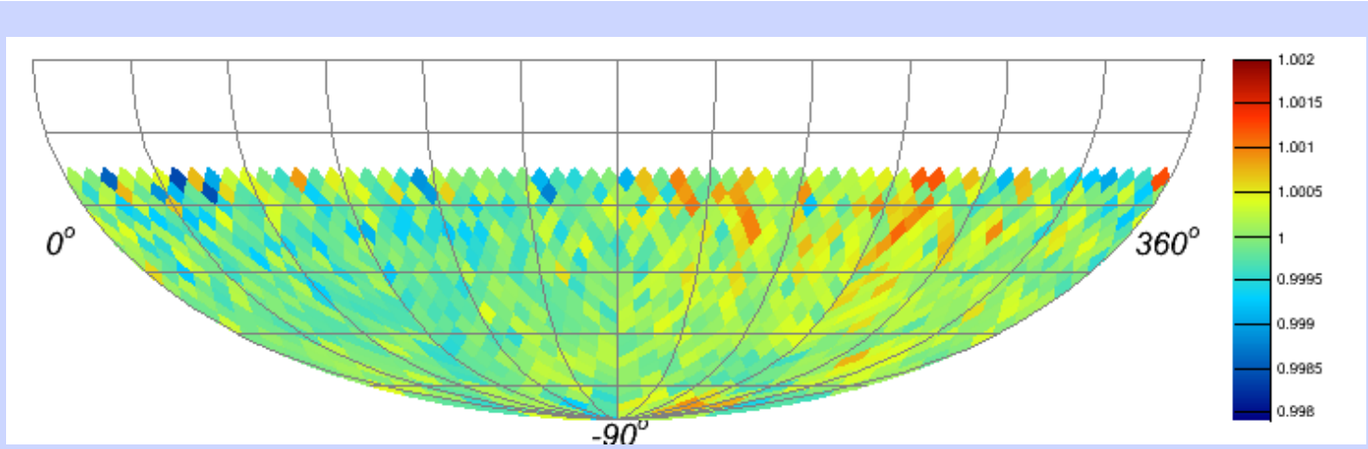

20 TeV

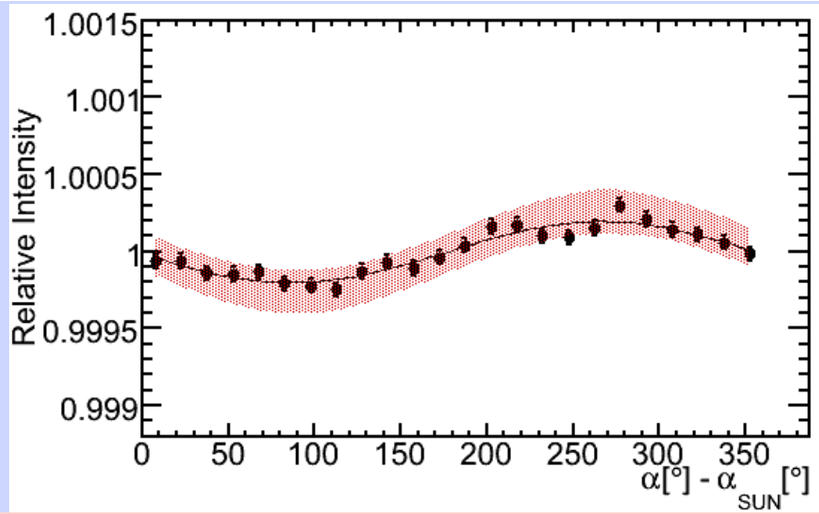

Abbasi et al., ApJ, **746**, 33, 2012

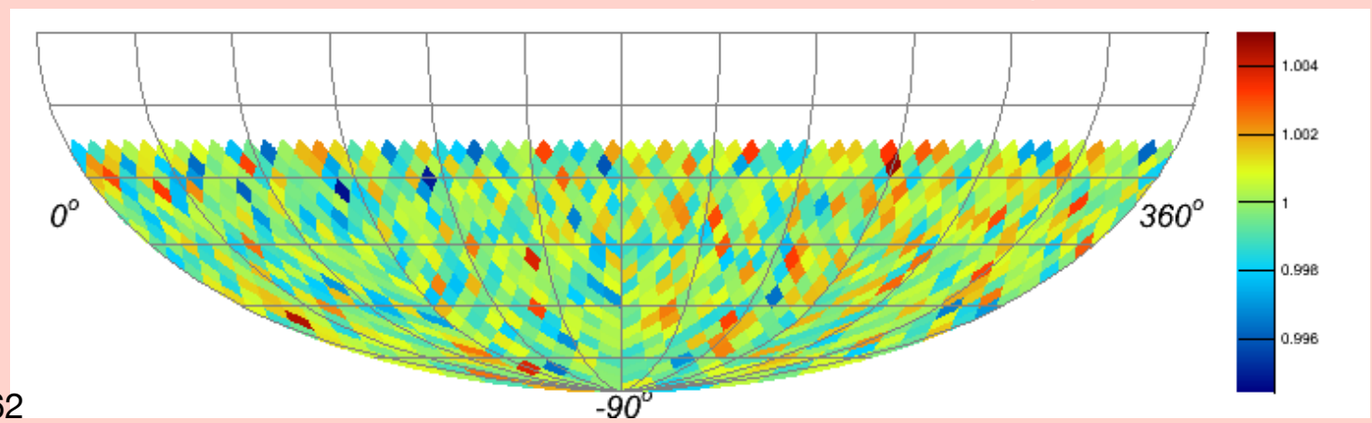

400 TeV

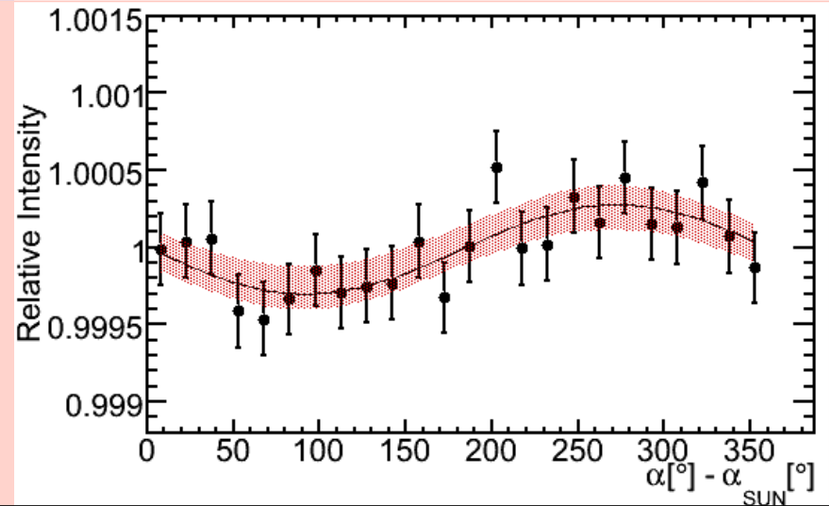

origin of large scale anisotropy : Compton-Getting Effect ?

Compton & Getting, Phys. Rev. 47, 817 (1935)
Gleeson, & Axford, Ap&SS, 2, 43 (1968)

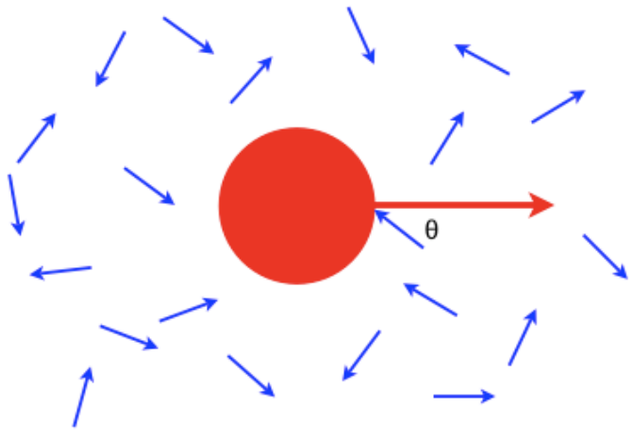

$$\frac{\Delta I}{I} = (\gamma + 2)\frac{v}{c}\cos\theta$$

- motion of solar system around galactic center ~ 220 km/s
- reference system of cosmic rays is **unknown**
  - at most one dipole component of the observation

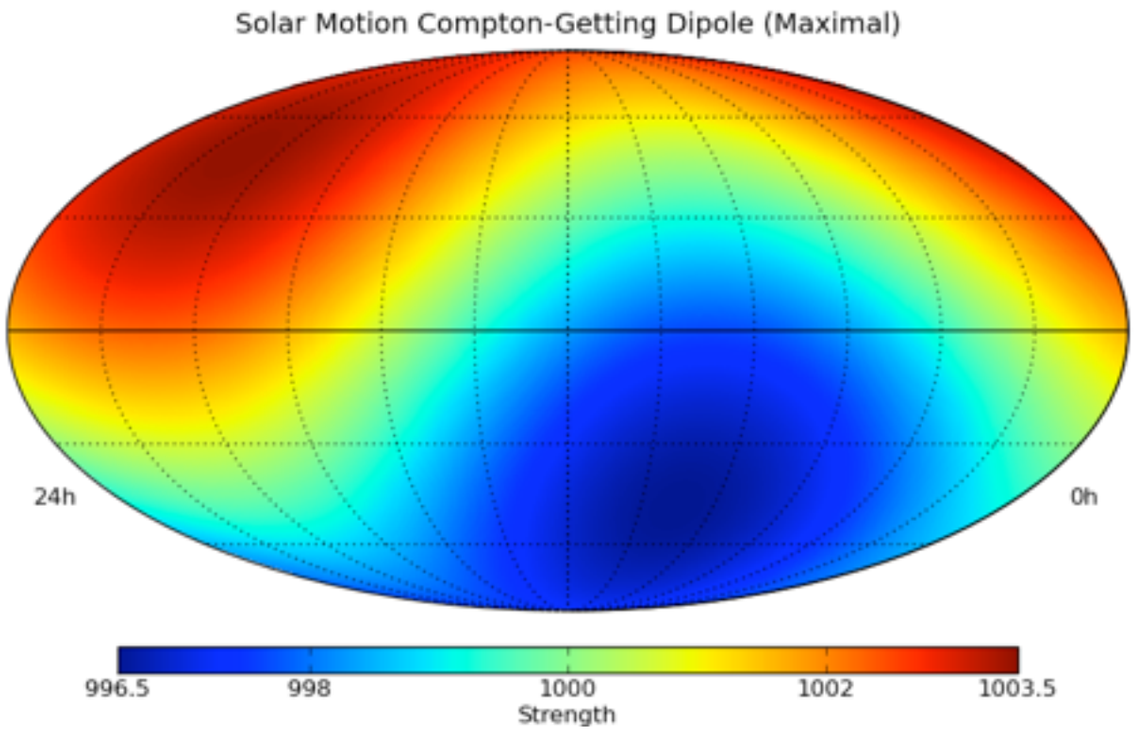

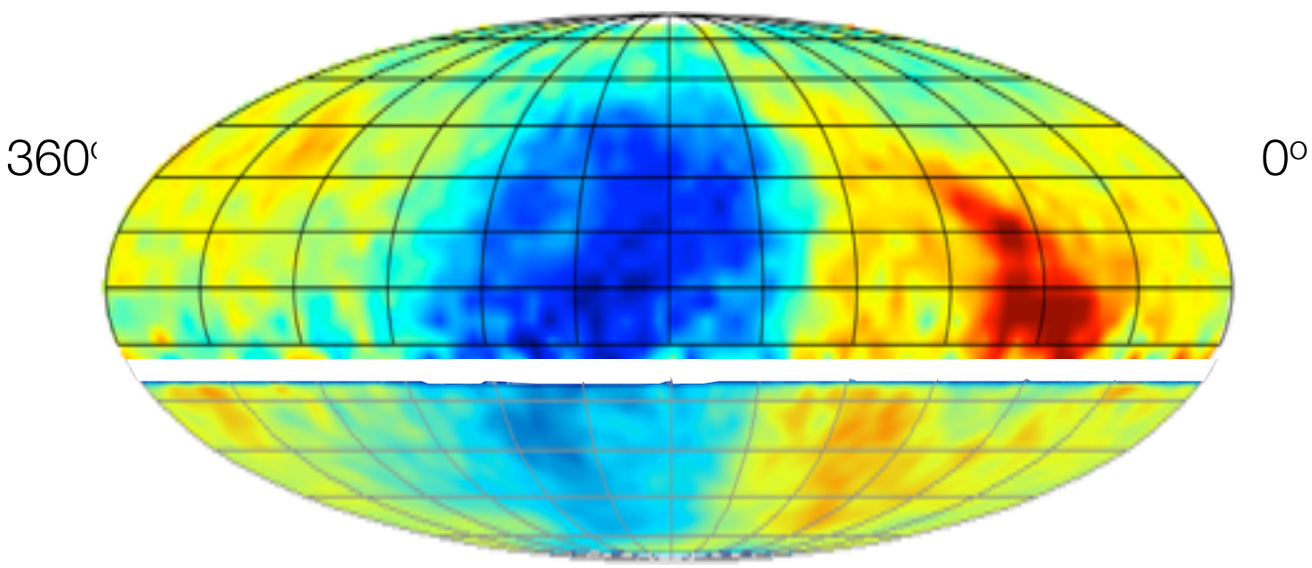

anti-/extended-sidereal distributions vs energy in IceCube-59

anti-sidereal distribution ~ solar dipole variability

extended-sidereal distribution ~ sid. anis. variability

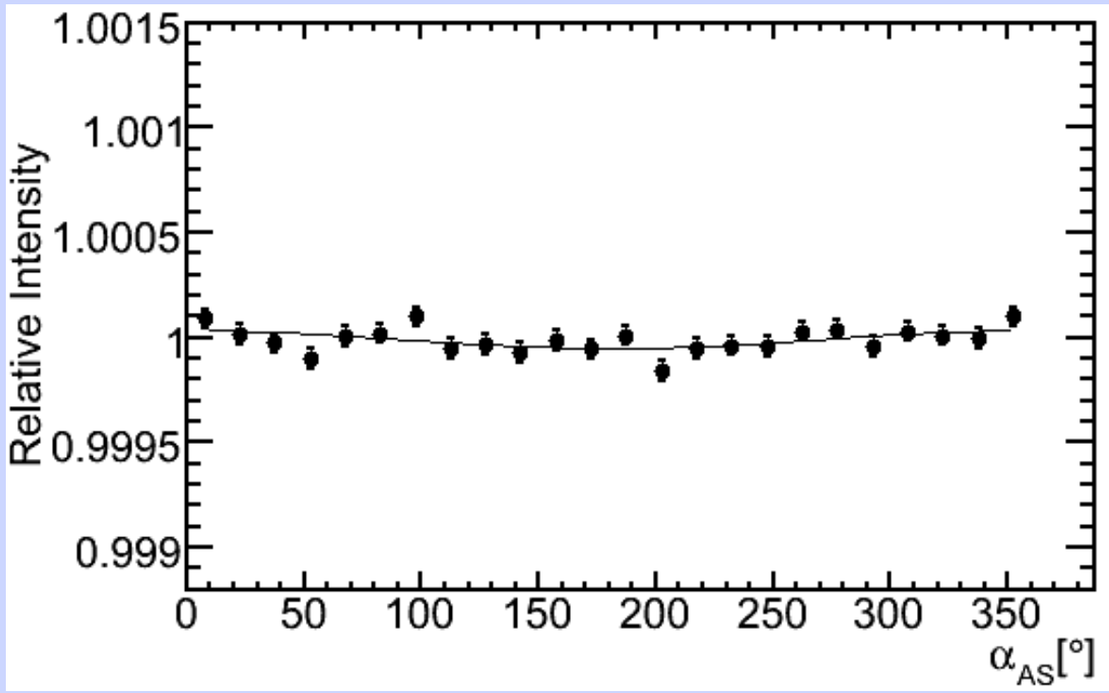

20 TeV

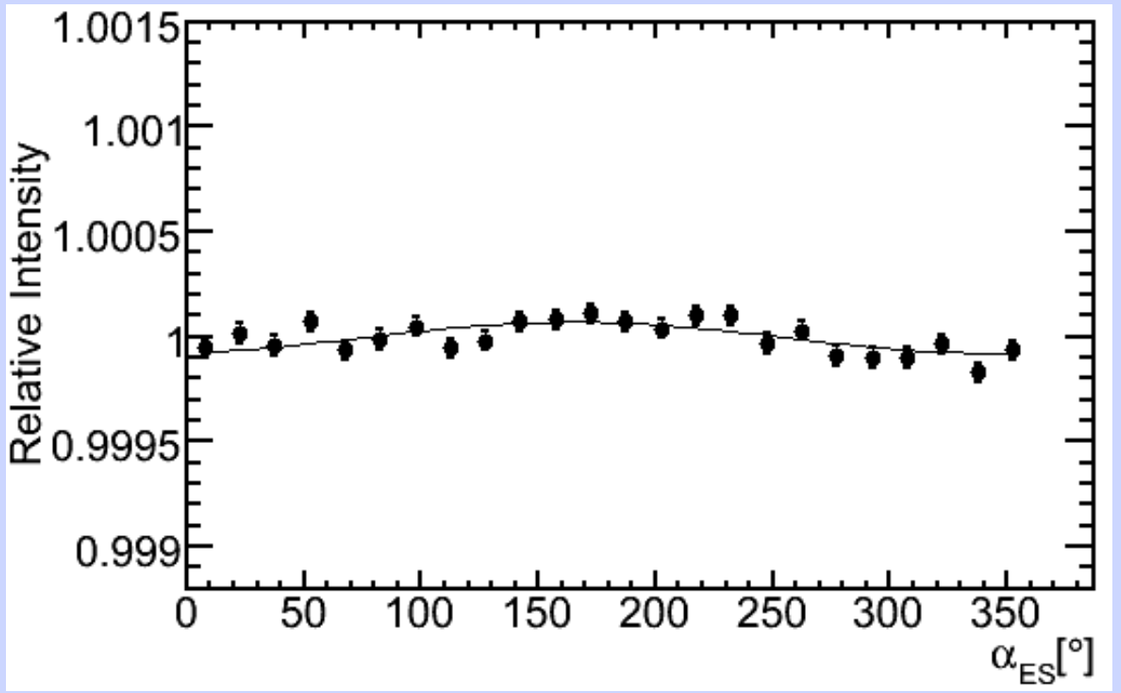

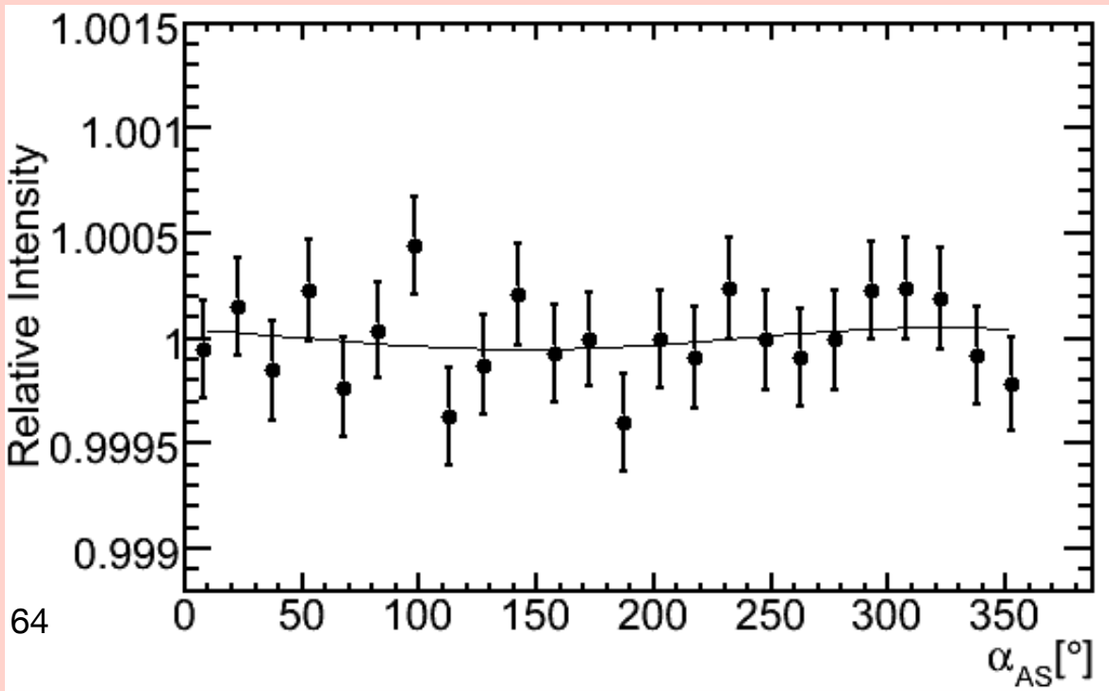

400 TeV

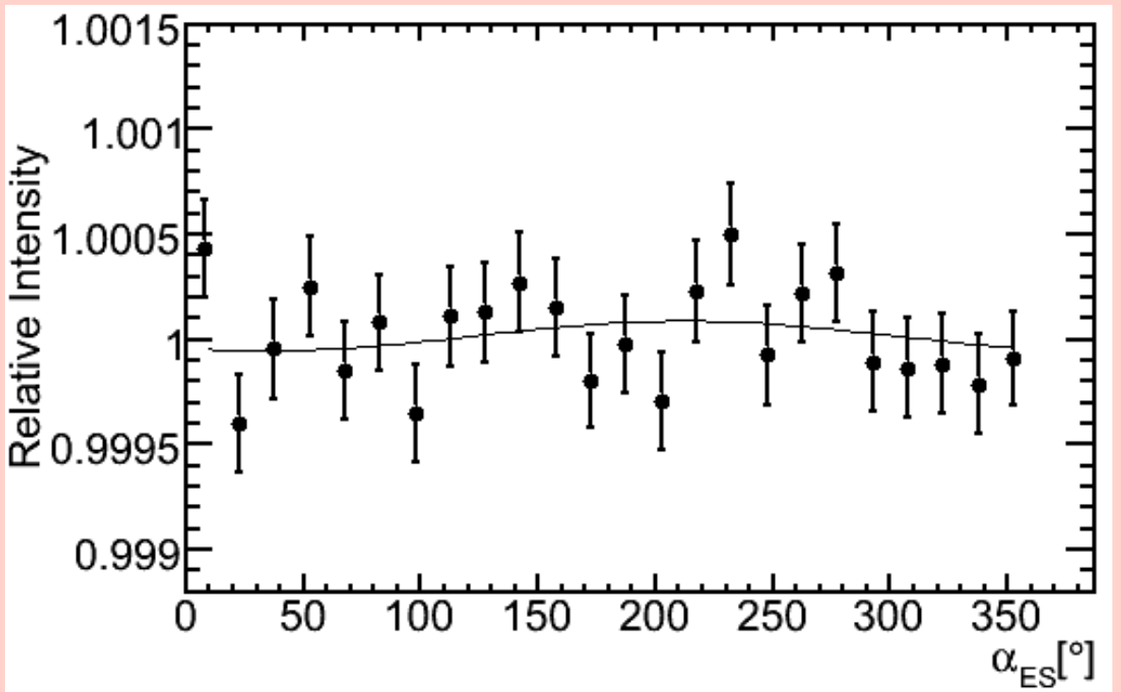

systematic uncertainties IceCube-59

statistical stability tests + anti-sidereal effect

extended-sidereal effect

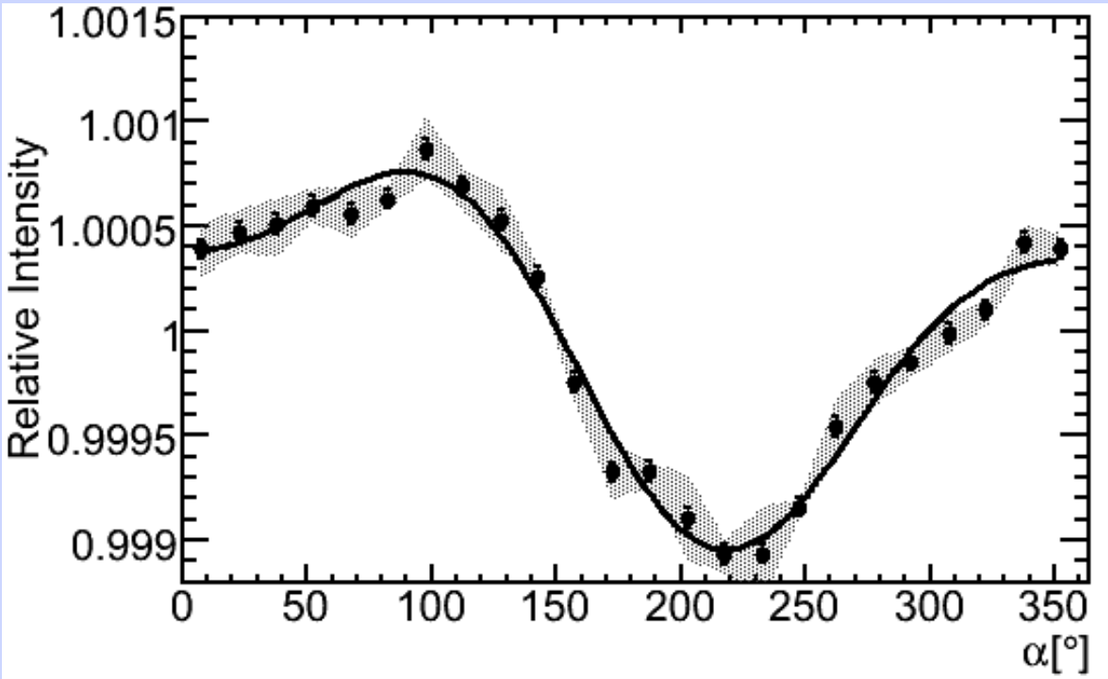

20 TeV

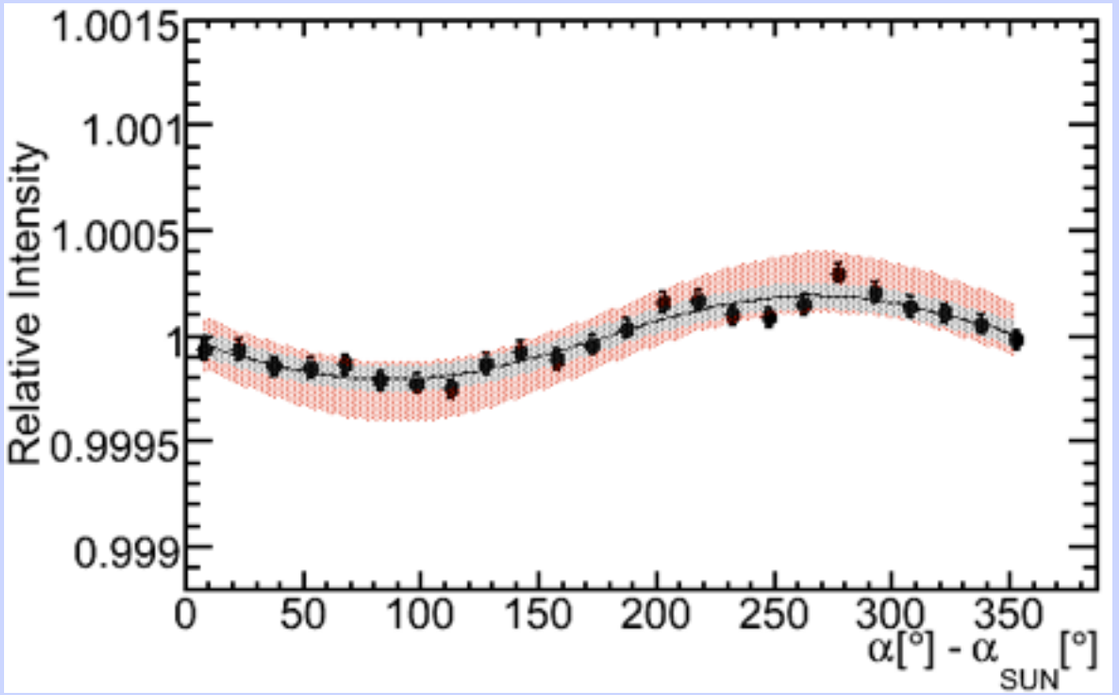

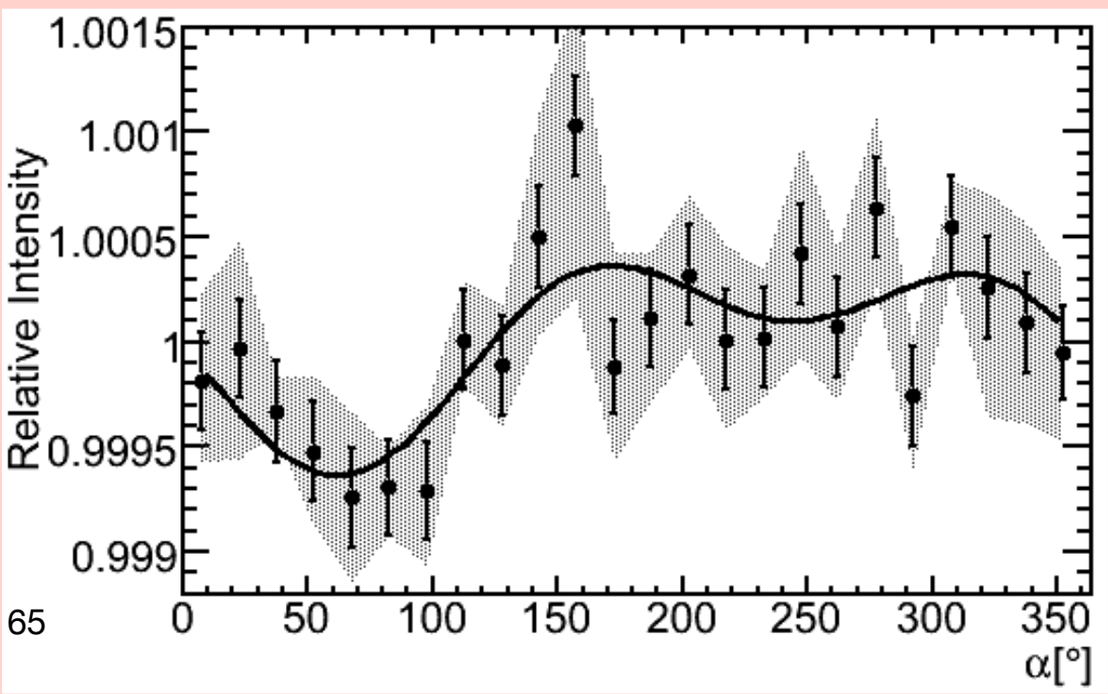

400 TeV

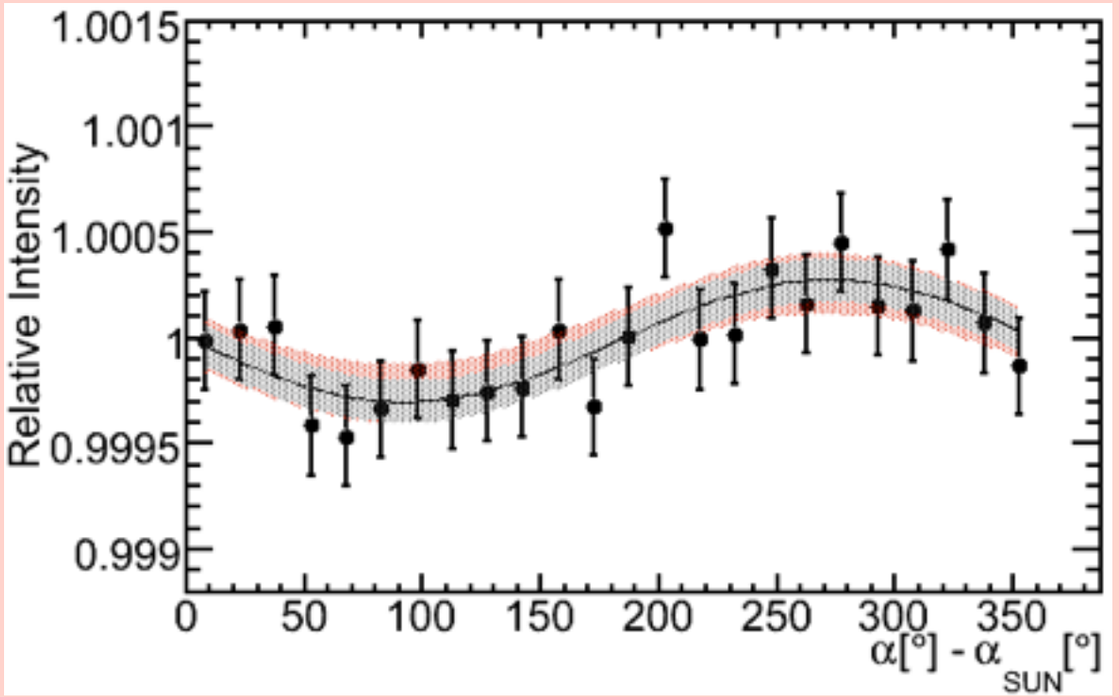

cosmic ray anisotropy small scale
IceCube

region	right ascension	declination	optimal scale	peak significance	post-trials	**IC79 (post-trials)**
1	$(122.4^{+4.1}_{-4.7})^\circ$	$(-47.4^{+7.5}_{-3.2})^\circ$	22°	7.0σ	5.3σ	6.8σ
2	$(263.0^{+3.7}_{-3.8})^\circ$	$(-44.1^{+5.3}_{-5.1})^\circ$	13°	6.7σ	4.9σ	5.4σ
3	$(201.6^{+6.0}_{-1.1})^\circ$	$(-37.0^{+2.2}_{-1.9})^\circ$	11°	6.3σ	4.4σ	6.4σ
4	$(332.4^{+9.5}_{-7.1})^\circ$	$(-70.0^{+4.2}_{-7.6})^\circ$	12°	6.2σ	4.2σ	6.1σ
5	$(217.7^{+10.2}_{-7.8})^\circ$	$(-70.0^{+3.6}_{-2.3})^\circ$	12°	-6.4σ	-4.5σ	-6.1σ
6	$(77.6^{+3.9}_{-8.4})^\circ$	$(-31.9^{+3.2}_{-8.6})^\circ$	13°	-6.1σ	-4.1σ	-4.3σ
7	$(308.2^{+4.8}_{-7.7})^\circ$	$(-34.5^{+9.6}_{-6.9})^\circ$	20°	-6.1σ	-4.1σ	-4.4σ
8	$(166.5^{+4.5}_{-5.7})^\circ$	$(-37.2^{+5.0}_{-5.7})^\circ$	12°	-6.0σ	-4.0σ	-6.4σ

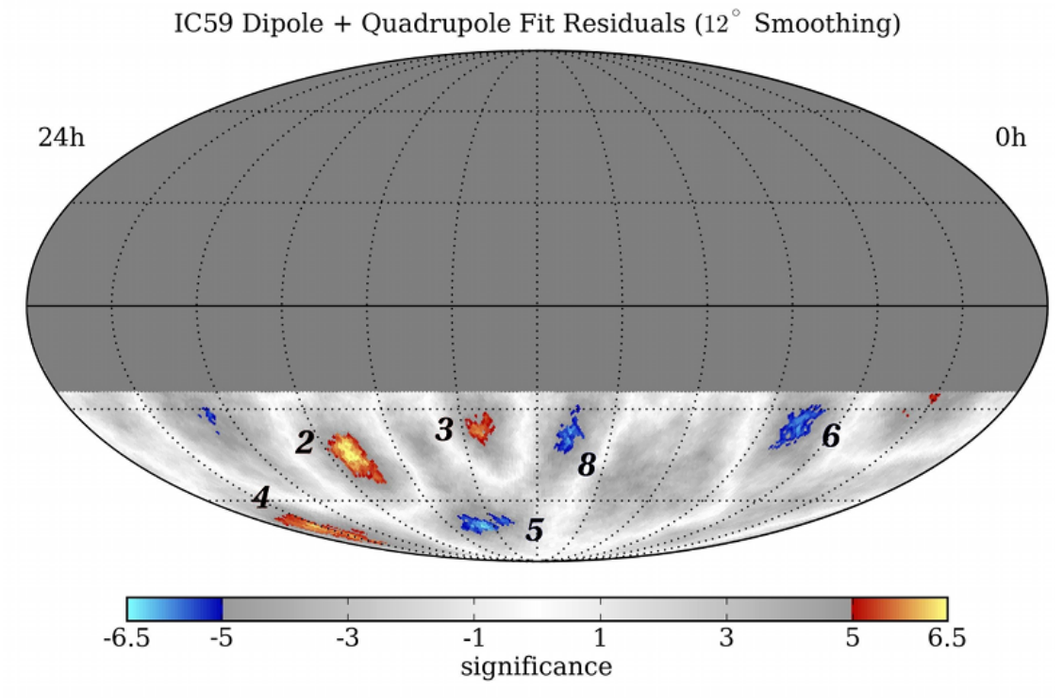

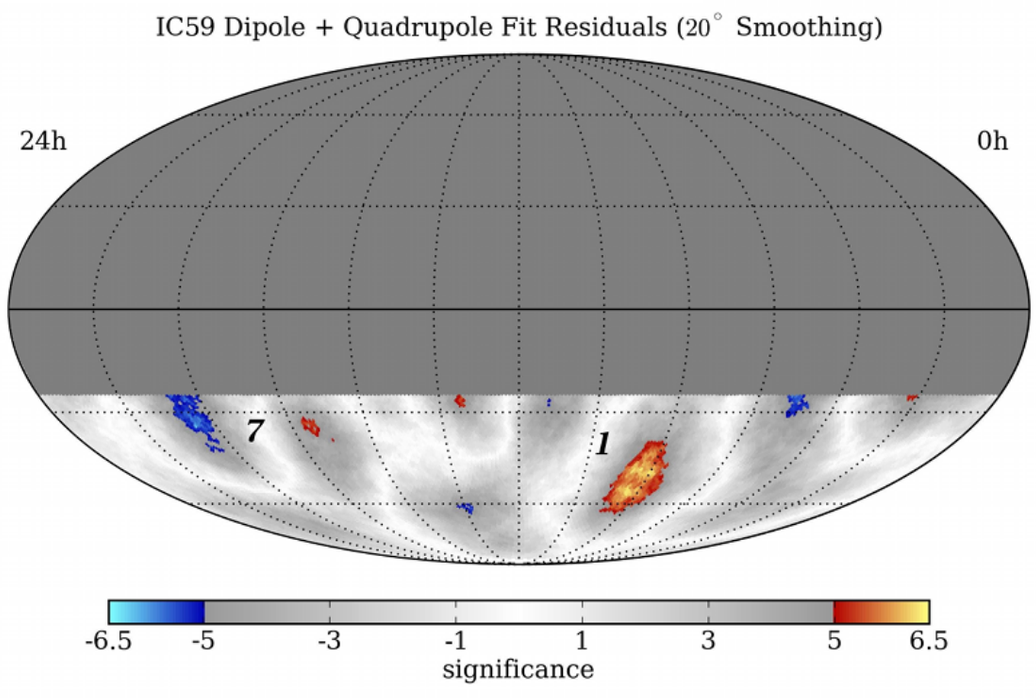

anisotropy vs. angular scale

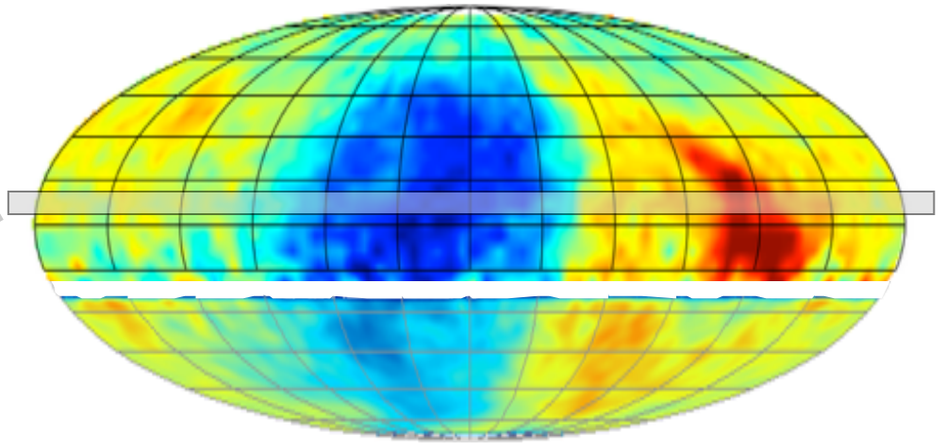

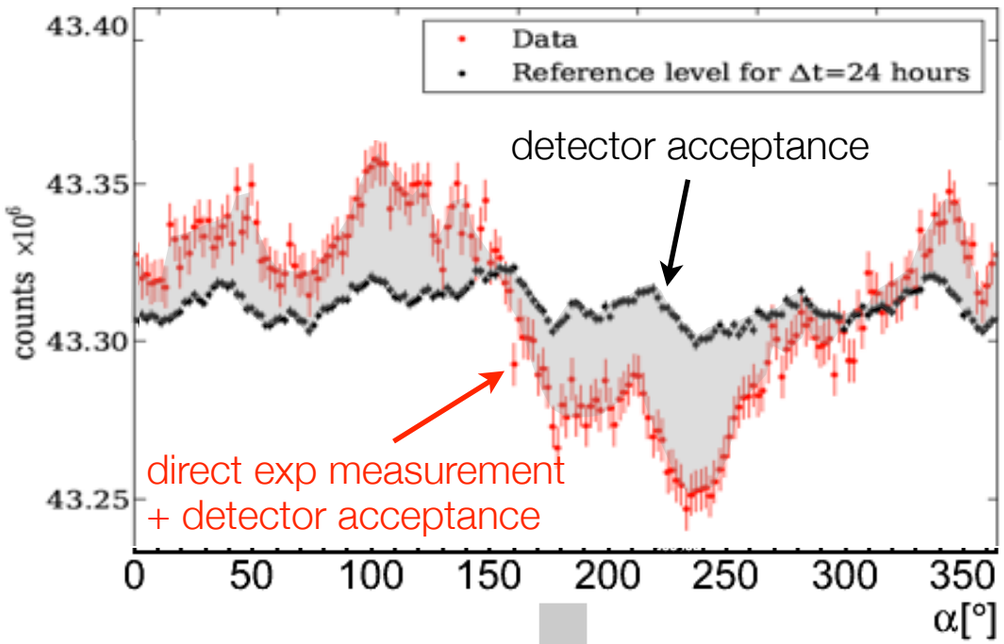

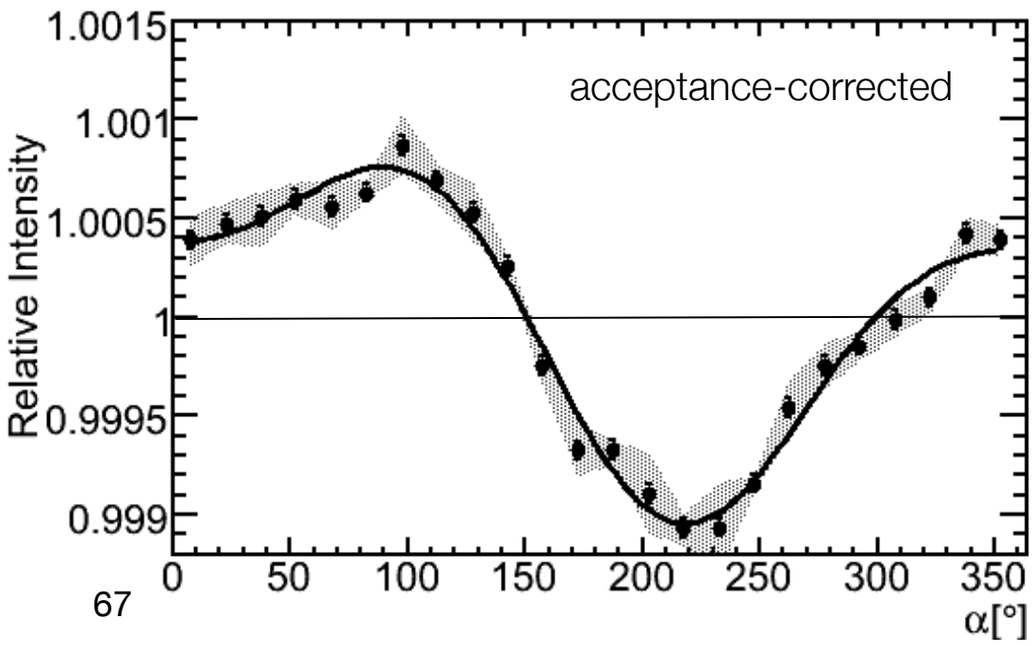

large vs small scale anisotropy

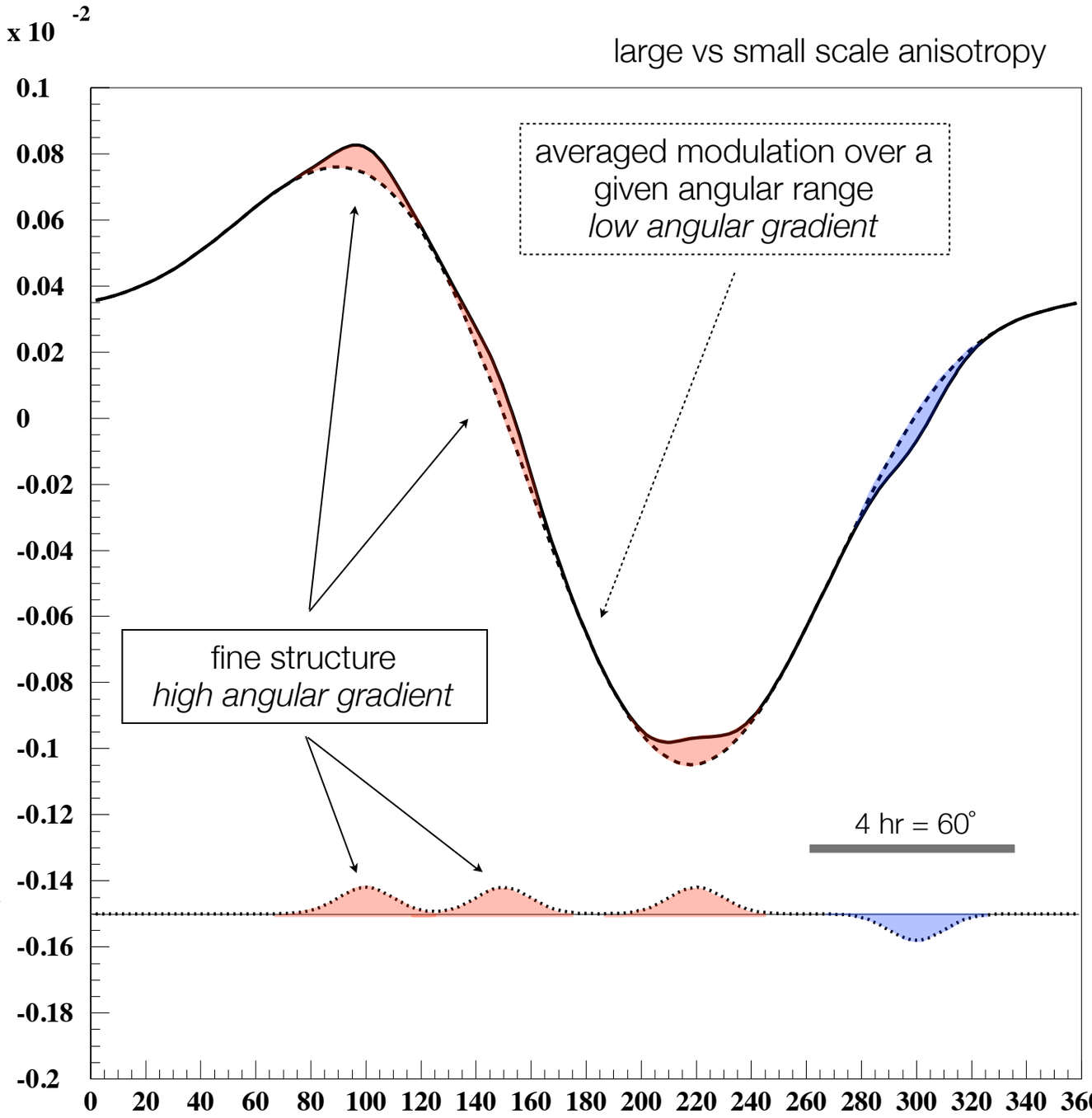

cosmic ray anisotropy

AMANDA-IceCube 2000-2011

Preliminary

Period	Detector	Start	End	Live-time (days)	No. of events ($\times 10^9$)	χ^2/dof	p-value
1	AM-II	02/13/2000	11/02/2000	213.4	1.4	11.3/15	0.73
2	AM-II	02/11/2001	10/19/2001	235.3	2.3	16.6/15	0.34
3	AM-II	01/01/2002	08/02/2002	169.2	2.4	26.0/15	0.04
4	AM-II	02/09/2003	12/17/2003	236.0	2.2	19.3/15	0.20
5	AM-II	01/05/2004	11/02/2004	225.8	2.5	14.3/15	0.50
6	AM-II	12/30/2004	12/23/2005	242.9	2.6	21.0/15	0.14
7	AM-II	01/01/2006	09/13/2006	213.1	2.4	24.4/15	0.06
8	IC22	06/01/2007	03/30/2008	269.4	5.3	45.2/15	7×10^{-5}
9	IC40	04/18/2008	04/30/2009	335.6	18.9	12.8/15	0.62
10	IC59	05/20/2009	05/30/2010	335.0	33.8	11.1/15	0.75
11	IC79	05/31/2010	05/12/2011	299.7	39.1	6.5/15	0.97
12	IC86	05/13/2011	05/14/2012	332.9	52.9	8.9/15	0.88

statistical uncertainties only

cosmic ray anisotropy

probing heliospheric magnetic structure

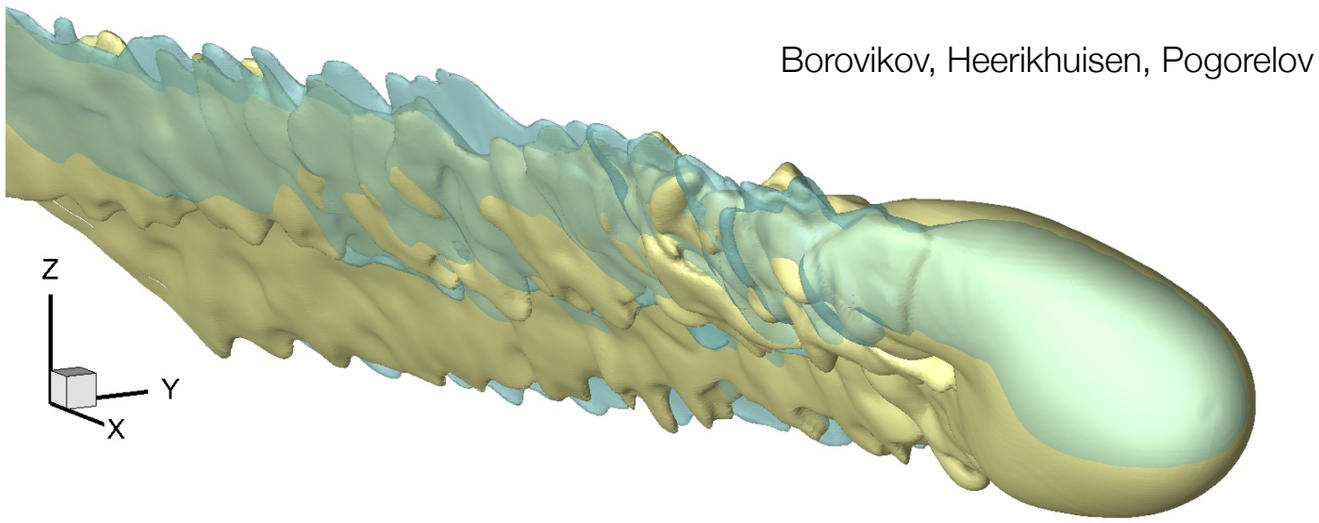

Borovikov, Heerikhuisen, Pogorelov

downstream instabilities on the flanks of heliotail

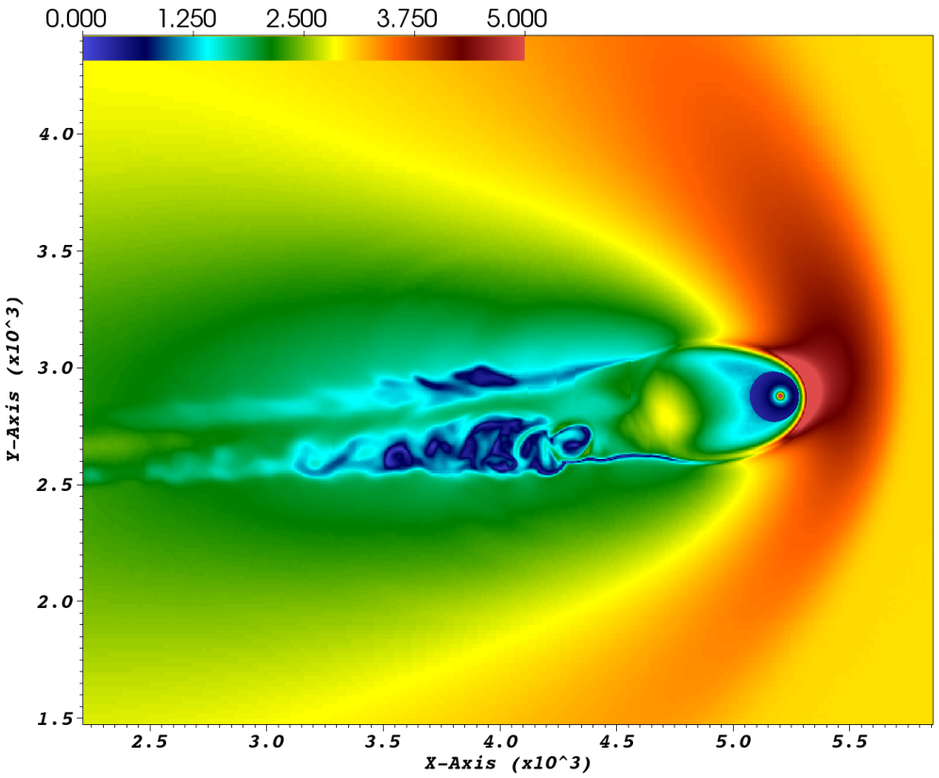

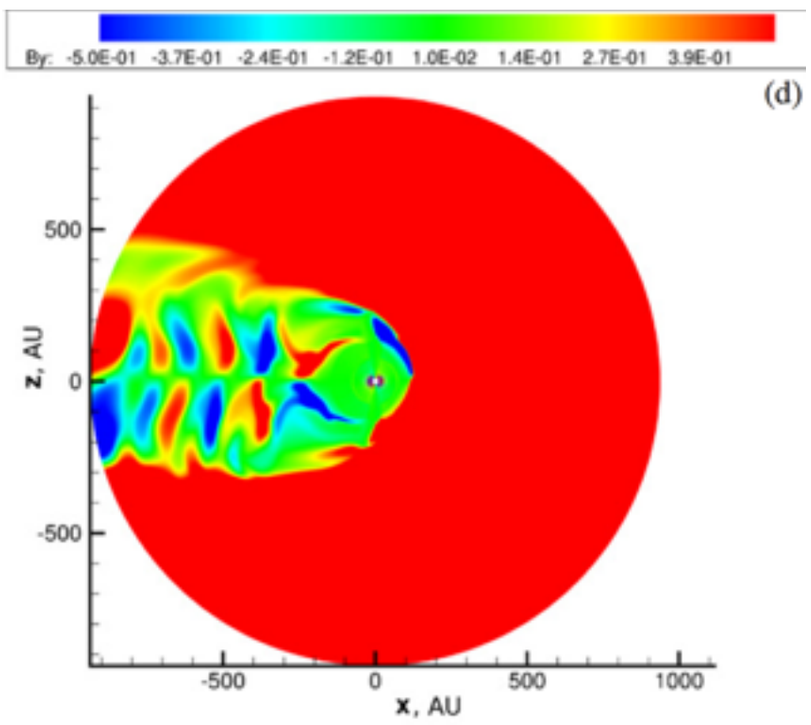

Pogorelov et al., 2009

effects of magnetic polarity reversals from solar cycles